Advanced fabrication

Denys Makarov

Advanced fabrication: Possible topics to be covered

Bulk materials (thermodynamic equilibrium)

Bulk materials (far-out-of equilibrium)

Thin film materials

Lithographically structured thin films

Self-assembly

Guided self-assembly

Magnetic composites

2D materials and heterostructures

Flexible vs rigid substrates

Printed materials

3D printed materials

Curvilinear materials

Electroplating

…

Bulk: soft and hard magnetic materials

Key aspect: power losses in electrical motors and generators

- Investigate the magnetization processes in magnetic materials
- Study the role of domain processes on power loss

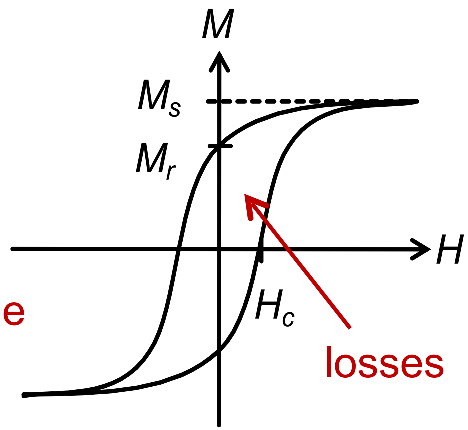

Losses in ferromagnets limit the performance of generators

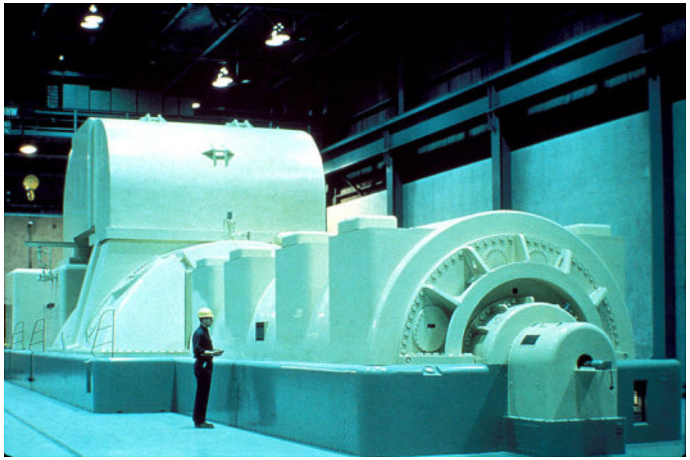

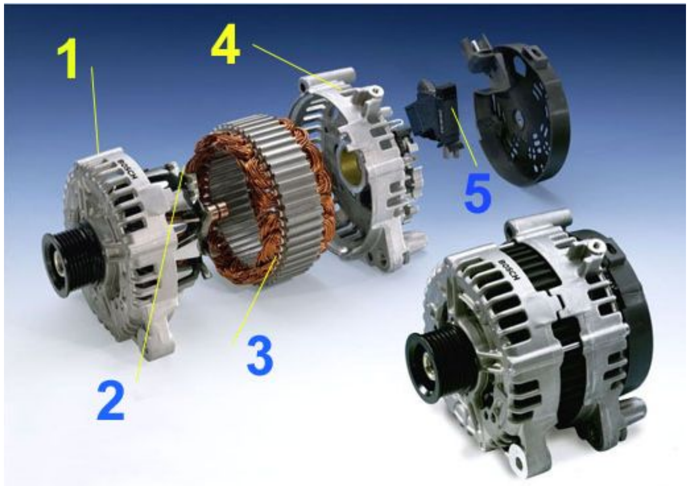

http://www.kfztech.de/kfztechnik/technikprofi/der-moderne-generator.htm

Change of magnetic domain pattern

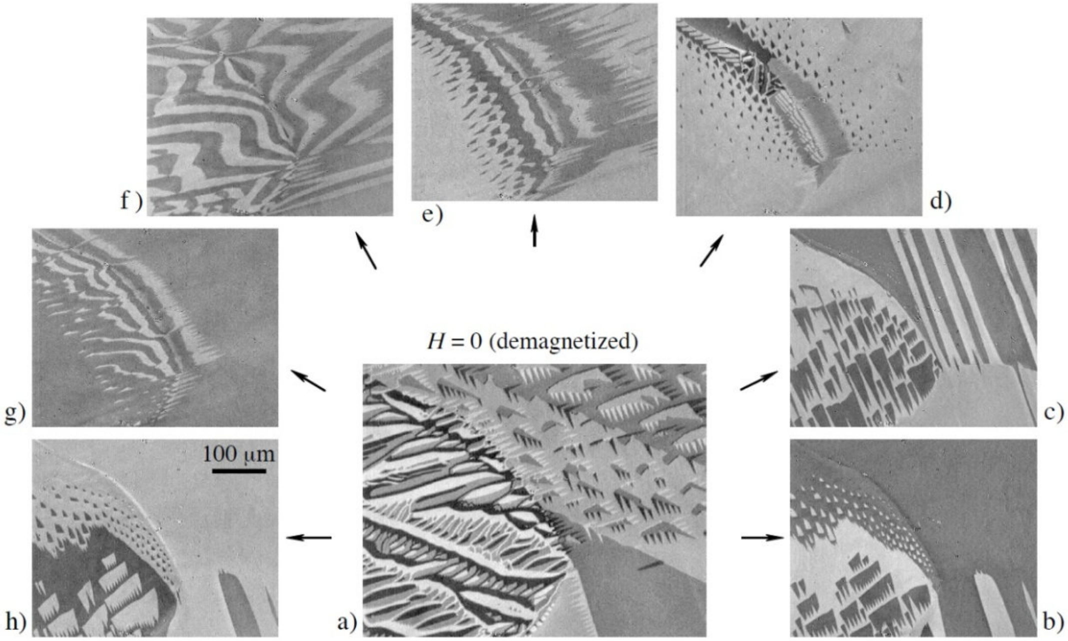

Prof. Rudolf Schäfer (Leibniz IFW Dresden)

Dr. Denys Makarov I E-Mail: d.makarov@hzdr.de I Intelligent Materials and Systems

Flexible: Magnetic tape recording

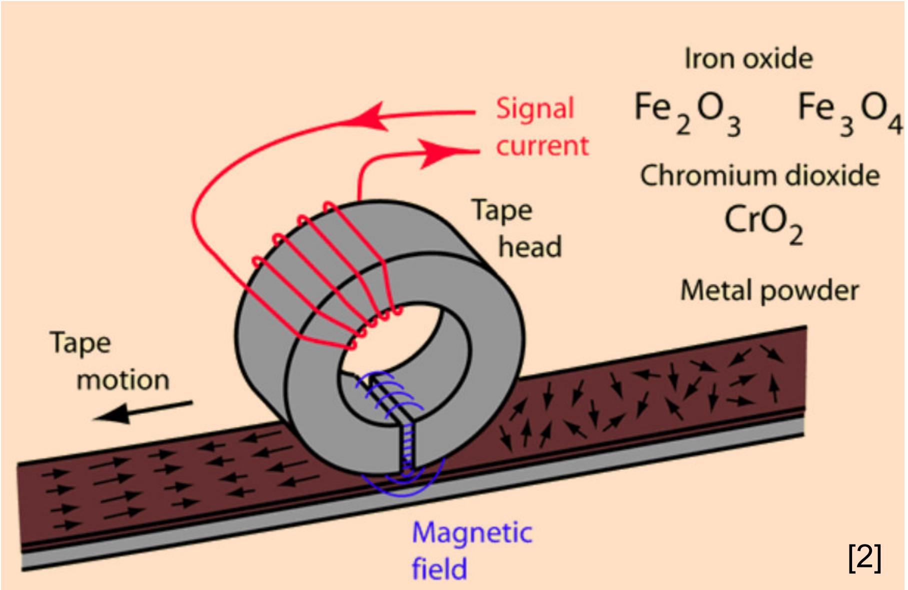

[1]
http://www.mtap.iasa-web.org/

[2]
http://hyperphysics.phy-astr.gsu.edu/hbase/Audio/tape2.html

Thin films: Application scenarios

Reservoir computing based on skyrmions

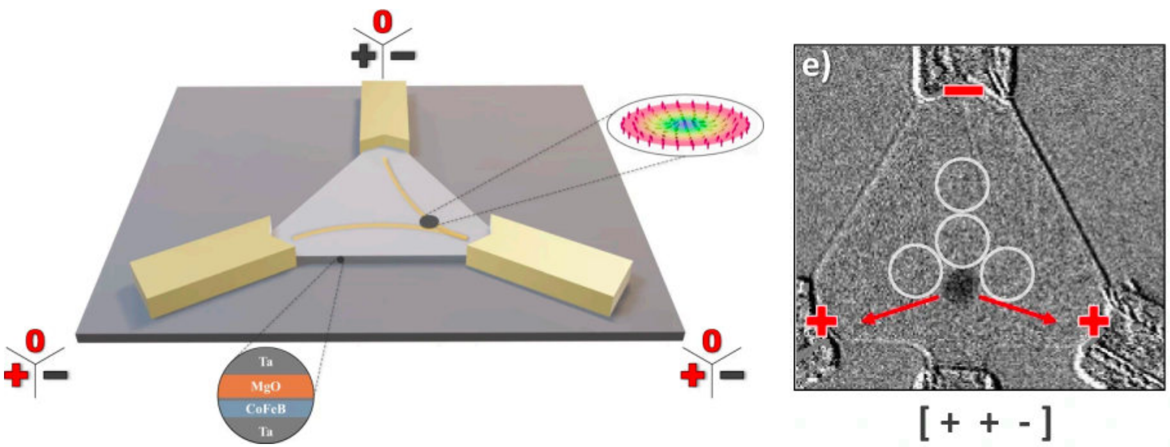

K. Raab et al., *Nature Comm.* **13**, 6982 (2022)

Racetrack memory

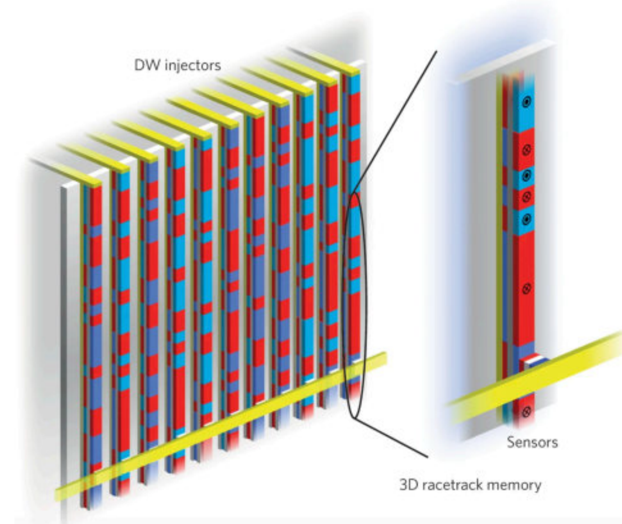

S. Parkin et al., *Nature Nano.* **10**, 195 (2015)

Racetrack of skyrmions / antiskyrmions

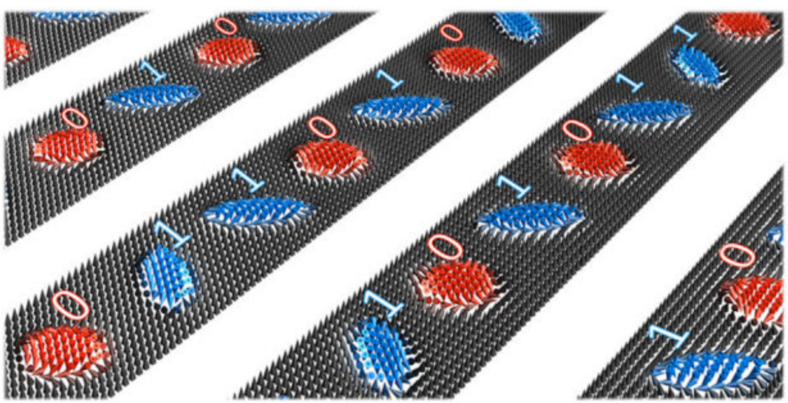

Jena et al., *Nature Comm.* **11**, 1115 (2020);

Inter chip communication

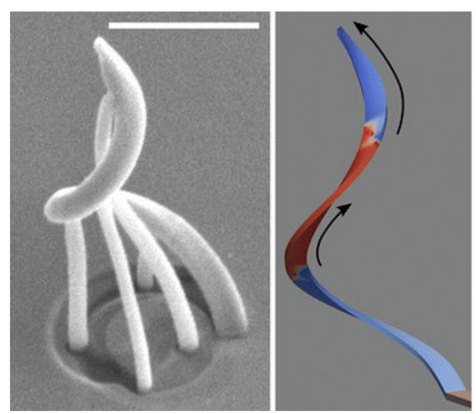

Skoric et al., *ACS Nano* **16**, 8860 (2022);

3D racetrack memory

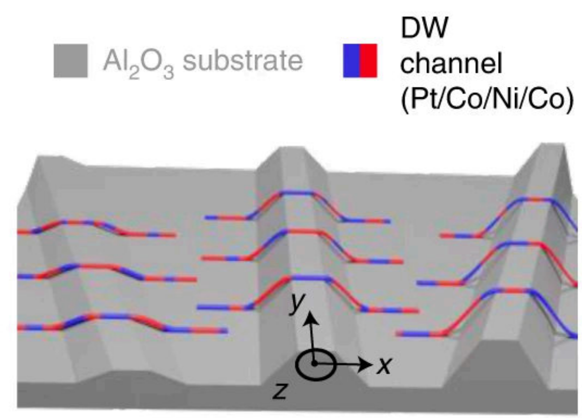

Gu et al., *Nature Nano.* **17**, 1065 (2022)

Composites: Ultrathin & ultrafast magnetic soft robots

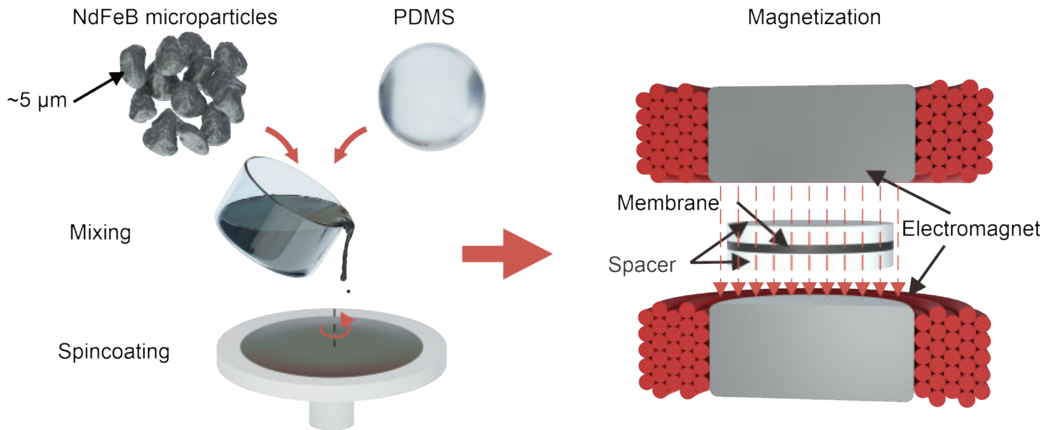

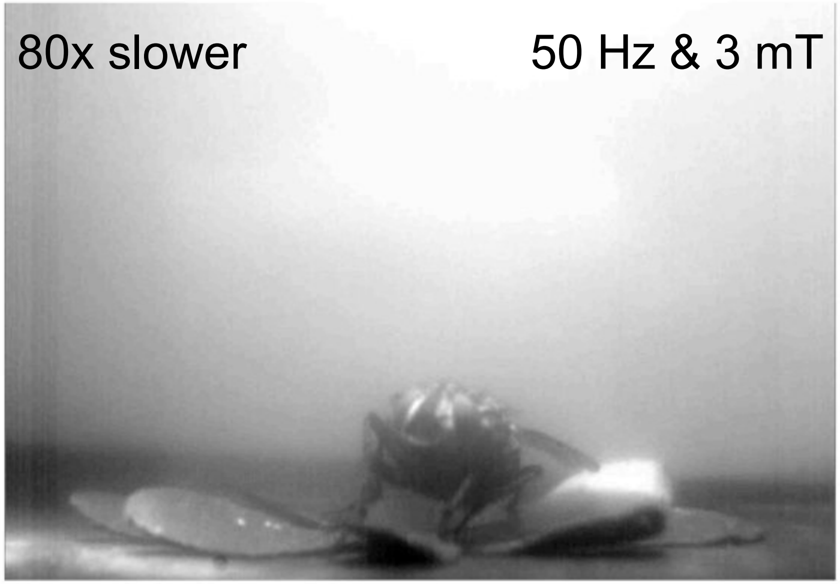

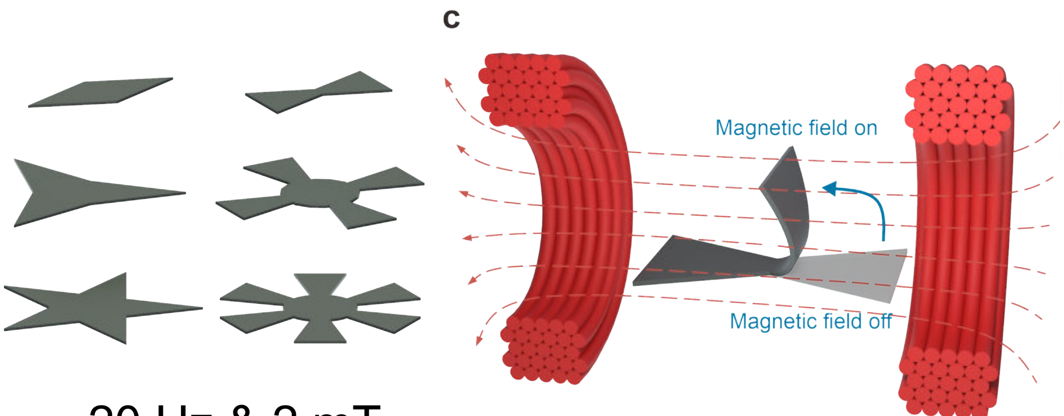

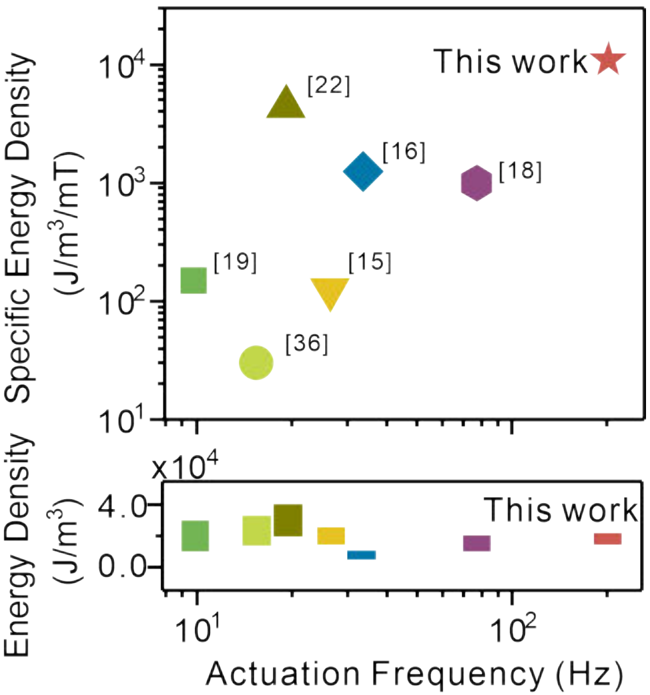

20 Hz & 2 mT

Test start

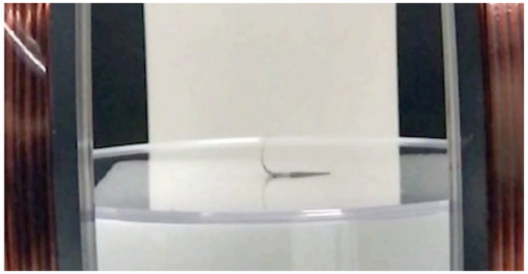

After 2.1 million cycles

Xu Wang, DM et al., *Communications Materials* **1**, 67 (2020)

2D magnetic materials and heterostructures

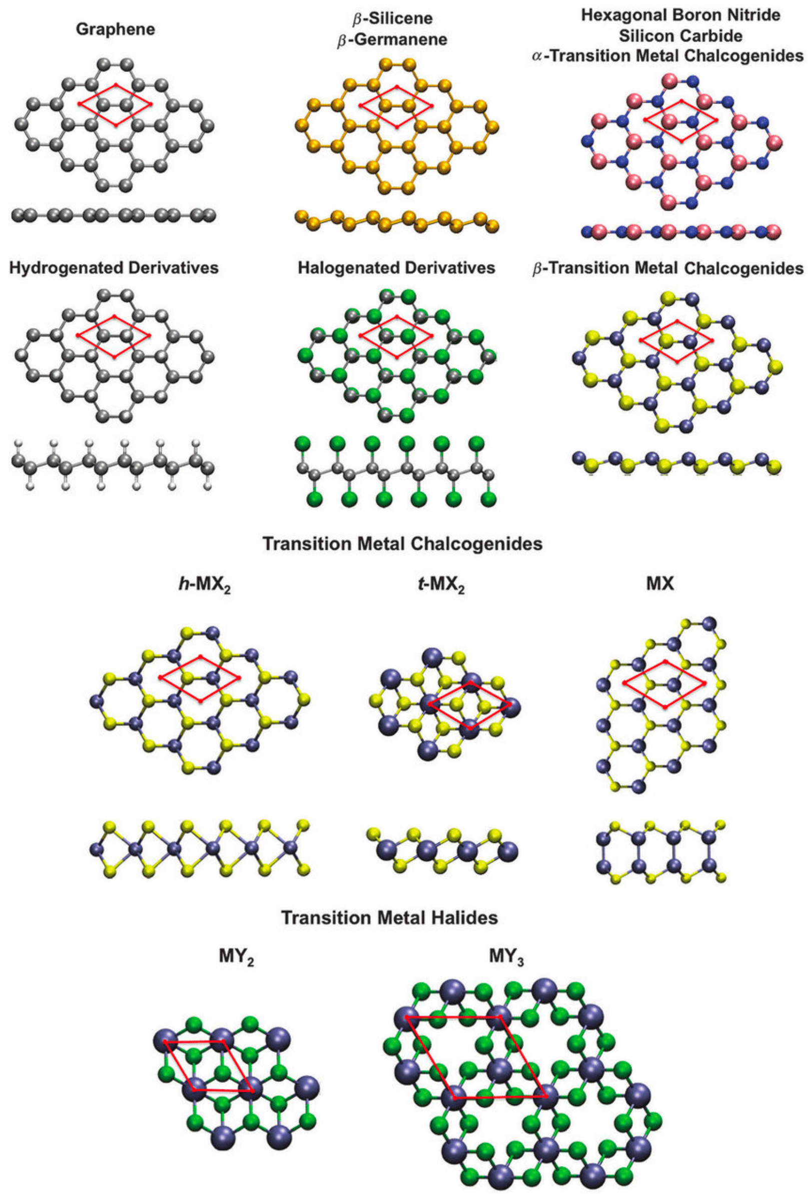

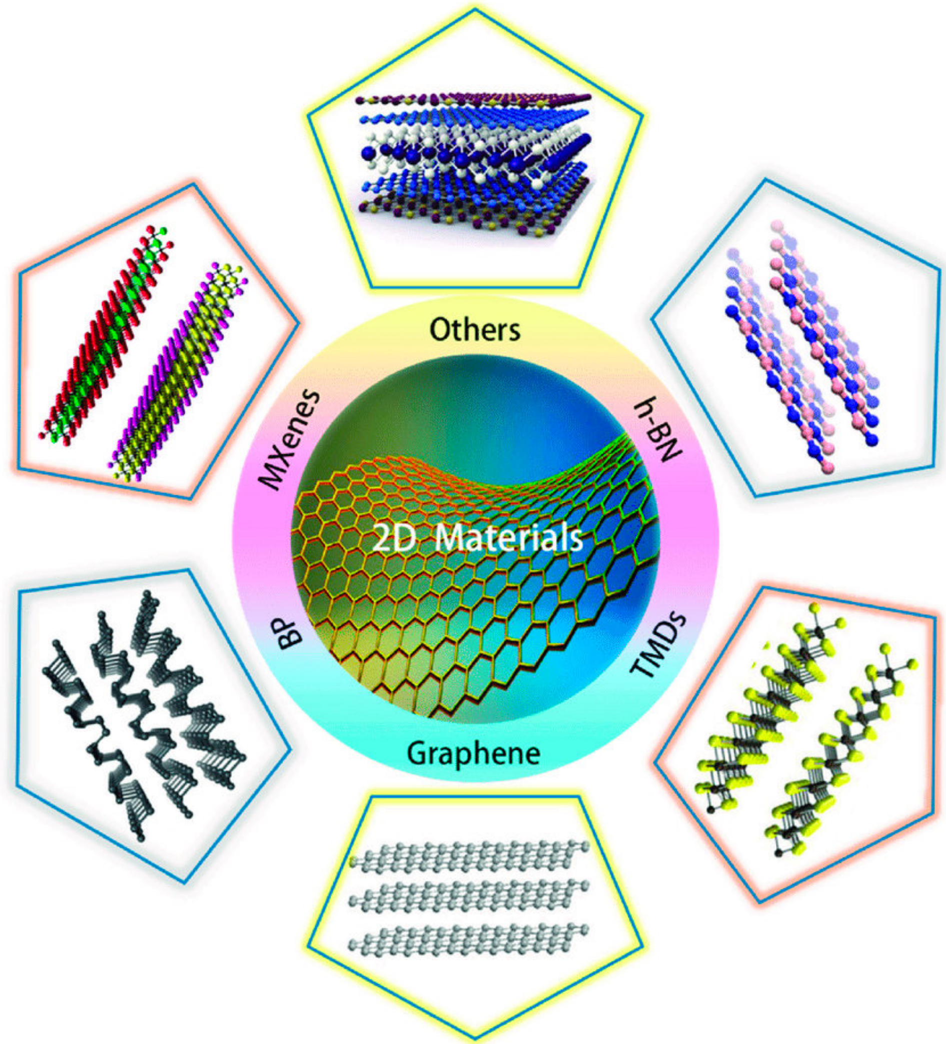

Molecules **24**, 88 (2019)

Chem. Soc. Rev. **43**, 6537 (2014)

Magnetic 2D material: CrI_3

- Semiconducting layered vdW material
- Undergoes low-temperature magnetic phase transition
- Exhibits different forms of magnetic order

Magnetization and magnetic susceptibility measurements show that bulk CrI_3 is a strongly anisotropic ferromagnet below the Curie temperature (T_C = 61 K), with its easy axis pointing perpendicular to the layers, and a saturation magnetization consistent with a spin S = 3/2 state of the Cr atoms

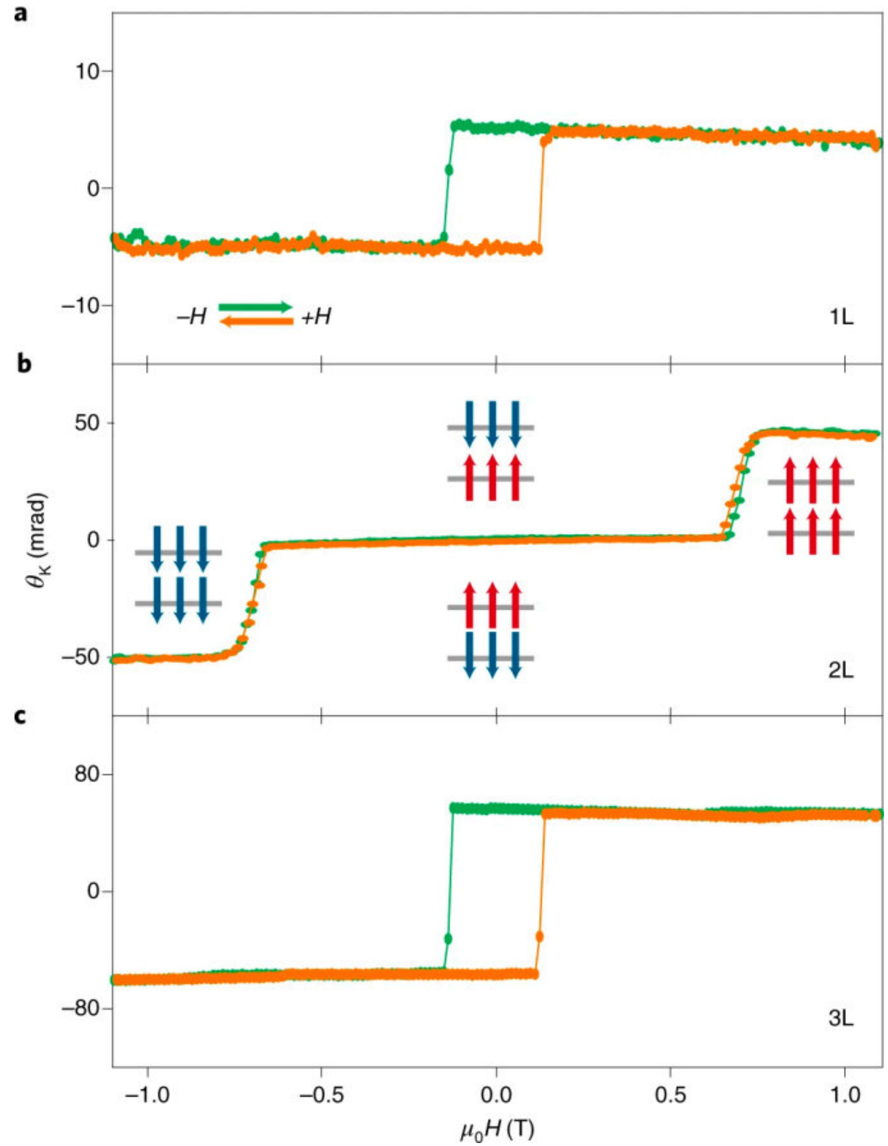

Nature **546**, 270–273 (2017)

https://www.nature.com/articles/s41565-019-0438-6

Magnetic domains in CrI_3 studied via NV microscopy

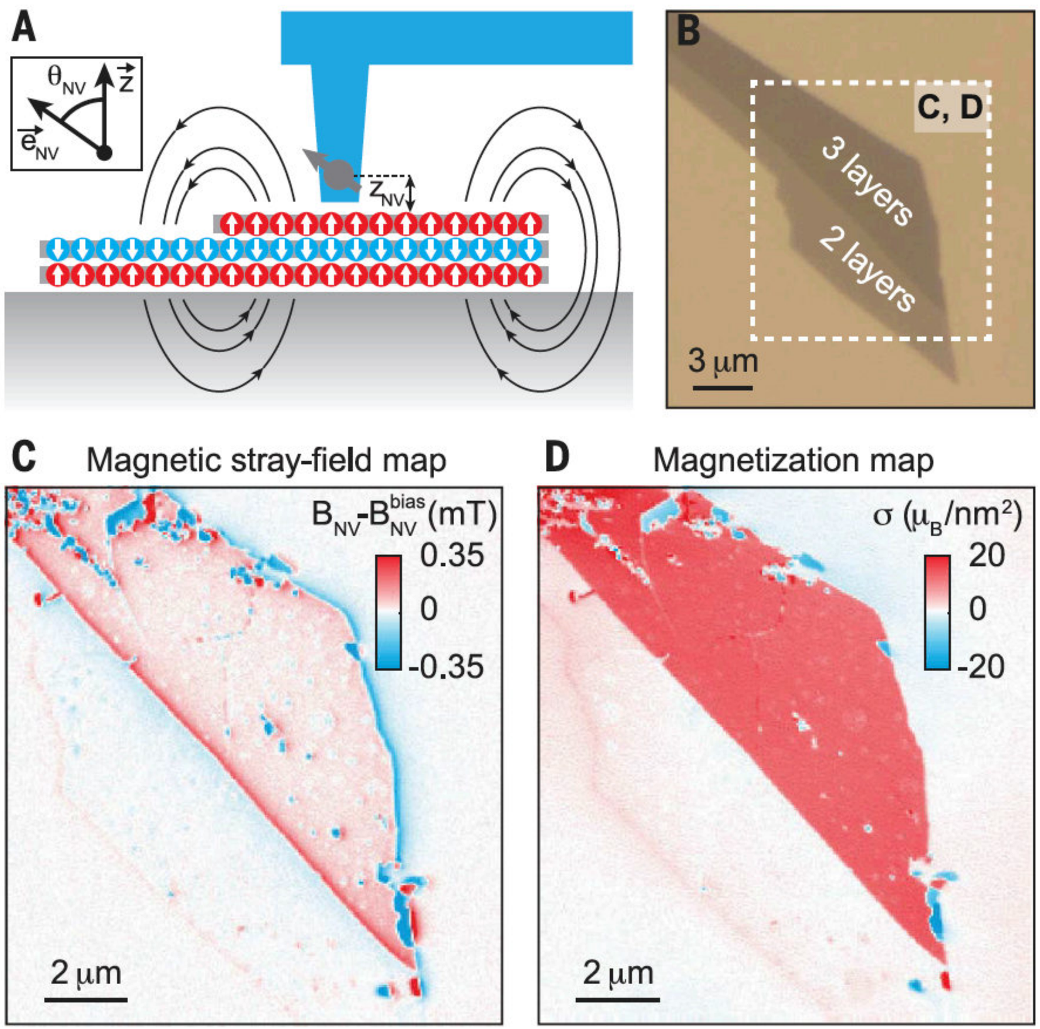

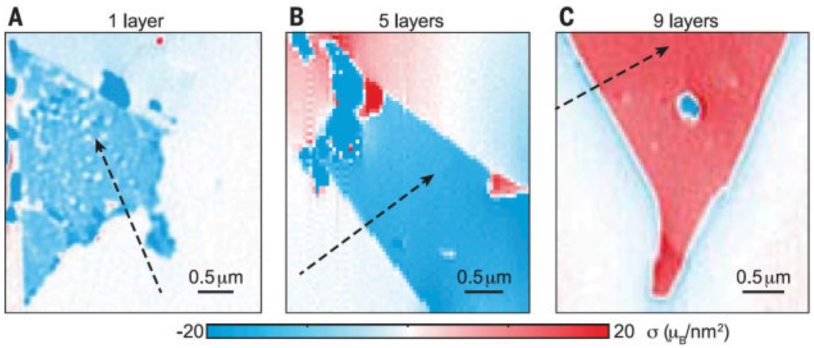

Imaging of a 9-layer flake

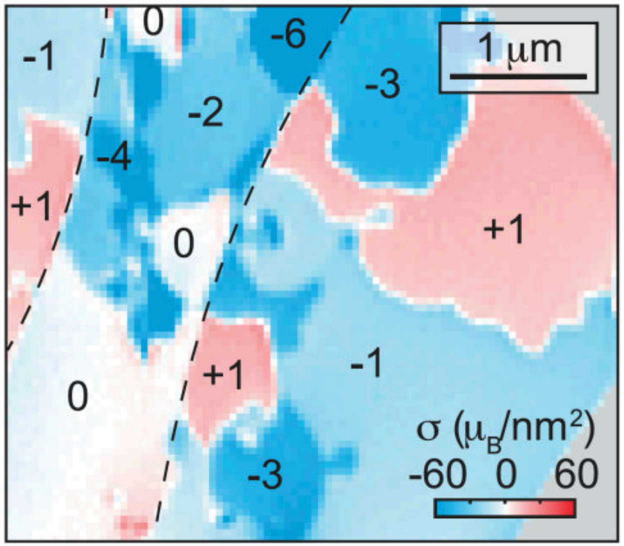

Thiel et al., *Science* **364**, 973 (2019)

Bulk materials

Dr. Denys Makarov I E-Mail: d.makarov@hzdr.de I Intelligent Materials and Systems

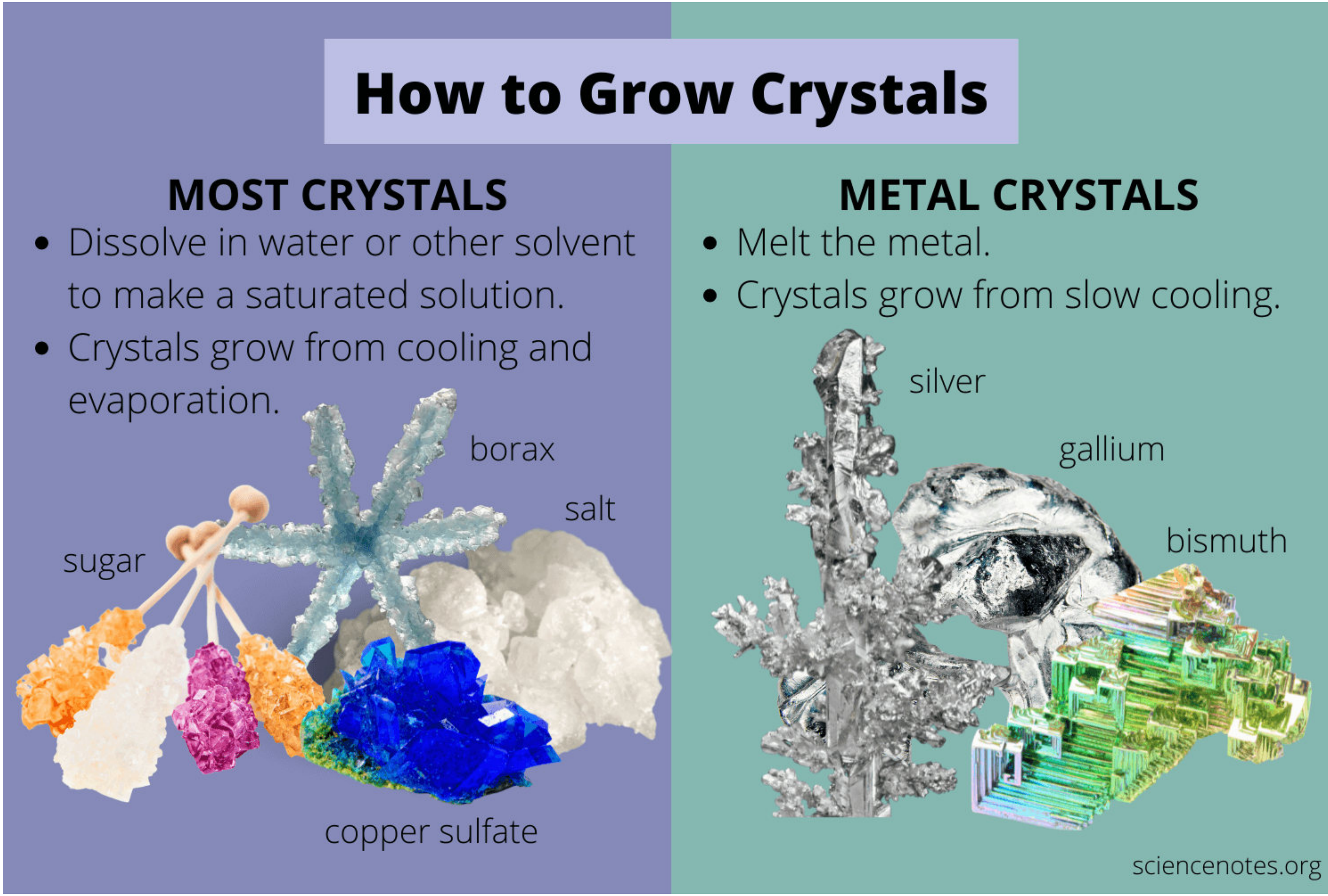

https://sciencenotes.org/how-to-grow-crystals/#google_vignette

Dr. Denys Makarov I E-Mail: d.makarov@hzdr.de I Intelligent Materials and Systems

Conventional / Classical synthesis methods

Arc-melting

Induction melting

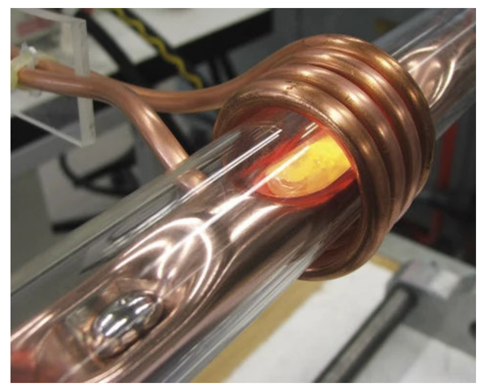

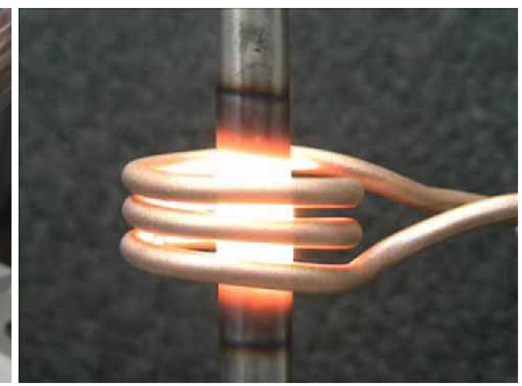

Ampule synthesis

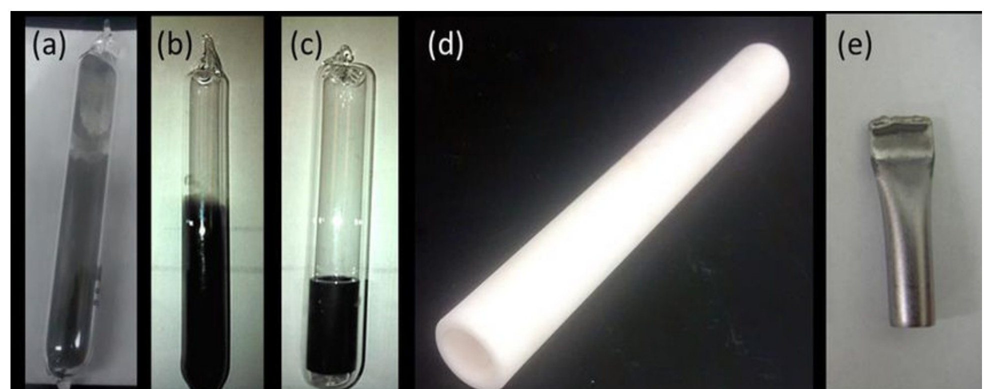

Courtesy: Dr. Ihor Veremchuk (HZDR)

Liquid Encapsulated Czochralski

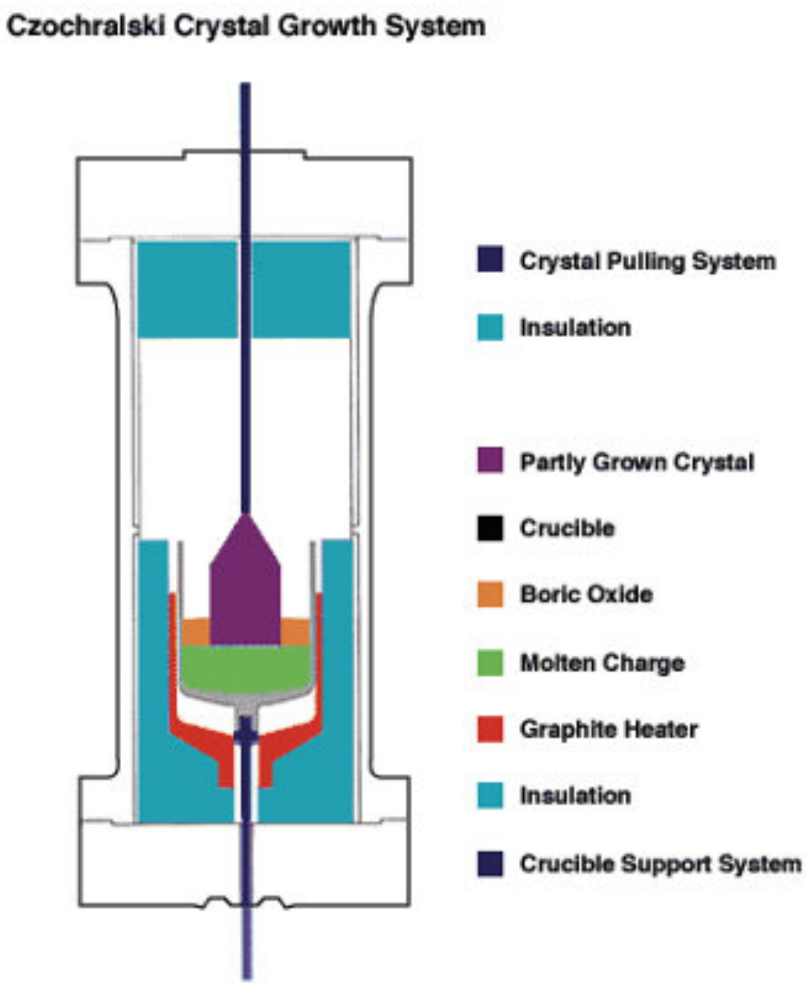

Courtesy: Dr. Ihor Veremchuk (HZDR)

Used for the manufacture of single crystals

The starting materials (either pre-synthesised polycrystalline chunks or, in the case of semi-insulating GaAs, elemental Ga and As) are placed in the growth crucible along with a pellet of boron trioxide. The crucible is placed inside a high pressure crystal puller and heated up.

At 460°C the boron trioxide melts to form a thick, viscous liquid which coats the entire melt, including the crucible (hence, liquid encapsulated). This layer, in combination with the pressure in the crystal puller, prevents sublimation of the volatile group V element.

The temperature is increased until the compound synthesises (temperatures and pressures are varied depending on which material is being produced). A seed crystal is then dipped, through the boron trioxide layer, into the melt. The seed is rotated and slowly withdrawn and a single crystal propagates from the seed.

Crystal growth is monitored by the use of cameras and measurements of weights, temperatures and pressures are made at regular intervals.

Horizontal Synthesis (e.g., semiconductors, TMD and CrI_3)

Used for producing stoichiometric polycrystalline bars of the compounds

High purity elements (Ga, As, In and/or P) are contained within a quartz boat, sealed in a quartz ampoule and placed into a furnace chamber. The furnace chamber is heated up and a temperature gradient is then moved along the boat. Temperatures and pressures are dependant on the compound being synthesised.

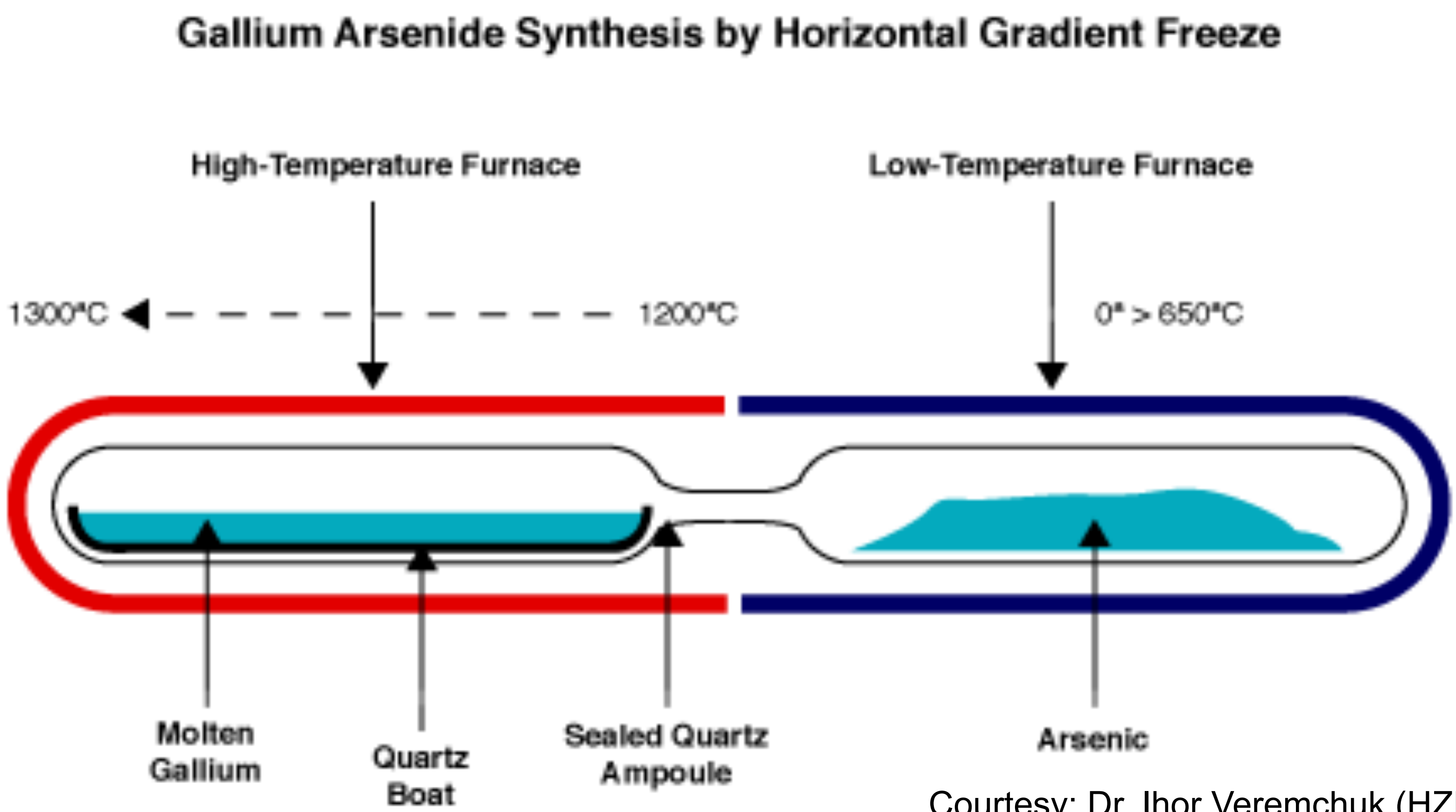

Courtesy: Dr. Ihor Veremchuk (HZDR)

Vertical Gradient Freeze

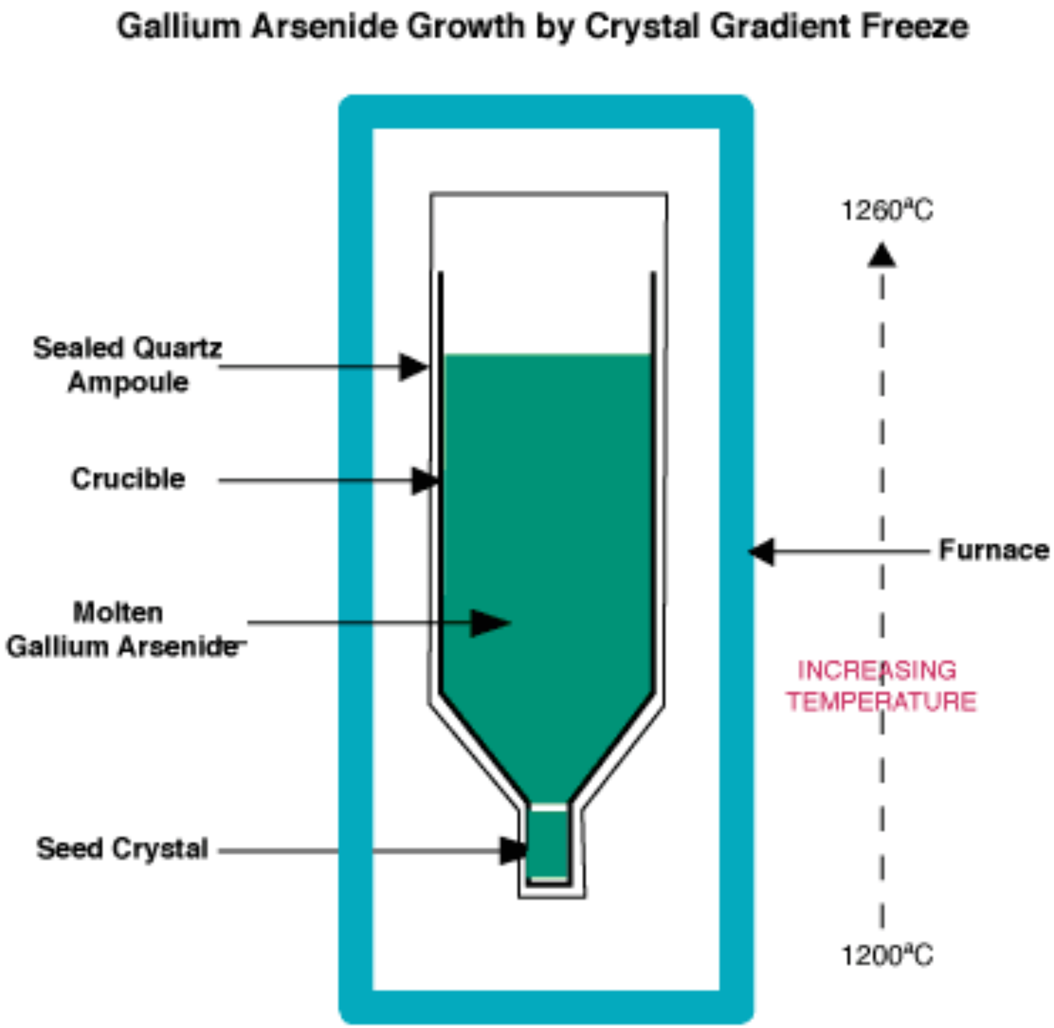

Used for producing low dislocation density GaAs crystals

Chunks of polycrystalline GaAs, produced by horizontal synthesis, are placed in a crucible with a seed crystal of the required orientation. The crucible is then placed vertically in a furnace and a temperature gradient is moved up the length of the crystal (away from the seed).

Single crystal growth propagates from the seed crystal and, because the crystal forms in the shape of the crucible, diameter control of the ingot is relatively simple.

Courtesy: Dr. Ihor Veremchuk (HZDR)

Liquid metal synthesis solvents for metallic crystals

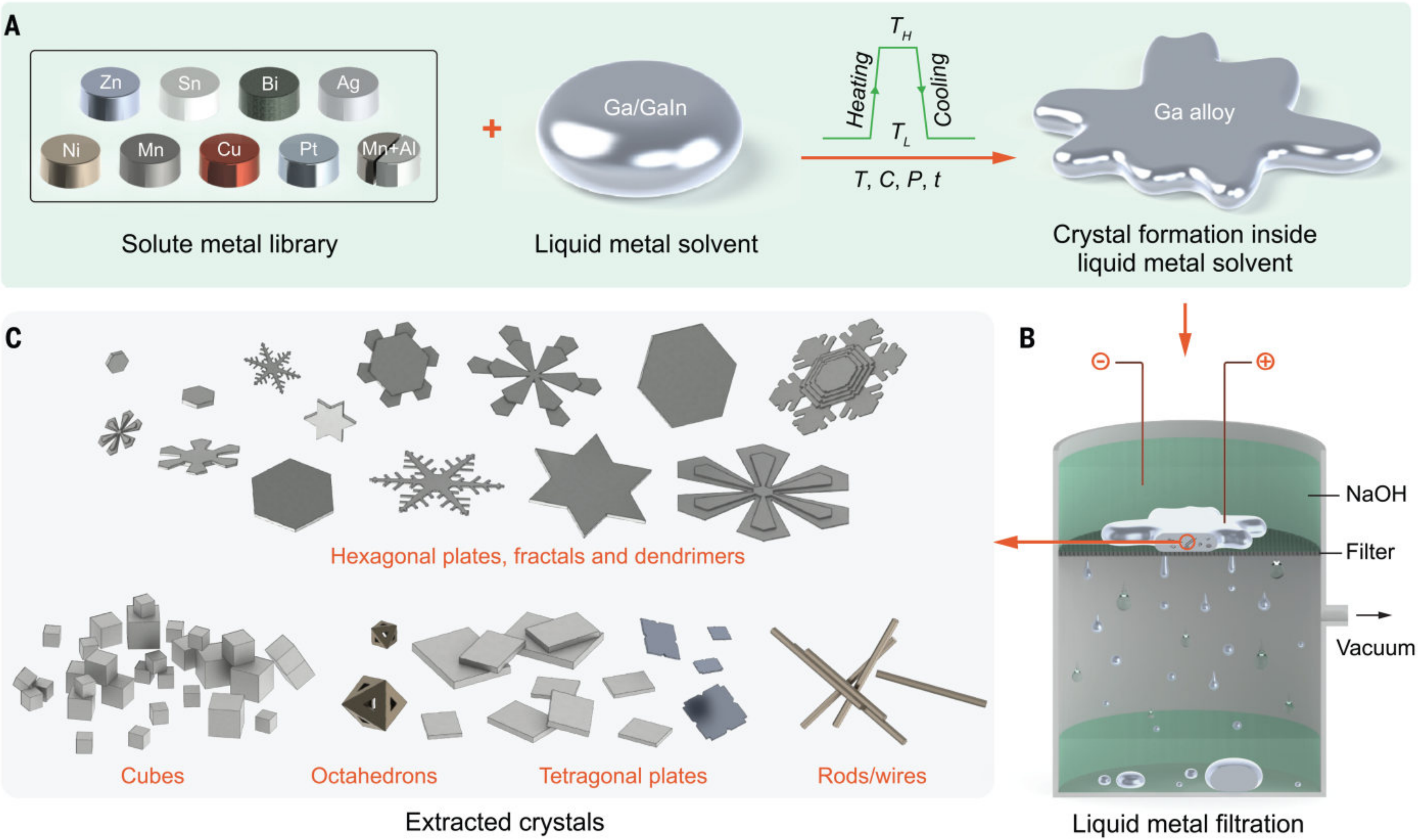

Idrus-Saidi et al., Science 378, 1118–1124 (2022)

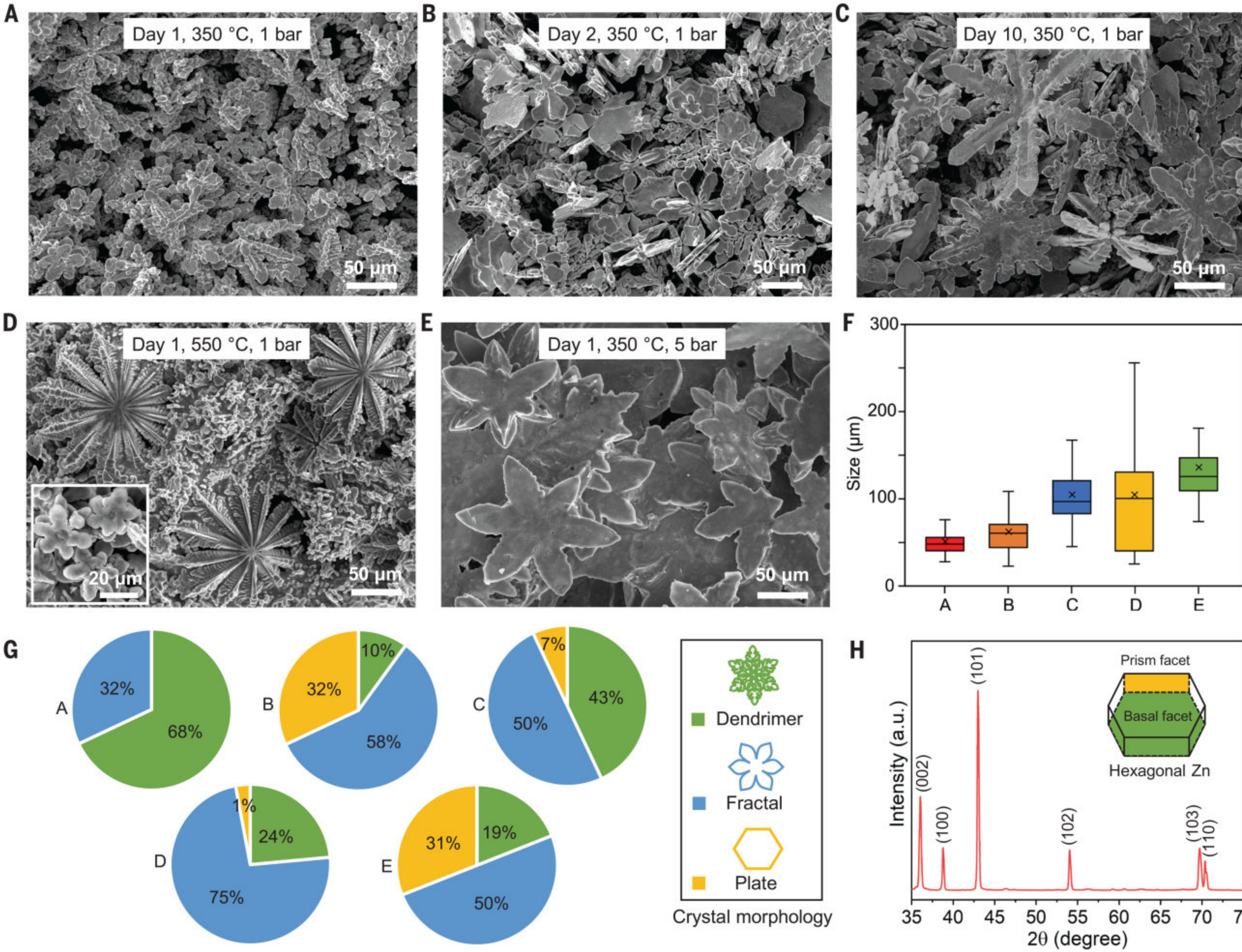

Idrus-Saidi et al., Science 378, 1118–1124 (2022)

Spark Plasma Sintering (SPS) synthesis method

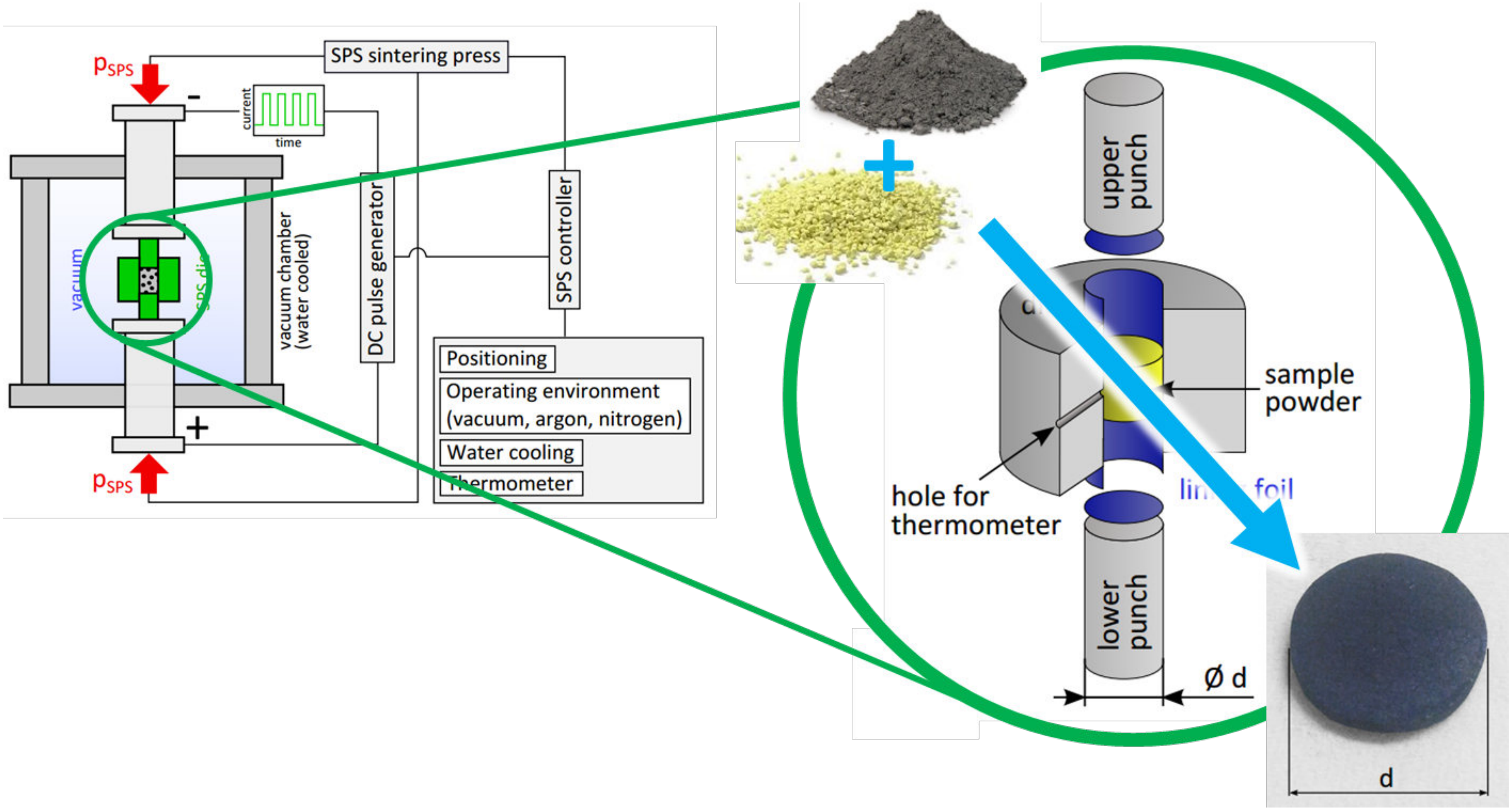

Courtesy: Dr. Ihor Veremchuk (HZDR)

SPS synthesis method

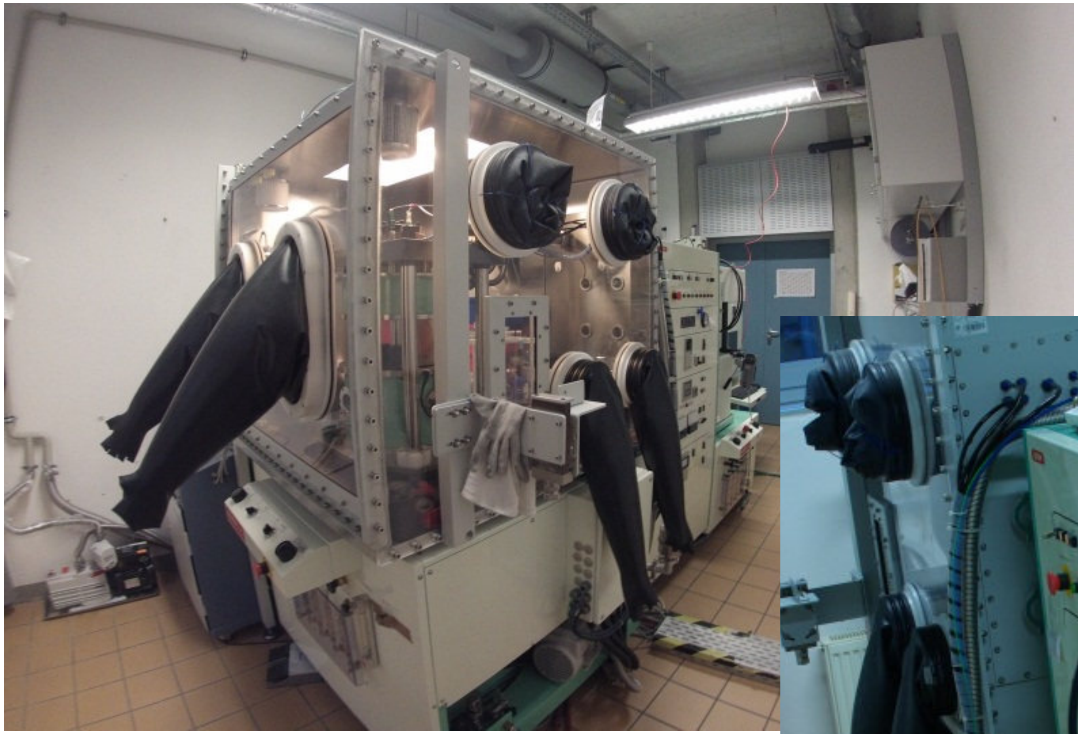

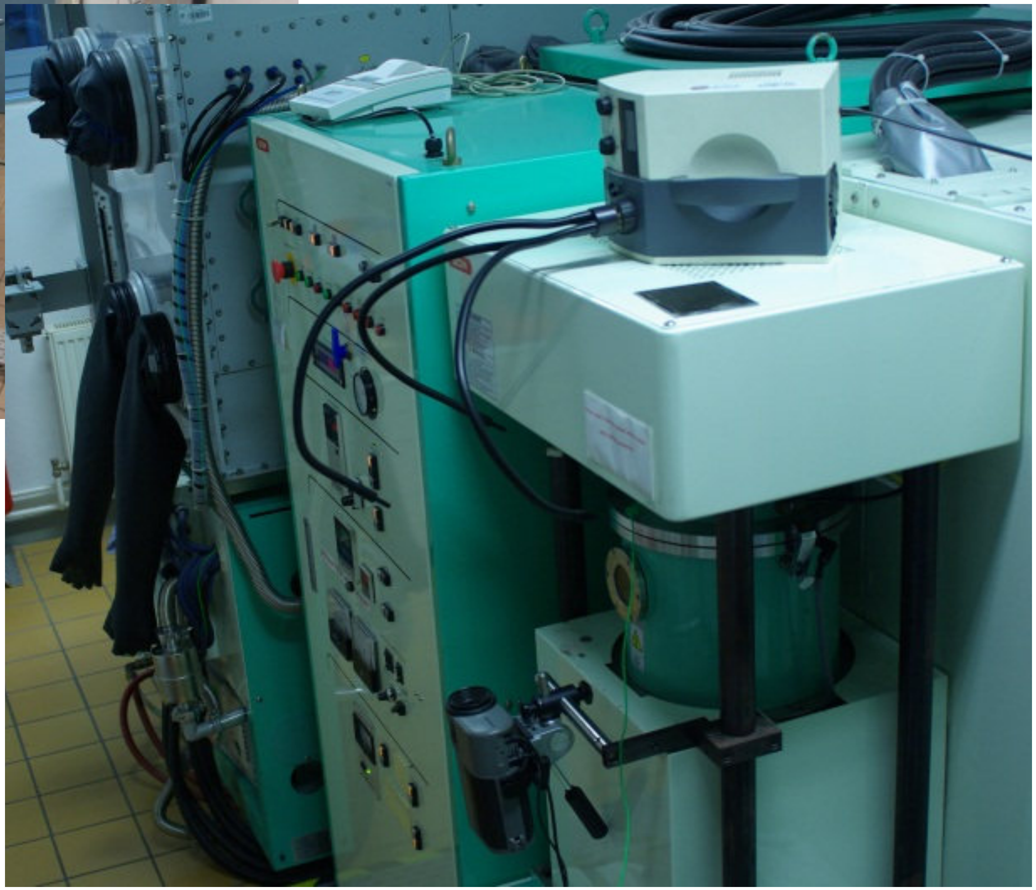

Dr. Ihor Veremchuk
at MPI CPfS Dresden

SPS synthesis method

Magnetism and magnetoelectricity of textured polycrystalline bulk Cr_2O_3 sintered in conditions far out of equilibrium

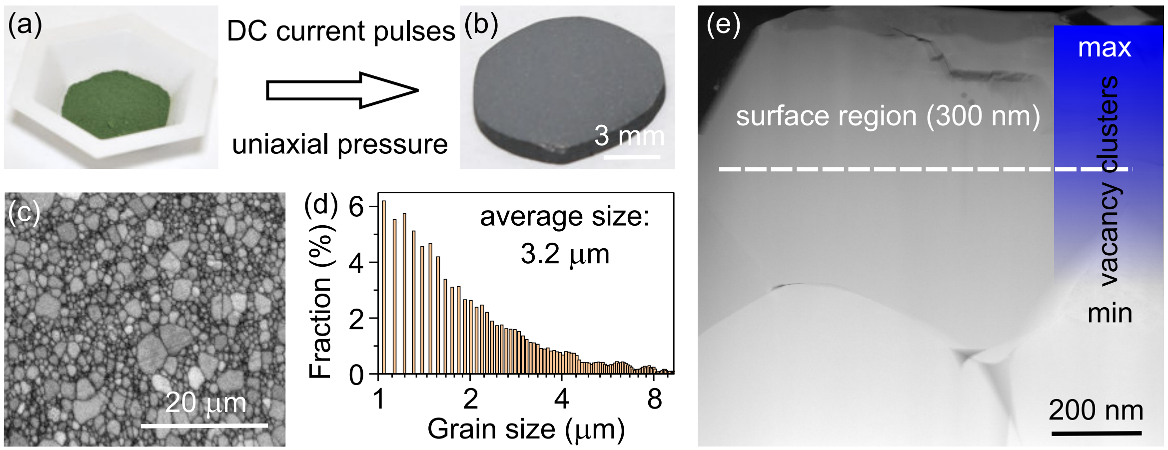

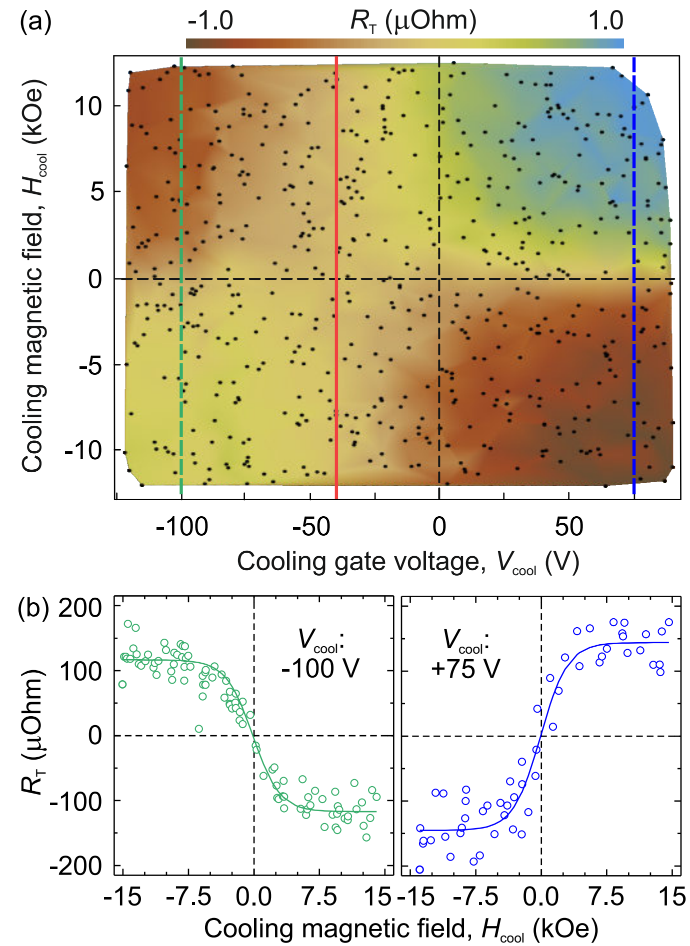

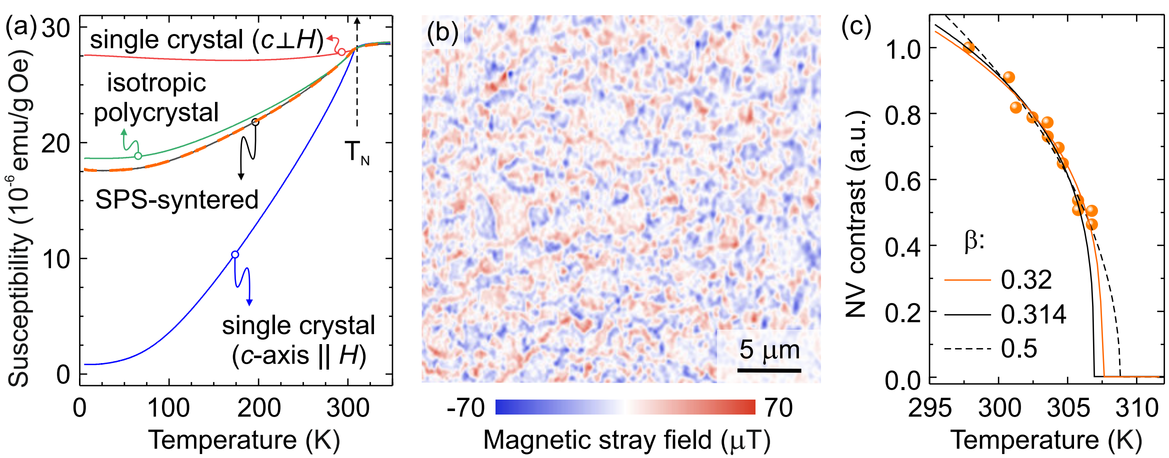

I. Veremchuk et al., ACS Appl. Electron. Mater. 4, 2943 (2022)

Top-down processes: Milling

Major industrial importance: High energy ball milling

Powders crushed mechanically in rotating drums (hard steel, tungsten carbide)

Milling under controlled atmospheric conditions (prevent unwanted oxidation)

Large reduction in grain size; mechanical cold welding and alloying of different compounds

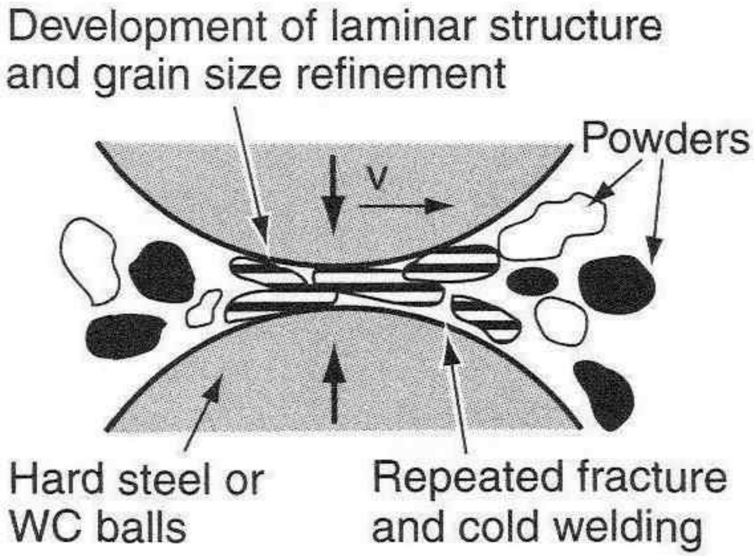

Figure 1.20 Schematic representation of the mechanical alloying process

Slide based on the lecture course at TU Chemnitz (with Prof. O. G. Schmidt)

Fabrication methods

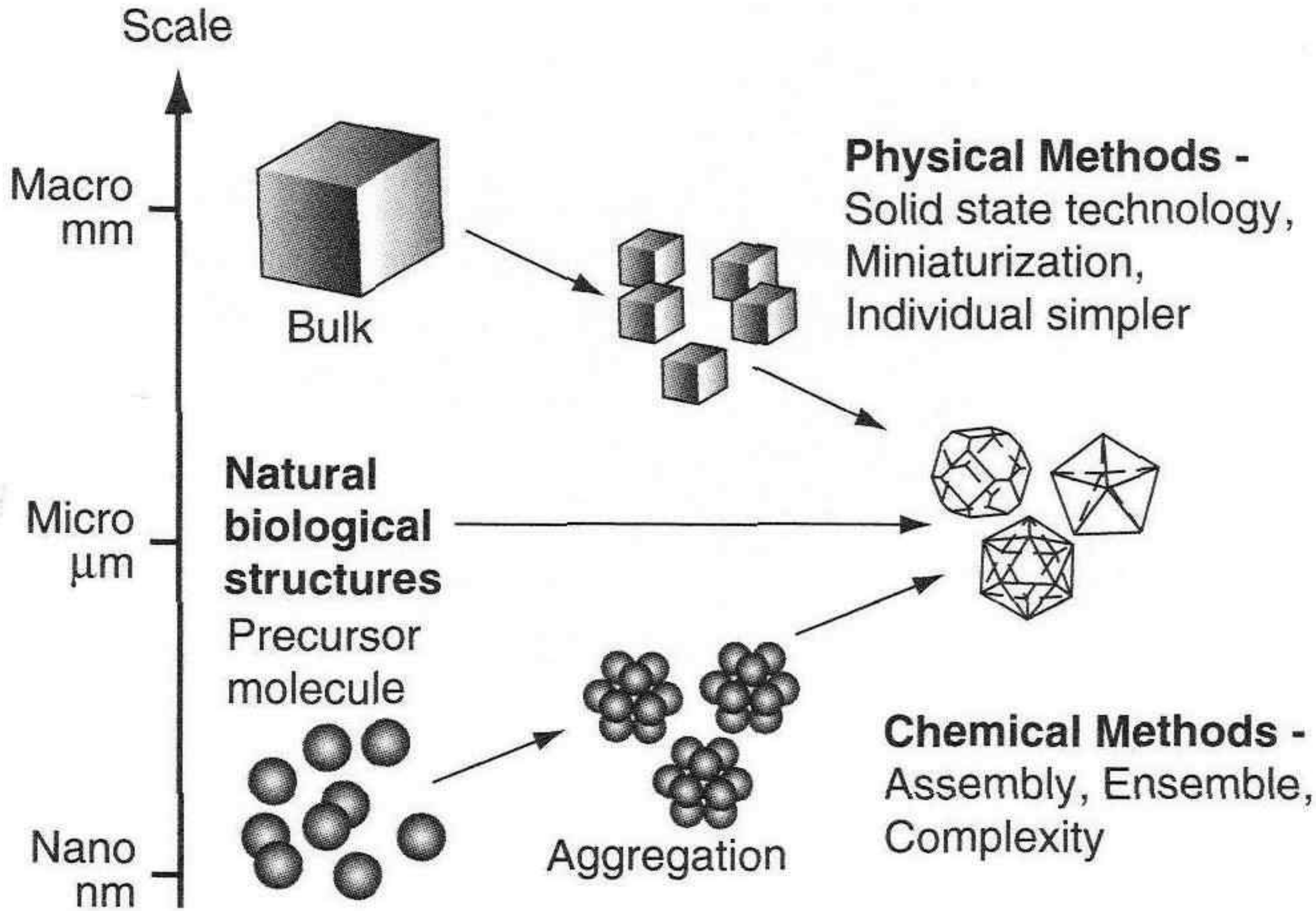

Figure 1.19 Schematic representation of the top-down and bottom-up processes and their relationship to biological processes and structures

Slide based on the lecture course at TU Chemnitz (with Prof. O. G. Schmidt)

„Top-Down“ and „Bottom-Up“ approach

„Top-Down“

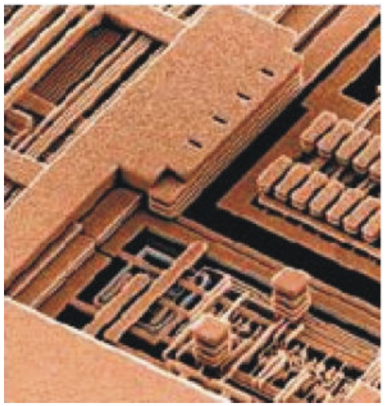

IBM

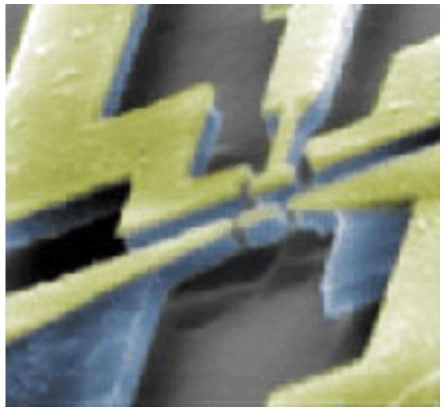

LMU, IBM, UC, SU, CU

Fabricating Nanostructures out of a macroscopic building block (e.g. Si substrate)

Advantages: Exact Addressing
→ Ultra-large scale integration

„Bottom-Up“ (Self-Organisation)

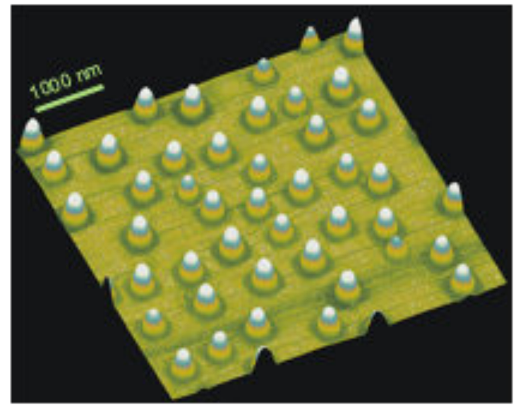

Quantum dots

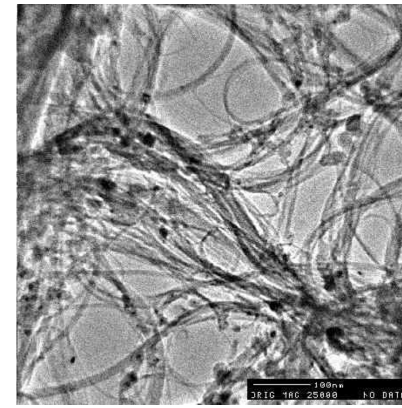

Carbon nanotubes, Delft

Atoms und Molecules self-assemble to form more complex structures

Pros: Self-formation
Complex Functionalities
But: Non-integrative

Slide based on the lecture course at TU Chemnitz (with Prof. O. G. Schmidt)

Dr. Denys Makarov I E-Mail: d.makarov@hzdr.de I Intelligent Materials and Systems

Bottom-up processes

- Vapour phase deposition methods

- Plasma-assisted deposition processes

- Molecular Beam Epitaxy and metal organic vapour phase epitaxy

- Liquid phase methods

- Colloidal methods

- Sol-gel methods

- Electro(chemical) deposition

Molecular Beam Epitaxy (MBE)

Epitaxis: From greek epi = “upon”; taxis = „ordered”

Atoms and molecules impinge on the surface of a heated crystalline substrate (e.g. Si or GaAs wafer) under ultra high vacuum conditions. They diffuse on the surface and finally become incorporated to form a crystalline deposit.

MBE is a physical deposition technique. The growth is limited by kinetic processes like, for example, adsorption, desorption, surface diffusion.

Characteristic properties of MBE:

- Low growth temperatures → non-thermodynamically stable state

- Powerful in-situ characterisation possible (RHEED)

- Controlled and atomically flat deposition

Slide based on the lecture course at TU Chemnitz (with Prof. O. G. Schmidt)

Molecular Beam Epitaxy (MBE)

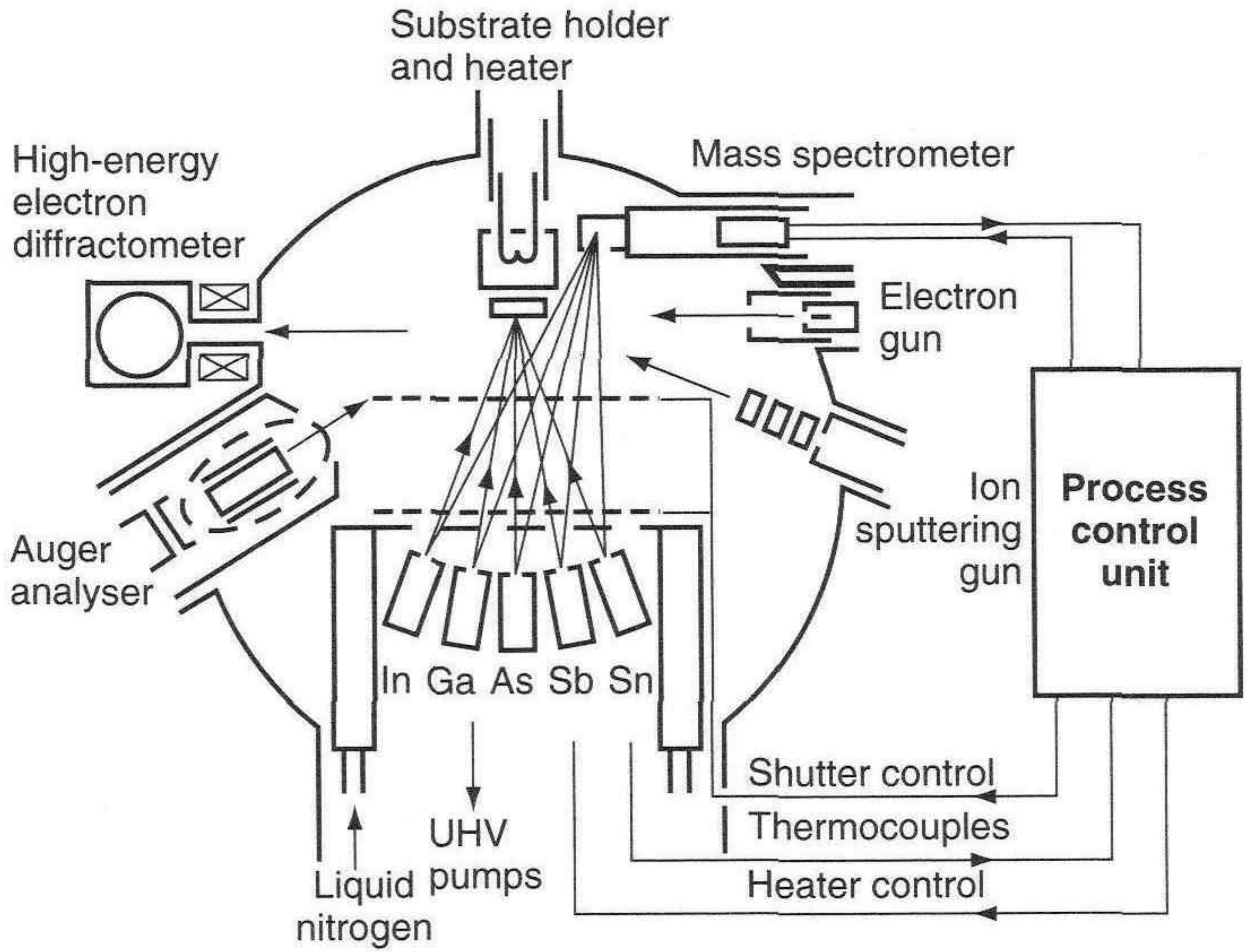

Schematic diagram of a molecular beam epitaxy thin film deposition system

Slide based on the lecture course at TU Chemnitz (with Prof. O. G. Schmidt)

Dr. Denys Makarov I E-Mail: d.makarov@hzdr.de I Intelligent Materials and Systems

Main chamber (many effusion cells) | Auxiliary chamber (annealing) | Load-lock chambers

Application: Production of quantum dots, quantum wells, 2D electron gas for lasers, quantum cascade lasers, quantum communication…

Slide based on the lecture course at TU Chemnitz (with Prof. O. G. Schmidt)

Growth modes (depending on the bond energy)

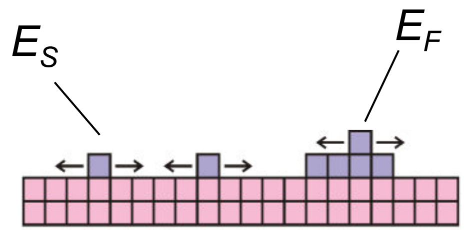

Layer-by-layer or Frank-van der Merwe (FM- mode)	Island or Volmer-Weber (VW-mode)	Layer-plus-island or Stranski-Krastanov (SK-mode)
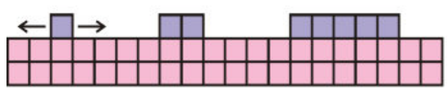	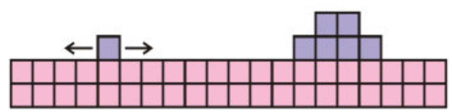	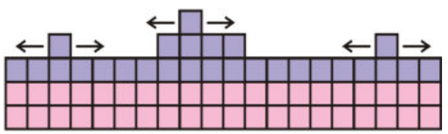
$E_S > E_F$	$E_S < E_F$	$E_S > E_F$
		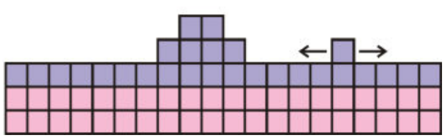
		$E_{F,n+1} > E_{F,n}$

E_S = Bond energy between substrate and adatoms

$E_{F,n}$ = Bond energy between the n^{th} epitaxial film layer and adatoms ($E_{F,1} = E_F$)

Wetting layer thickness of *n* monolayers.
e.g. $E_{F,n+1}$ increases due to strain relaxation.

Slide based on the lecture course at TU Chemnitz (with Prof. O. G. Schmidt)

Kinetic Monte Carlo (KMC) simulation

Rules

1. Atoms are randomly deposited at a rate F (ML/s).
2. All atoms on the surface can diffuse (hop) at the rate:

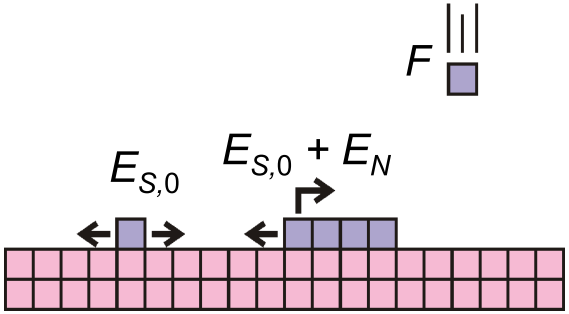

$$\boxed{R_n = (2k_B T/h)\exp(-(E_{S,0} + n\cdot E_N)/k_B T)}$$

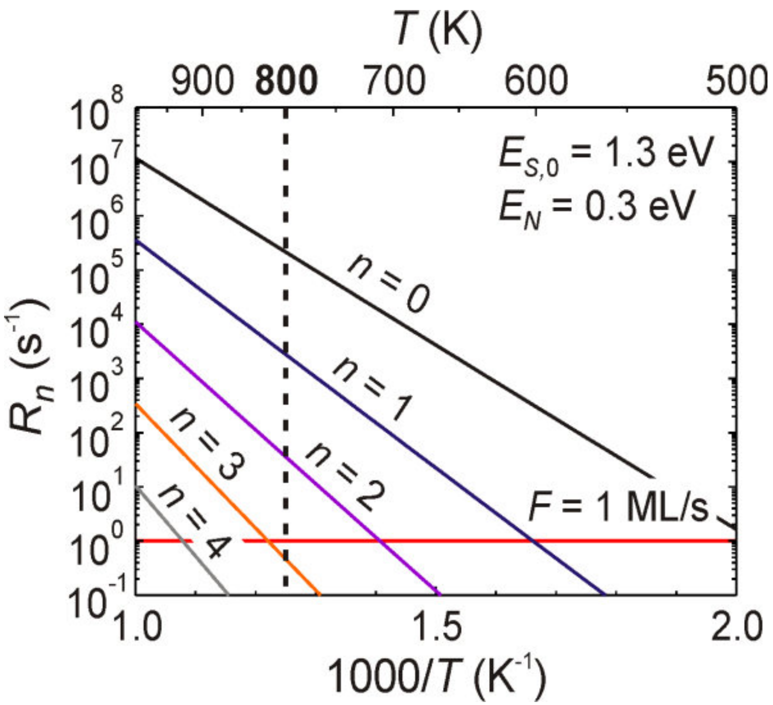

k_B : Boltzmann constant (1.38×10^{-23} J K^{-1})

T : Temperature

h : Planck constant (6.626×10^{-34} J s)

$E_{S,0}$: surface bond energy (without strain)

n : number of the nearest neighbor atoms

E_N : lateral nearest neighbor bond energy

ML: monolayer (here: atomic layer)

Adatom can hop 10^4 – 10^7 times before the next atom hits the surface

Slide based on the lecture course at TU Chemnitz (with Prof. O. G. Schmidt)

KMC simulation result: Surface morphology evolution

2D island growth in layer-by-layer growth mode

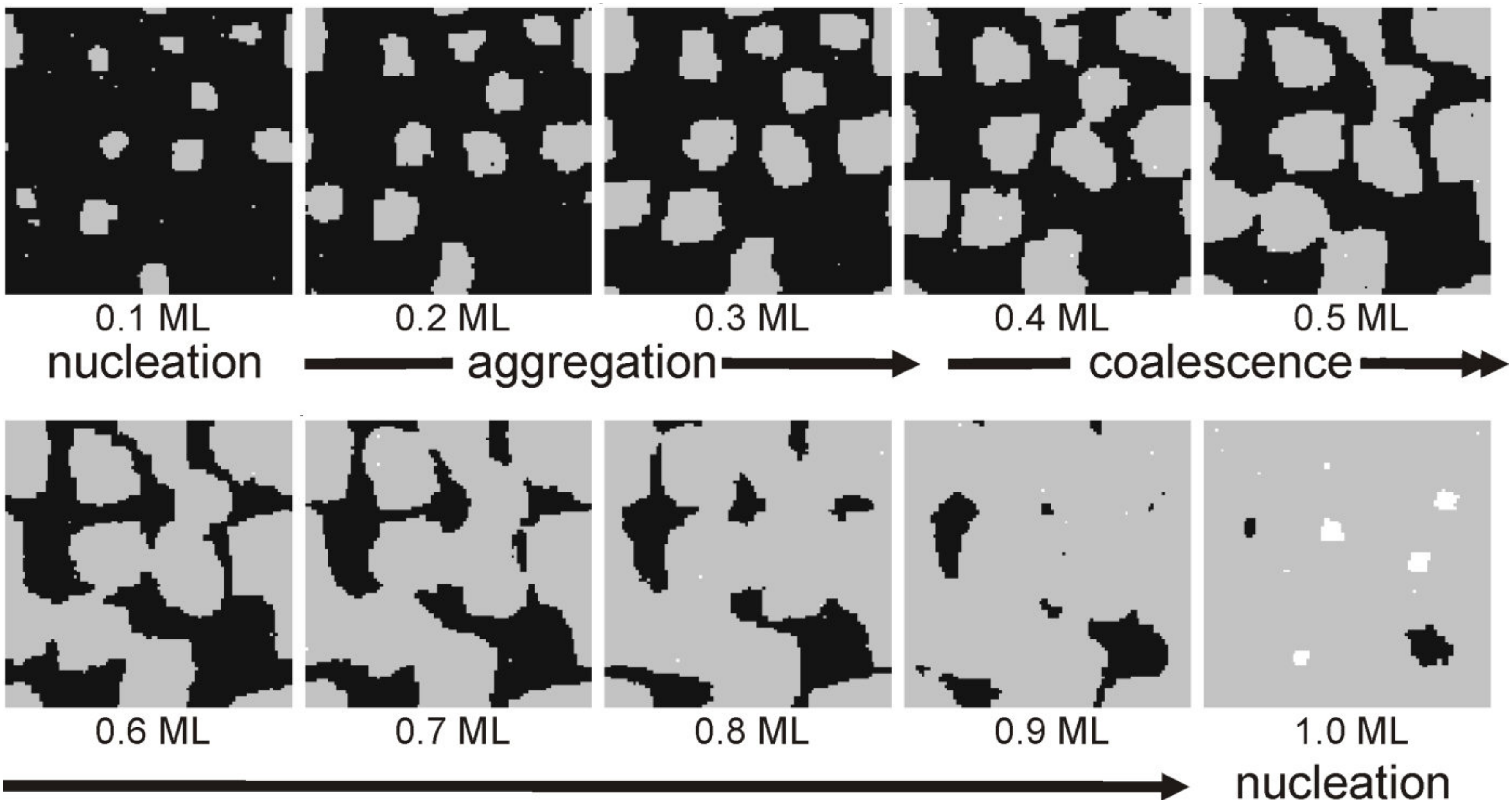

Slide based on the lecture course at TU Chemnitz (with Prof. O. G. Schmidt)

Lattice mismatch

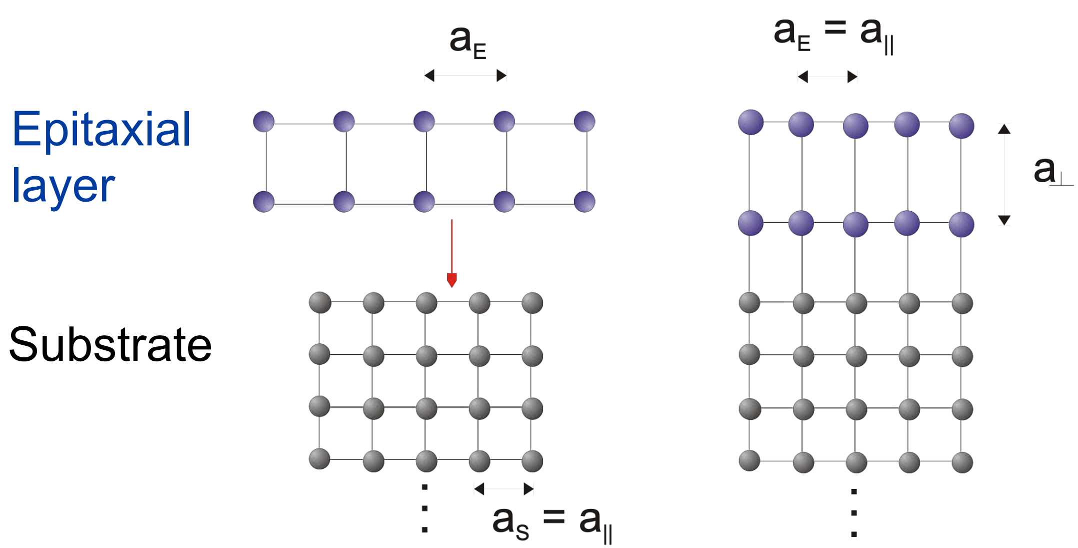

Pseudomorphic growth

Lattice mismatch for cubic crystals: $\mathbf{f = (a_S - a_E)/a_E}$ In-plane strain: $\varepsilon_{||} = \mathbf{(a_S - a_E)/a_E}$

Tetragonal strain: $\varepsilon_\perp = \xi\varepsilon_{||} = \mathbf{-2C_{12}/C_{11}}\varepsilon_{||}$ with C_{11}, C_{12} elasticity constants

$\varepsilon_{||} > 0$: tensile strain $\varepsilon_{||} < 0$: compressive strain

Example: $a_{Si} = 0.5431$ nm $a_{Ge} = 0.5657$ nm

Ge epitaxial layer pseudomorphically grown on Si experiences compressive strain of -4.0 %

Slide based on the lecture course at TU Chemnitz (with Prof. O. G. Schmidt)

Critical thickness for dislocation nucleation

The layer thickness,
beyond which dislocation
nucleation sets in,
Is defined as the

**„critical
thickness for dislocation
nucleation“**

(not to be confused with
the critical thickness for
island formation).

Thermodynamic model
knows three regimes:

I. Stable regime
II. Metastabe regime
III. Plastically relaxed regime

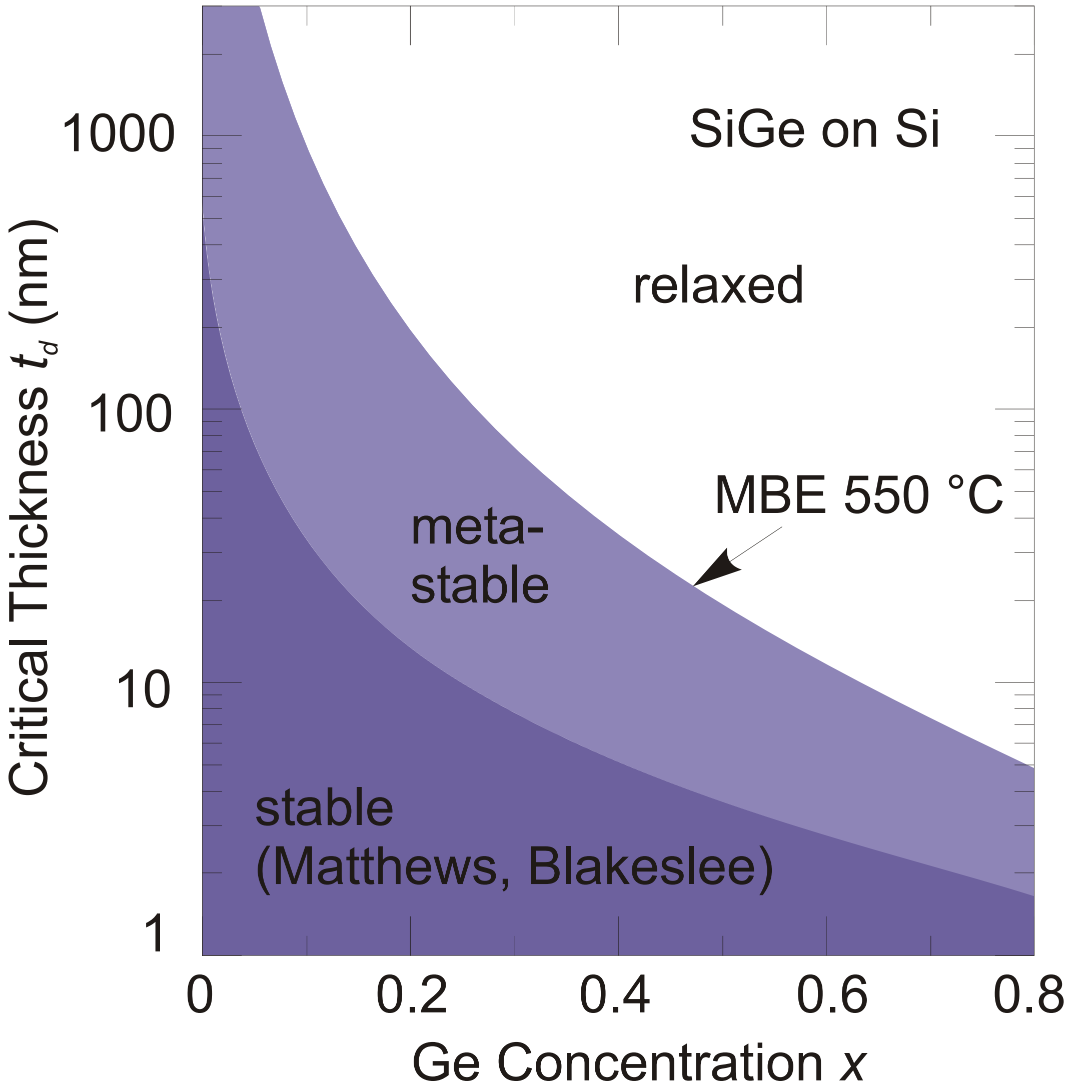

Slide based on the lecture course at TU Chemnitz (with Prof. O. G. Schmidt)

Thin films of Cr_2O_3 with a strain gradient

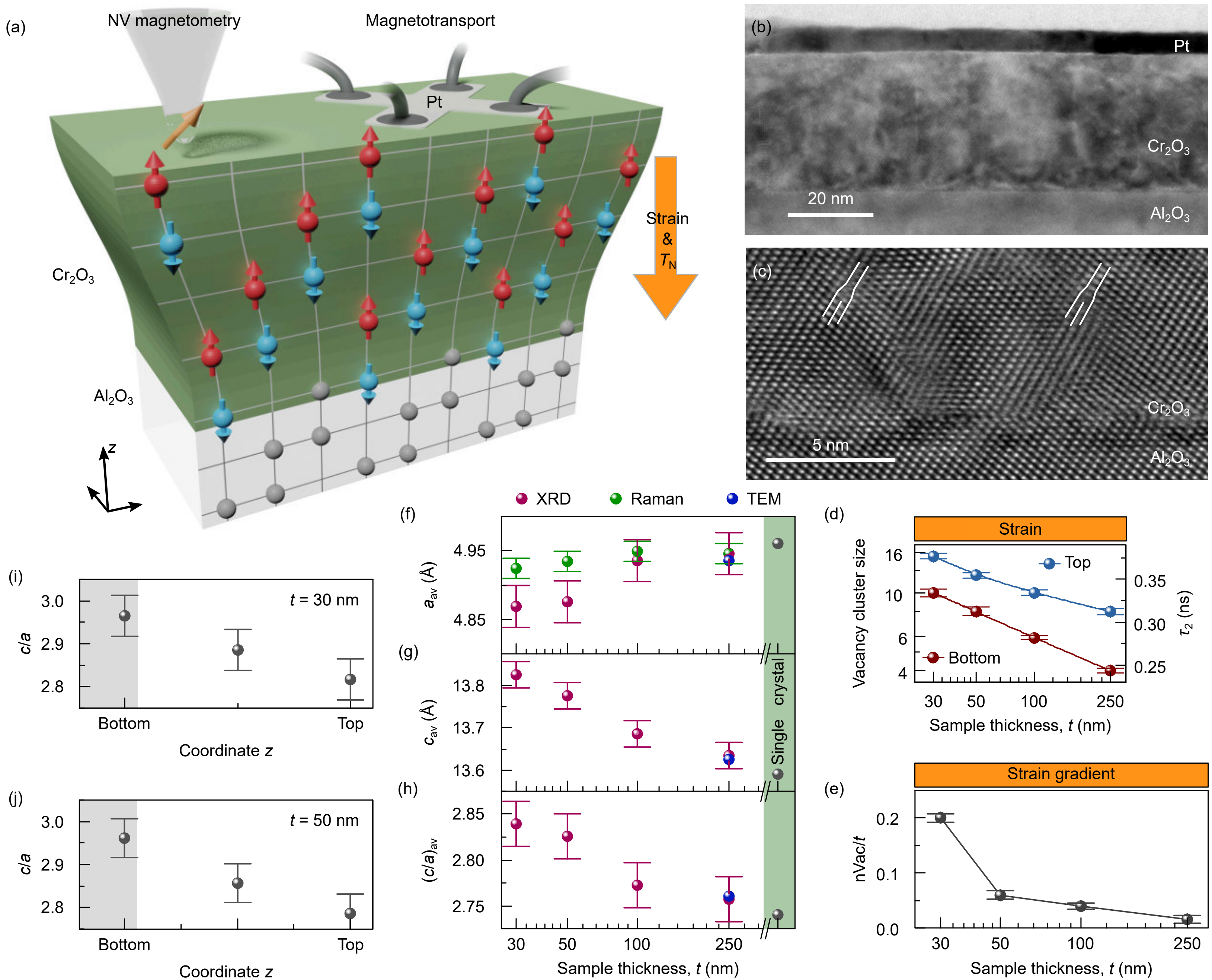

P. Makushko et al., *Nature Commun.* **13**, 6745 (2022)

Strain properties of a 30-nm-thick Cr_2O_3 thin film

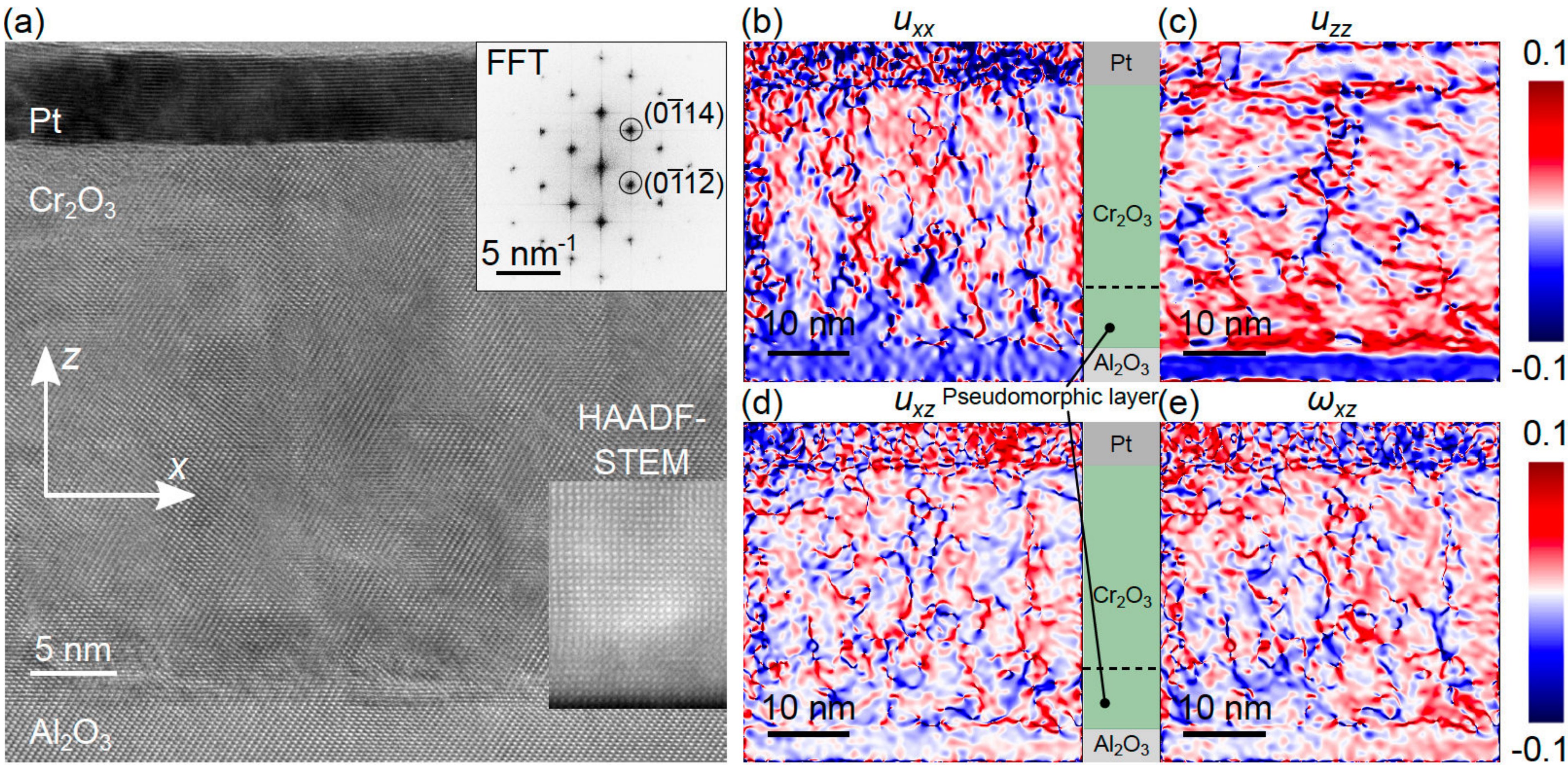

P. Makushko et al., *Nature Commun*. **13**, 6745 (2022)

Strain properties of a 30-nm-thick Cr_2O_3 thin film

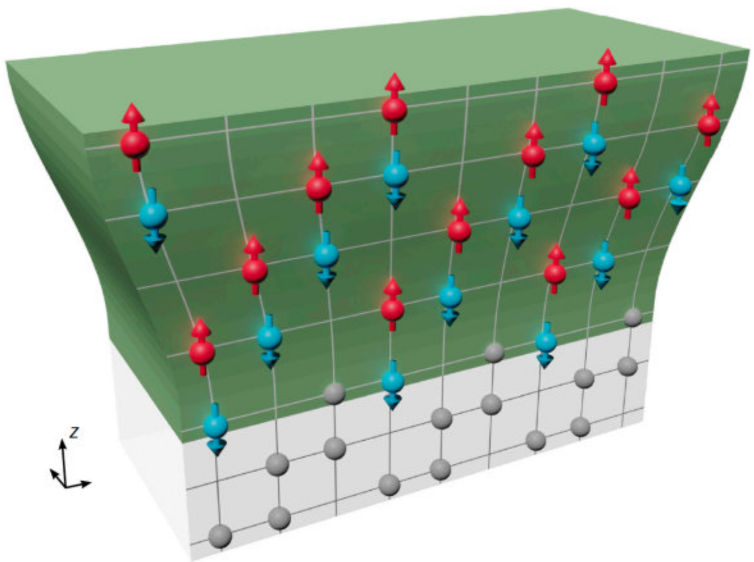

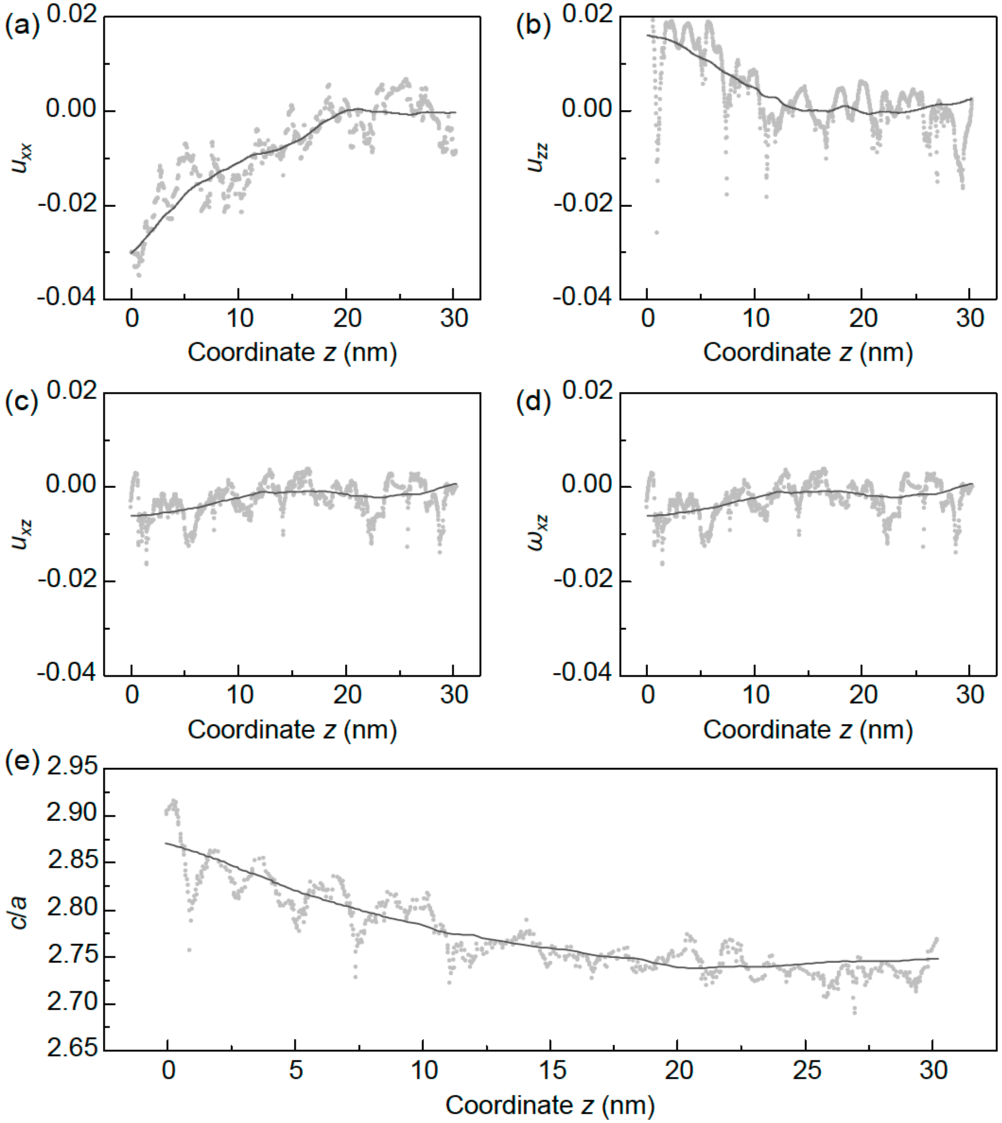

P. Makushko et al., *Nature Commun*. **13**, 6745 (2022)

Magnetization of Cr_2O_3 thin films

Source	Thickness, nm	Strain	Temperature	Value, $\mu_B\,\mathrm{nm}^{-2}$	Ref.
Uncompensated surface spins	200	–	$0.96T/T_N$	2.14 ± 1.5	[2]
	Single crystal	–	$0.98T/T_N$	2.2	[30]
	Single crystal	–	$0.96T/T_N$	2.3	[58]
Dislocations	200	✓	$0.95T/T_N$	0.455 ± 0.28	[1]
Flexomagnetism, Eq. (S26)	30	✓	$O(10^2\,\mathrm{K})$	0.65	This work
	50	✓	$O(10^2\,\mathrm{K})$	0.72	
Dzyaloshinskii-like [60, 61]	t	–	$\ll T_N$	$\sim 0.01t$	
Thermally induced, Eq. (S30)	$30\ldots50$	✓	T_N^{top}	~ 2	

Dzyaloshinskii-like mechanism (magnetization is induced at a non-collinear texture)

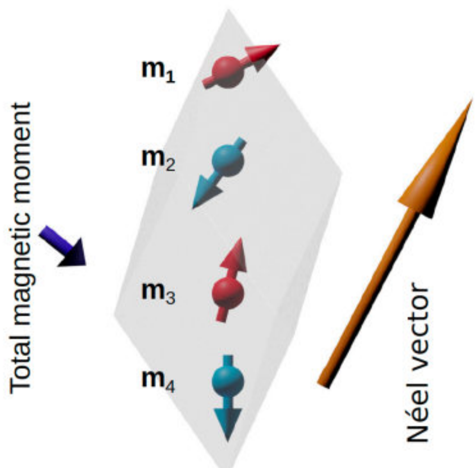

Flexomagnetism of the inhomogeneously strained thin films

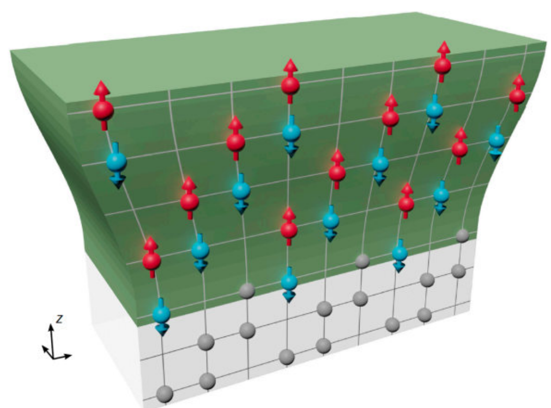

Ferromagnetism, induced by the inhomogeneous thermal reduction of the sublattice magnetization

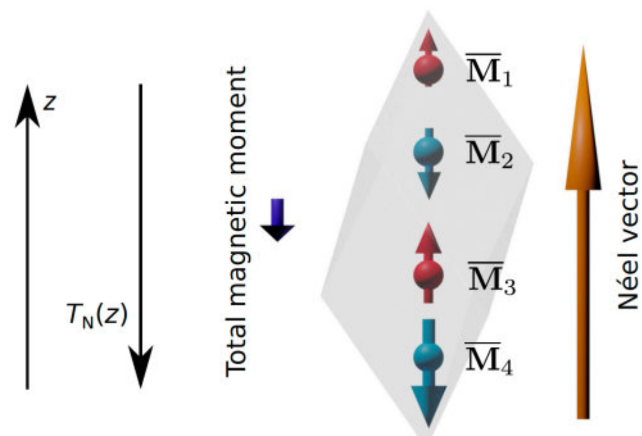

P. Makushko et al., *Nature Commun*. **13**, 6745 (2022)

Strain compensation

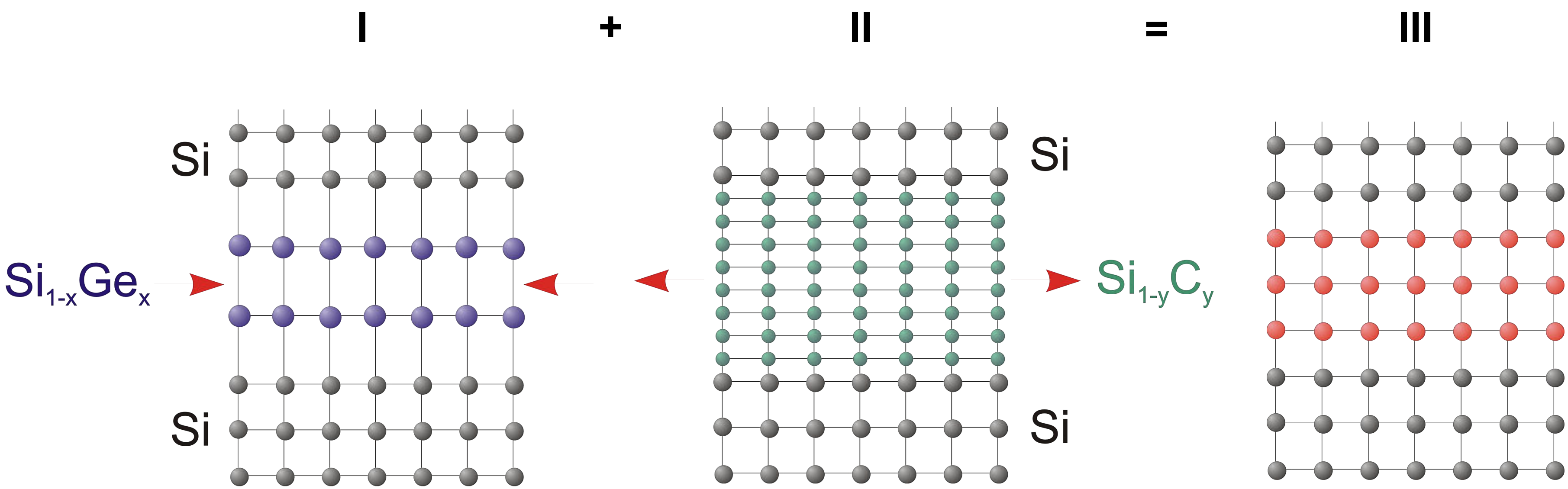

Compressively strained

Tensile strained

Exactly strain compensated

$Si_{1-x-y}Ge_xC_y$ at $\frac{x}{y} = 10$

Slide based on the lecture course at TU Chemnitz (with Prof. O. G. Schmidt)

Lithography

Lithographic processes

Most important steps for lateral structuring:

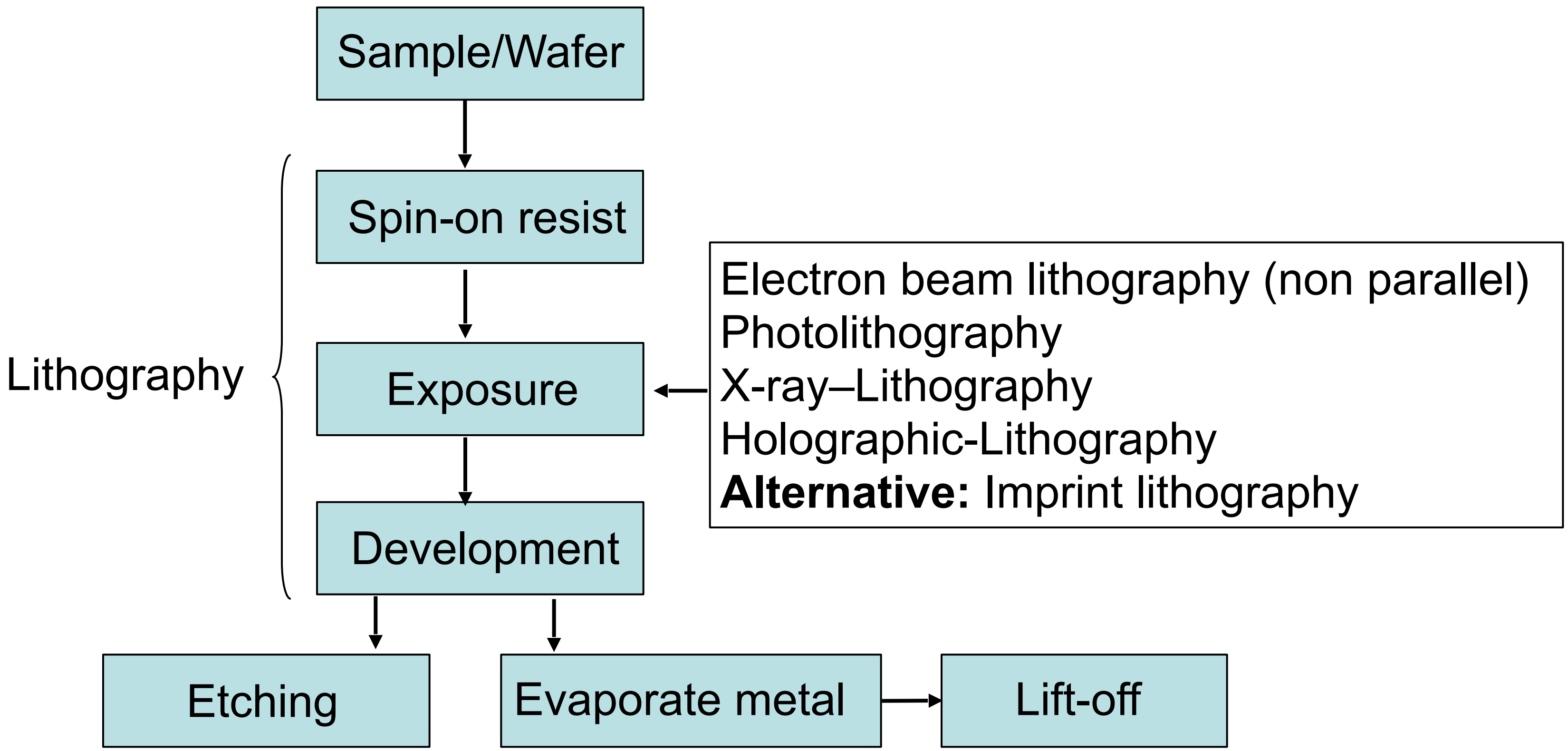

Block diagram can be followed through many times

Slide based on the lecture course at TU Chemnitz (with Prof. O. G. Schmidt)

Spin-on resist

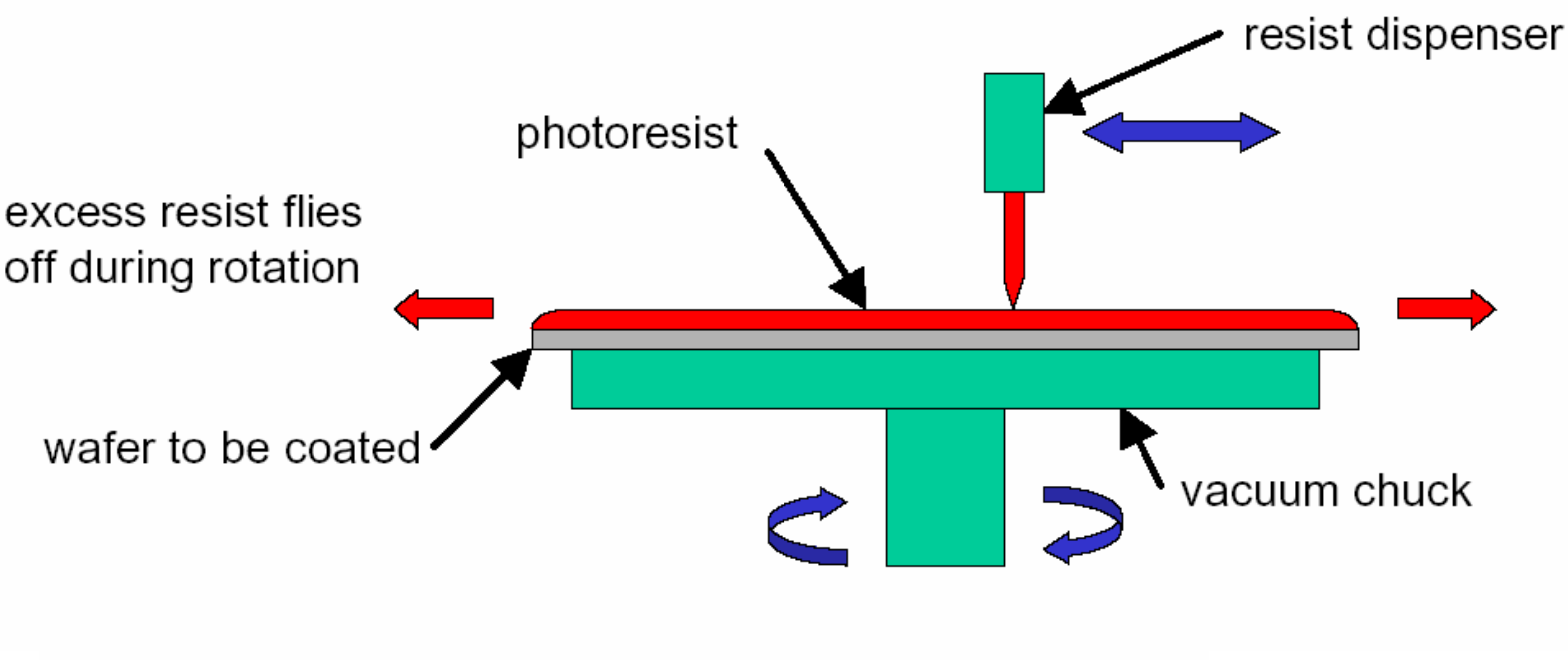

Thickness of PR $$t := K \cdot S \cdot \left(\frac{\nu}{\omega^2 \cdot R^2} \right)^{\frac{1}{3}}$$

t = thickness
K = constant
S= fraction of solids
υ= viscosity
ω= angular velocity
R = radius

Slide based on the lecture course at TU Chemnitz (with Prof. O. G. Schmidt)

Electron beam lithography

Smallest feature size: about 5 nm

Advantage:
Arbitrary geometries possible
Direct writing, no mask required

Disadvantage:
Long exposure times (can be days)
→ typically only small patterns possible (100 x 100 μm^2)

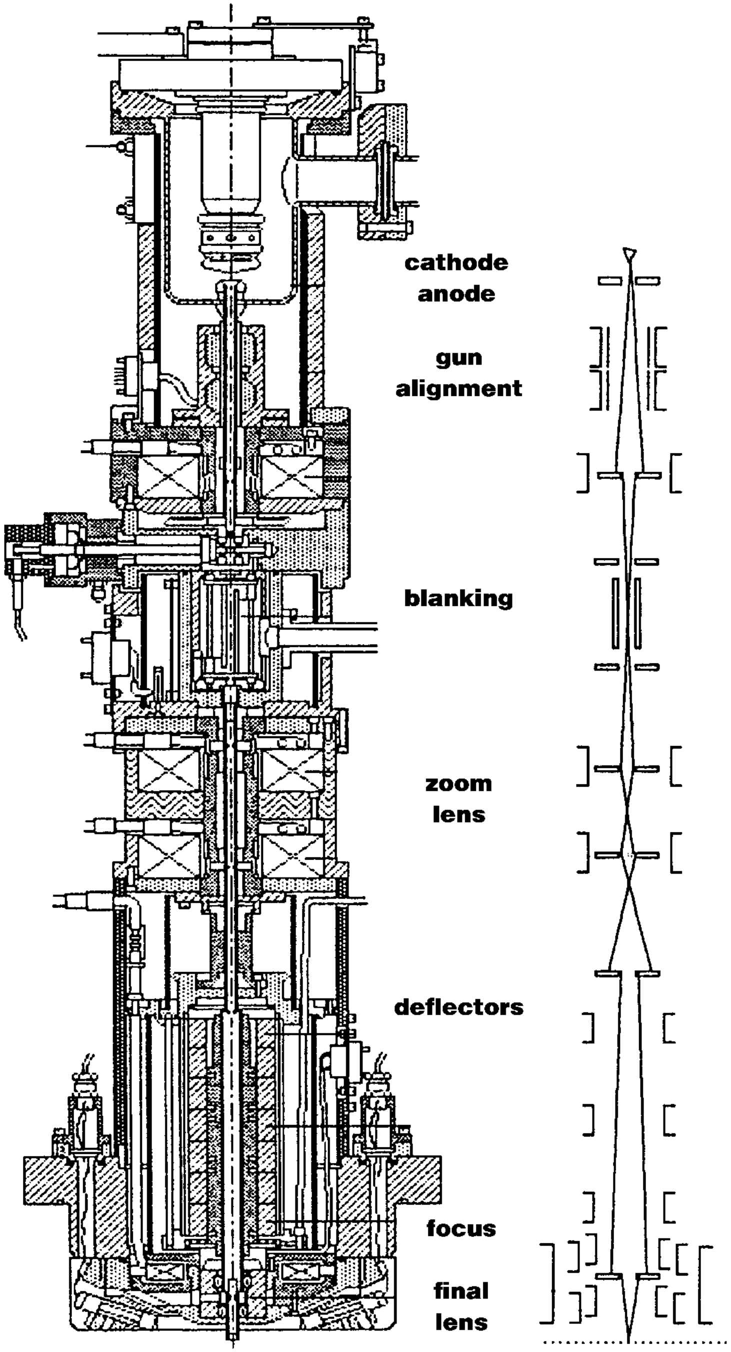

Slide based on the lecture course at TU Chemnitz (with Prof. O. G. Schmidt)

Dr. Denys Makarov I E-Mail: d.makarov@hzdr.de I Intelligent Materials and Systems

Photolithography

- Dominant method in industrial production

- Ultra-violet light (lamp/laser) passes through a mask and exposes a pattern in the resist on the wafer.

- In contact lithography the mask is in contact with the wafer. For more refined lithography additional optics are used to project the mask pattern on the wafer.

- The mask consists of a structured metal coating, which is applied to a quartz substrate. The metal coating can be structured by for example electron beam lithography.

- Once the mask is fabricated, large area complex structures can be defined on a wafer in very short times (seconds). Optical lithography therefore allows a high throughput of processed wafers.

Slide based on the lecture course at TU Chemnitz (with Prof. O. G. Schmidt)

Photolithography

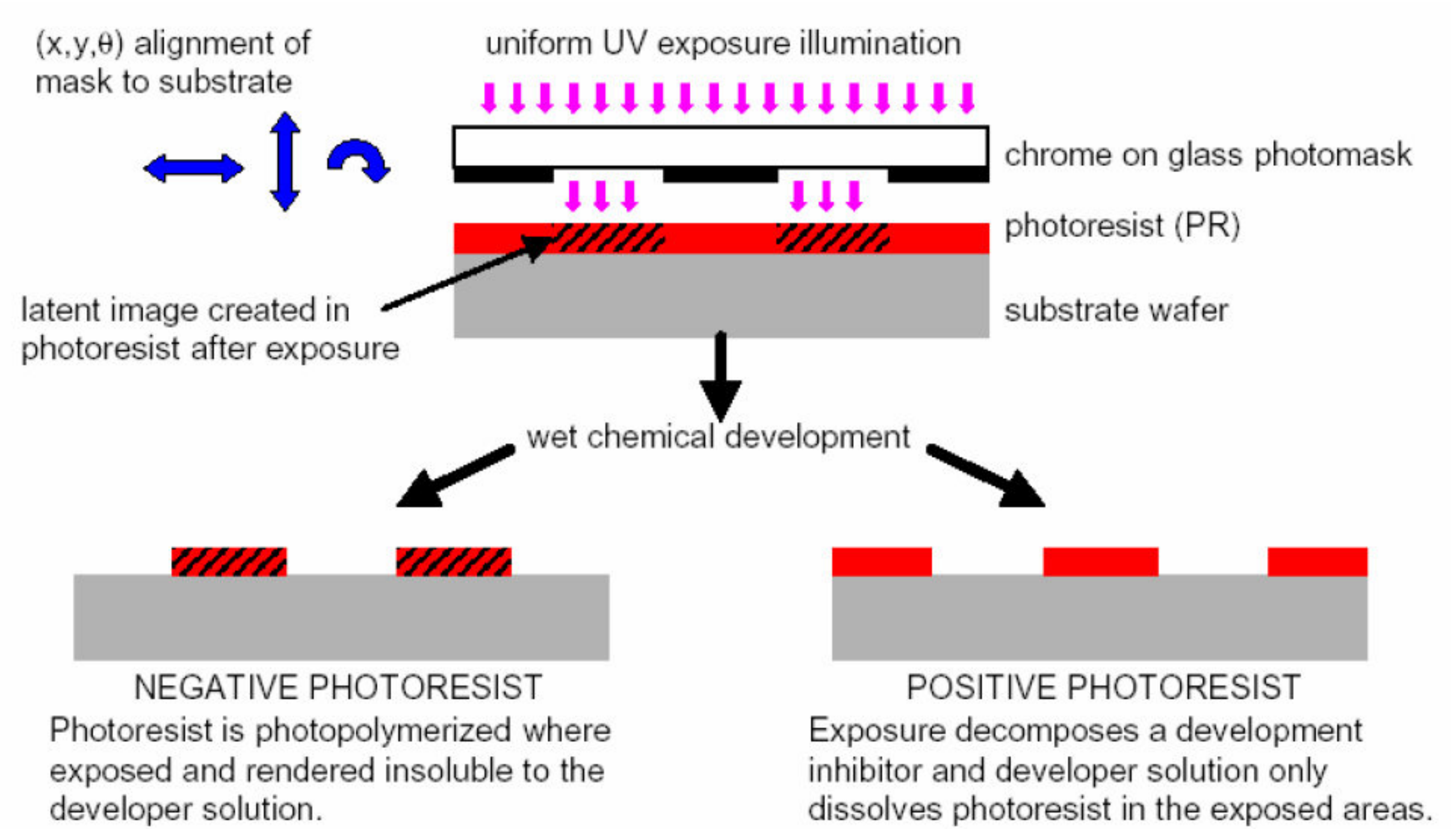

Slide based on the lecture course at TU Chemnitz (with Prof. O. G. Schmidt)

Challenge of optical lithography

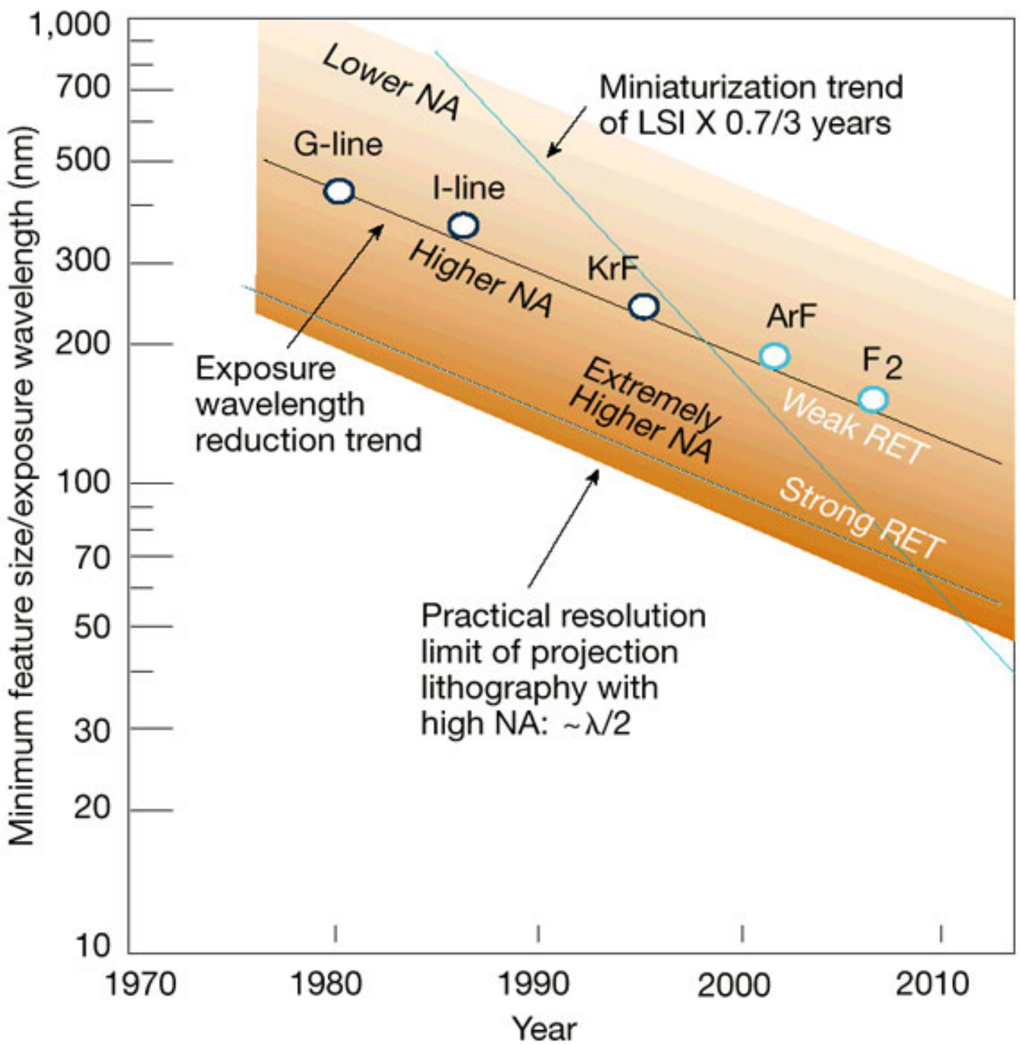

LSI : Large scale integration
NA : Numerical aperture
RET: resolution enhanced techniques

T. Ito et al., Nature 406, 1027 (2002)

Since 1998, the feature size is smaller than the wavelength of the exposure light.

Resolution is limited by **λ/NA k;** λ: wavelength, Numerical aperture, k: equipment dependent factor

Slide based on the lecture course at TU Chemnitz (with Prof. O. G. Schmidt)

To improve resolution, either the used wavelength needs to be reduced or complex phase shifting masks (PSMs) need to be developed. Clever mask design is required to correct proximity effects.

Resolution enhanced technique: Phase shifting mask (PSM)

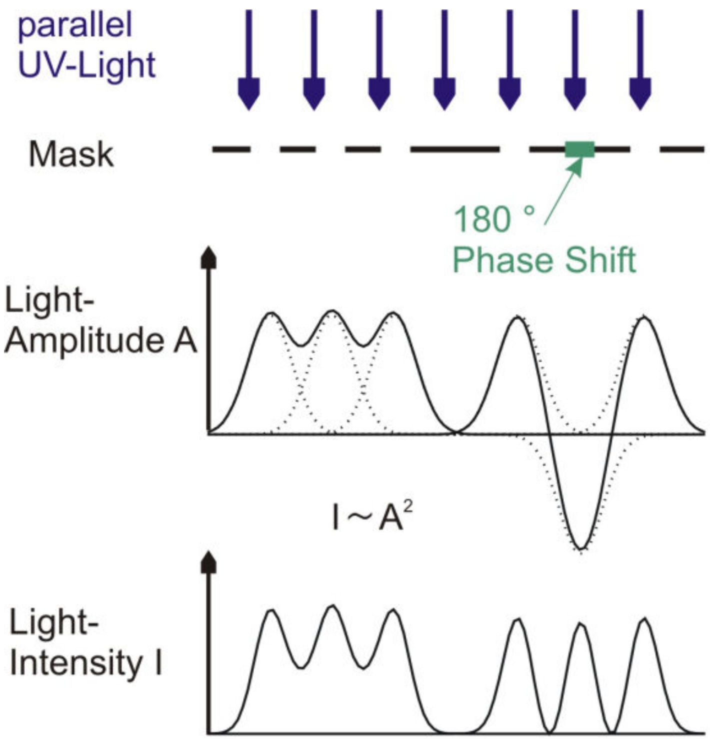

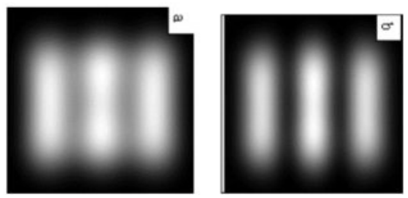

Optical proximity Correction (OPC)

Layout

Mask pattern

Wafer image

Slide based on the lecture course at TU Chemnitz (with Prof. O. G. Schmidt)

Extreme Ultraviolet Lithography (EUV)

- A laser-produced plasma or synchrotron radiation serves as the source of EUV (about 14 nm)

- A mask is produced by patterning an absorber material deposited on a multilayer coated silicon or glass mask blank.

Advantages:

- Extending minimum line width without throughput loss

Disadvantages:

- EUV is strongly absorbed in all materials, therefore the lithography process must be performed in vacuum

- Completely new development of mirror optics necessary

- Mask fabrication is difficult

Leading company for these devices: ASML (NL)

Slide based on the lecture course at TU Chemnitz (with Prof. O. G. Schmidt)

Extreme Ultraviolet Lithography (EUV)

Schematic set-up of EUV using mirror optics

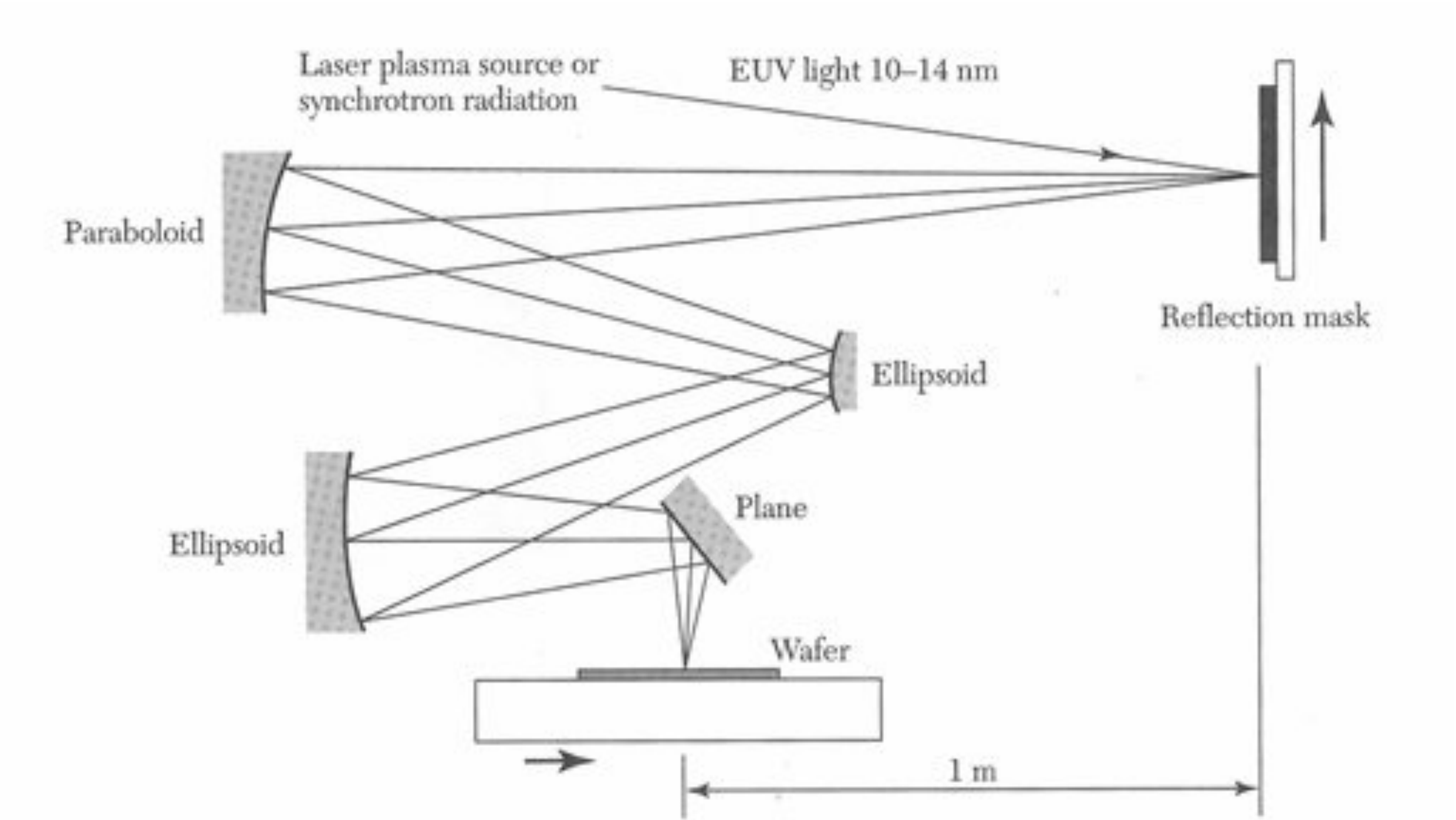

Slide based on the lecture course at TU Chemnitz (with Prof. O. G. Schmidt)

Nano-imprint lithography (NIL)

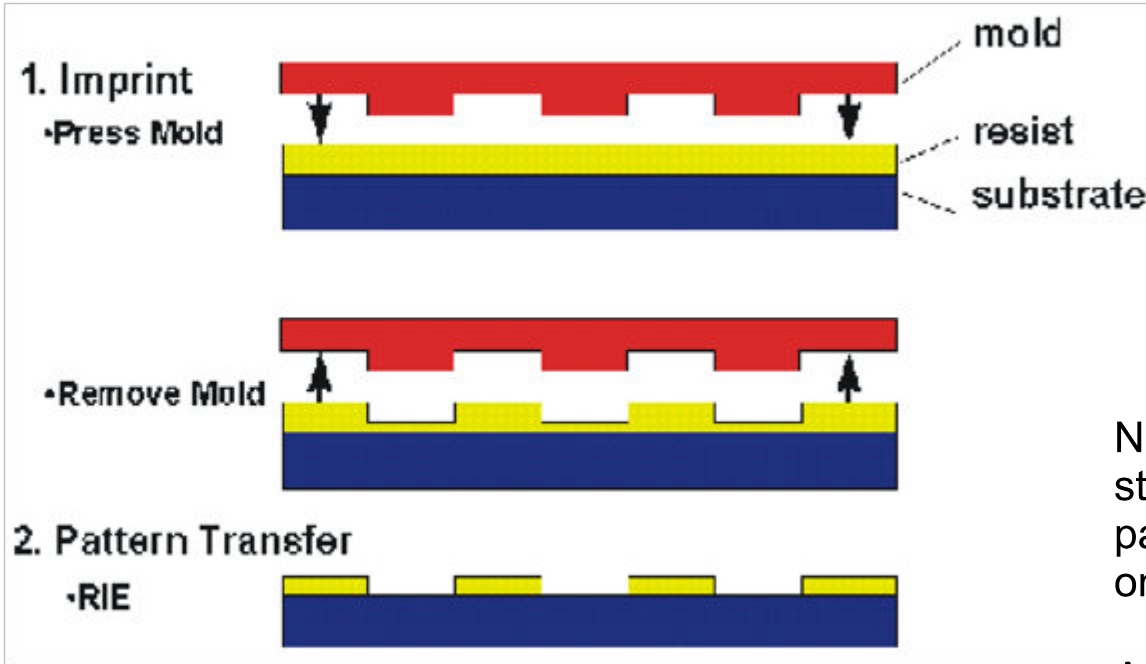

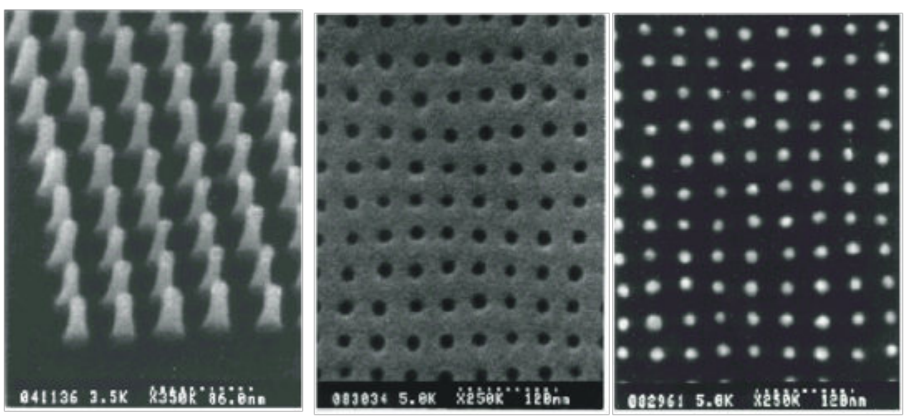

Nanoimprint Lithography structures a resist by pressing a patterned mold into a resist film on a substrate surface.

A chemical development of the resist is not required.

After empossing, the pattern is transferred into the substrate by etching techniques.

Feature sizes: 10 nm

Slide based on the lecture course at TU Chemnitz (with Prof. O. G. Schmidt)

Ultra-fast nano-imprint lithography

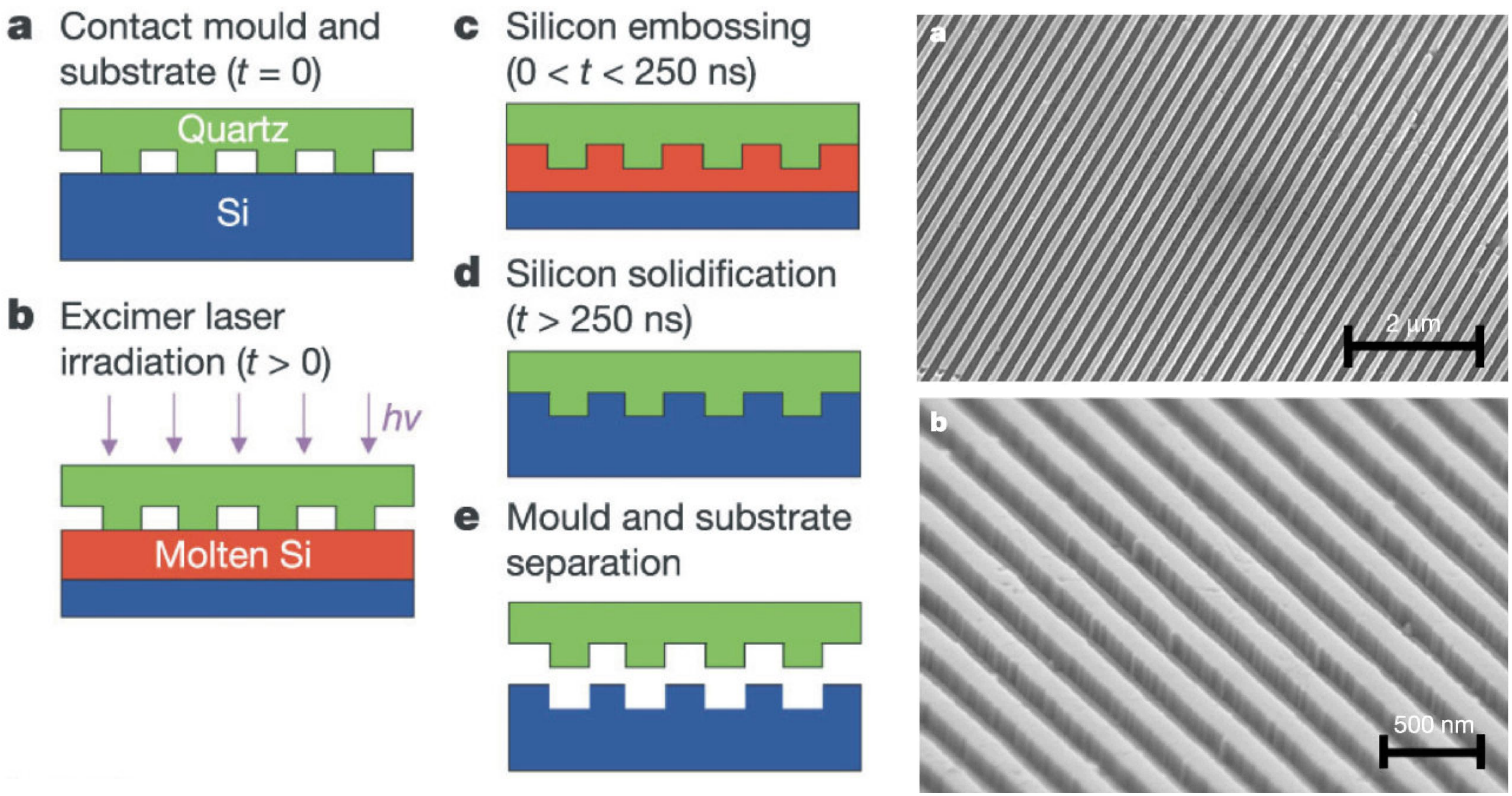

S. Y. Chu et al., Nature 417, 835 (2002)

Advantage of NIL: Parallel process, high throughput

Disadvantage: Overlay accuracy, limited feature size flexibility

Slide based on the lecture course at TU Chemnitz (with Prof. O. G. Schmidt)

Etching techniques

- Wet chemical etching
For structures in the sub-micrometer range wet-chemical etching is not well-suited because of a pronounced underetching effect (isotropic etching)

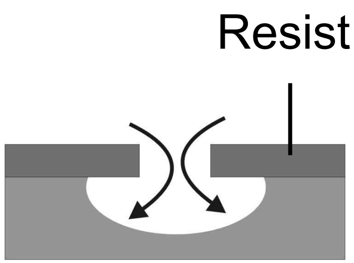

- Physical etching
Ion beam etching; positively charge Ar^+ ions are accelerated onto the sample surface and remove material from the sample.
High anisotropy, but small selectivity: resist and sample material experience similar etching rates
Produces extended crystal damage

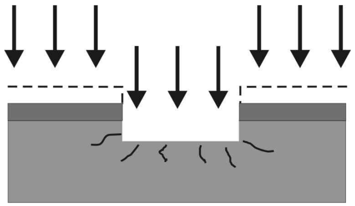

- Reactive ion etching
Gas discharge produces heavy ions in etching gas (e.g. $SiCl_4$), which are accelerated onto the sample surface, where they chemically and physically etch the sample
High selectivitiy (10:1), good anisotropy

Slide based on the lecture course at TU Chemnitz (with Prof. O. G. Schmidt)

Lift-off process for pattern transfer

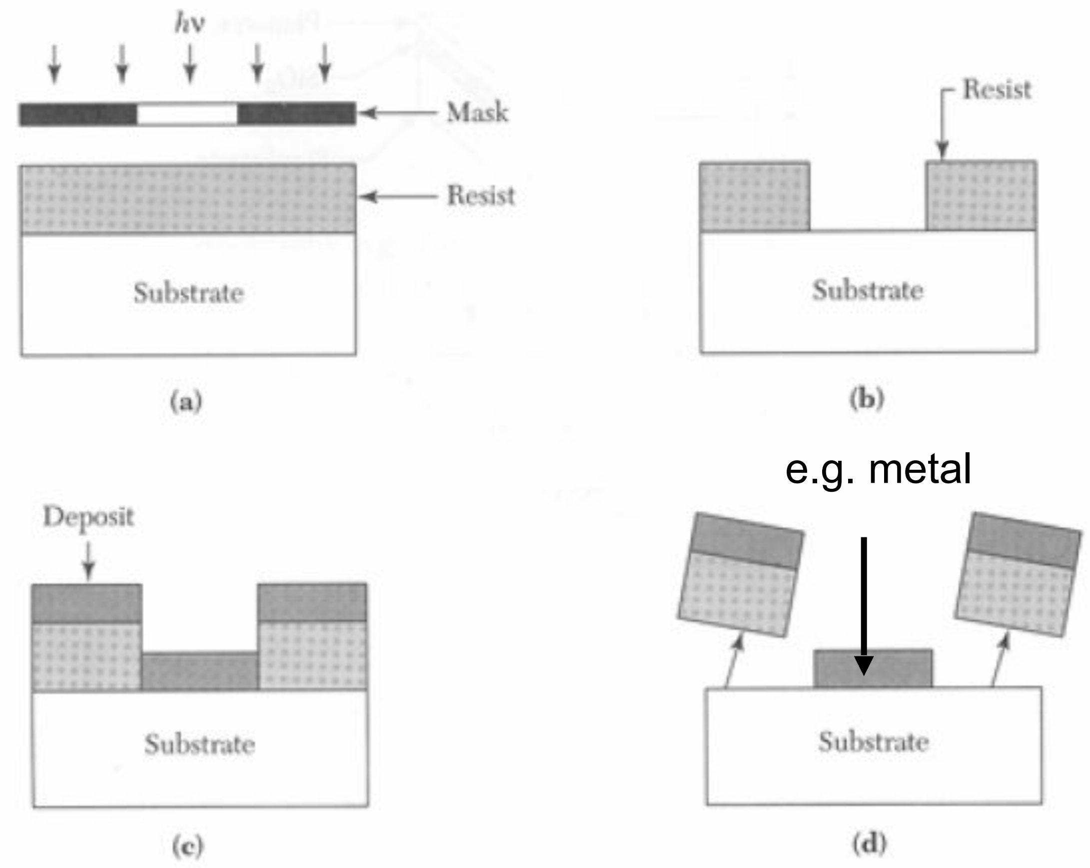

- Film thickness must be smaller than that of the resist
- Film on the resist is removed by selectively dissolving the resist layer in an appropriate liquid etchant

Slide based on the lecture course at TU Chemnitz (with Prof. O. G. Schmidt)

Magnetic nanostructures

Magnetic data storage

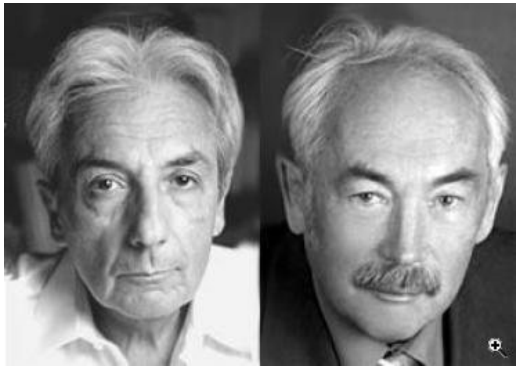

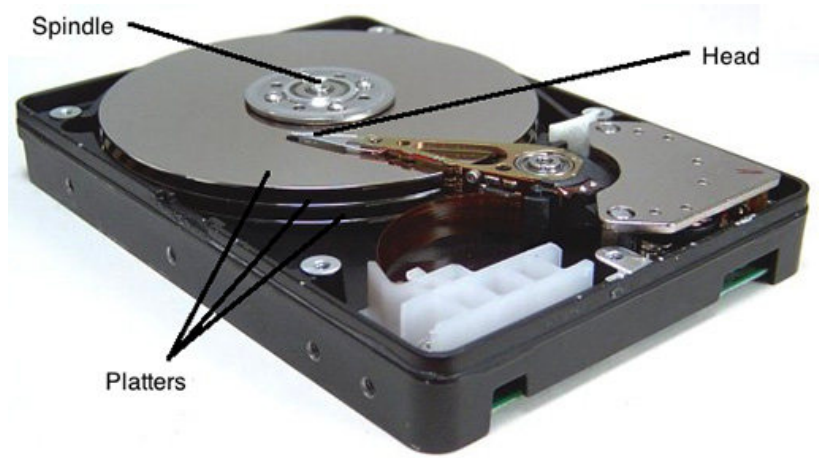

https://www.open.edu/openlearn/science-maths-technology/computing-ict/introducing-computing-and-it/content-section-5.1

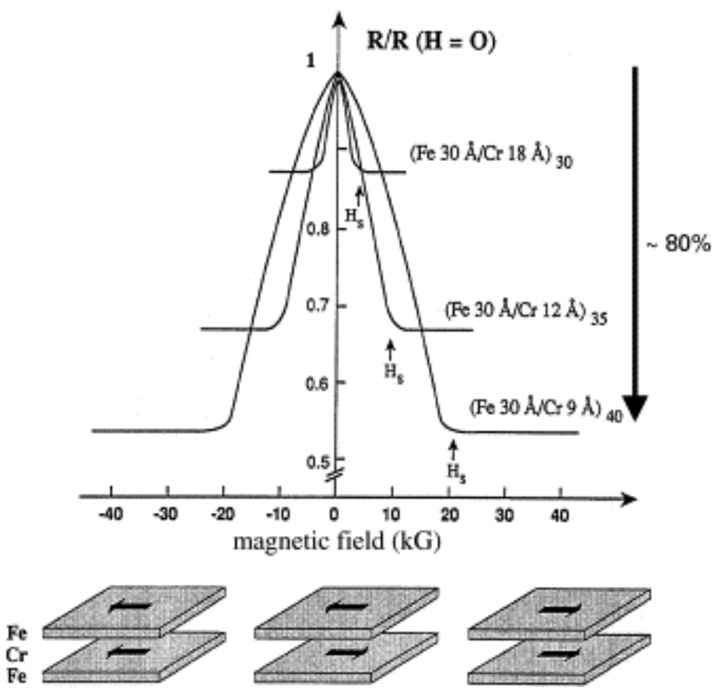

Barthélémy et al., JMMM 242-245, 68 (2002)

Magnetic data storage

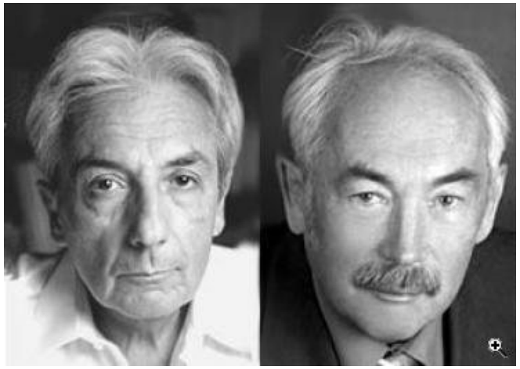

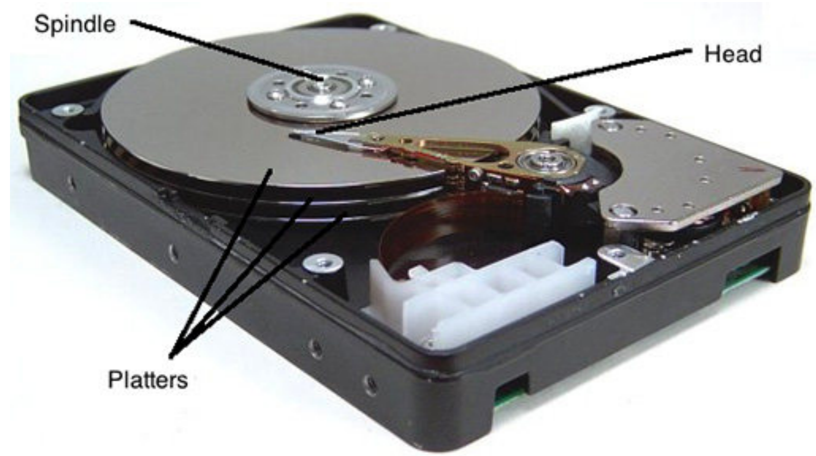

https://www.open.edu/openlearn/science-maths-technology/computing-ict/introducing-computing-and-it/content-section-5.1

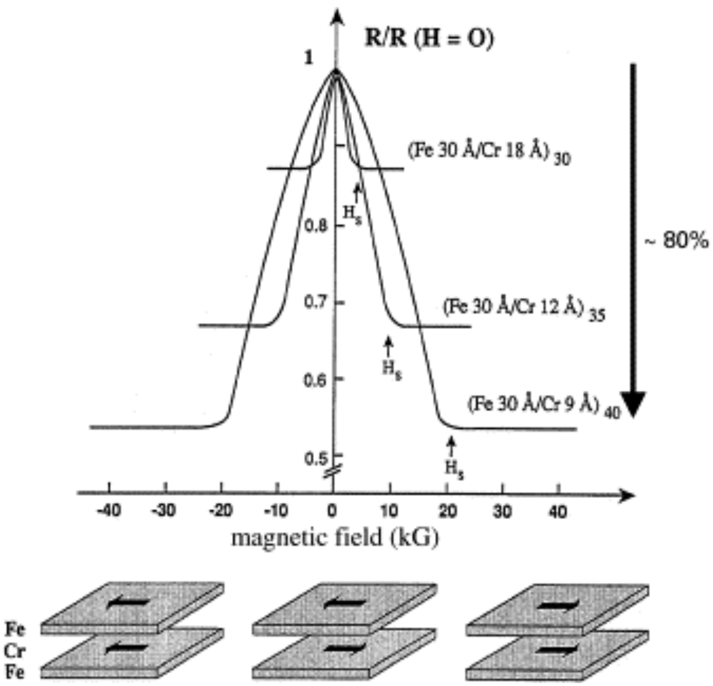

Barthélémy et al., JMMM 242-245, 68 (2002)

Cloud storage is based on HDDs

https://www.storage-insider.de/5-tipps-fuer-cloud-basiertes-backup-a-977818/

Magnetic data storage

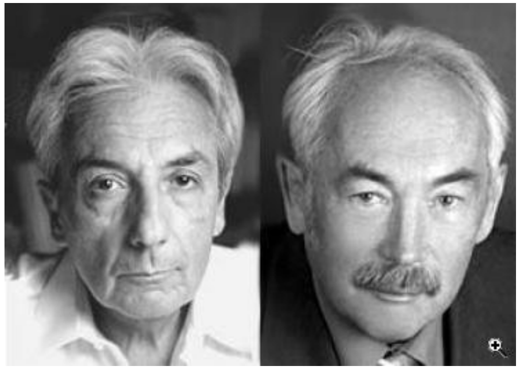

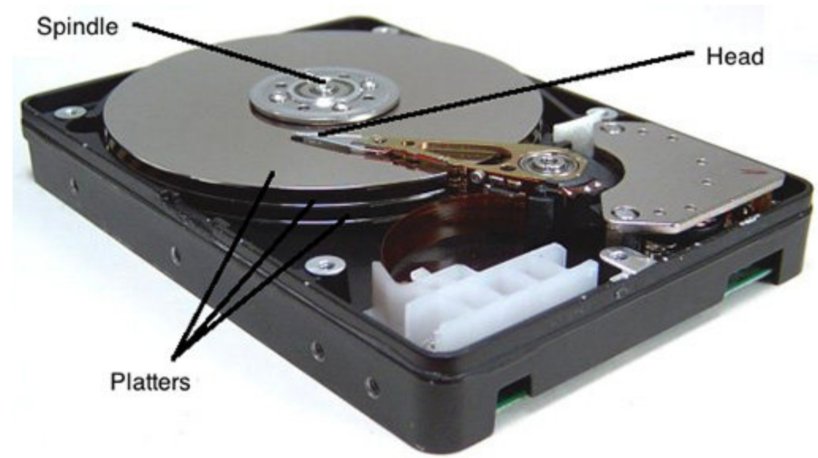

https://www.open.edu/openlearn/science-maths-technology/computing-ict/introducing-computing-and-it/content-section-5.1

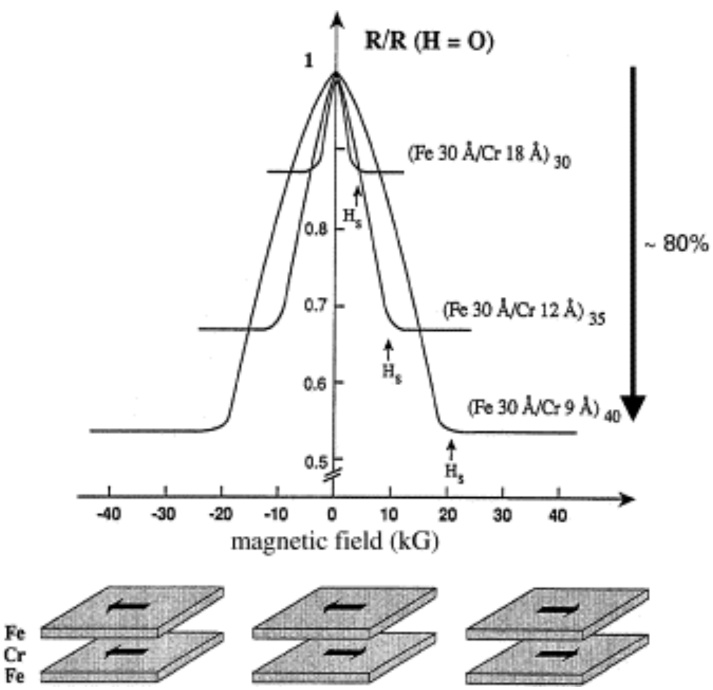

Barthélémy et al., JMMM 242-245, 68 (2002)

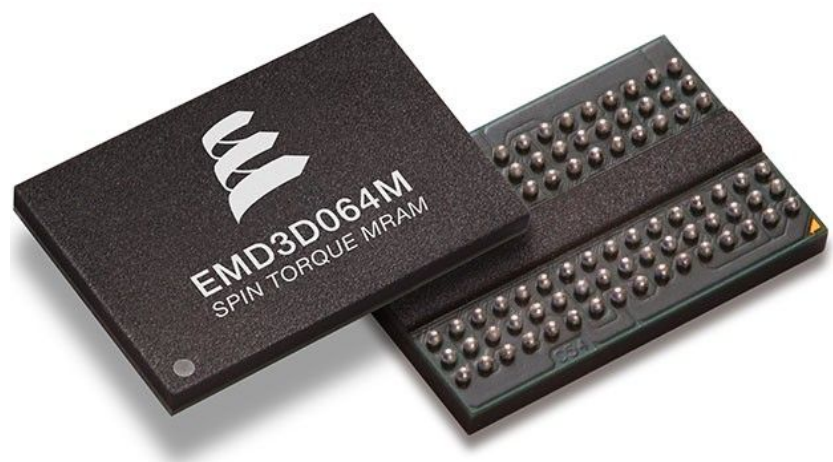

Courtesy: Everspin

Families of Magnetic RAM

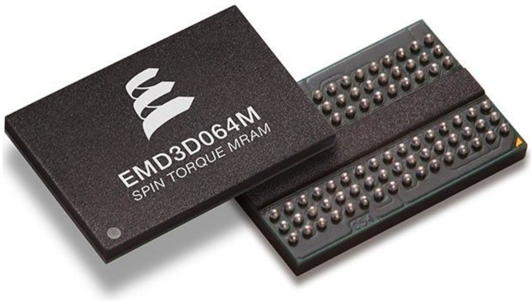

Courtesy: Everspin

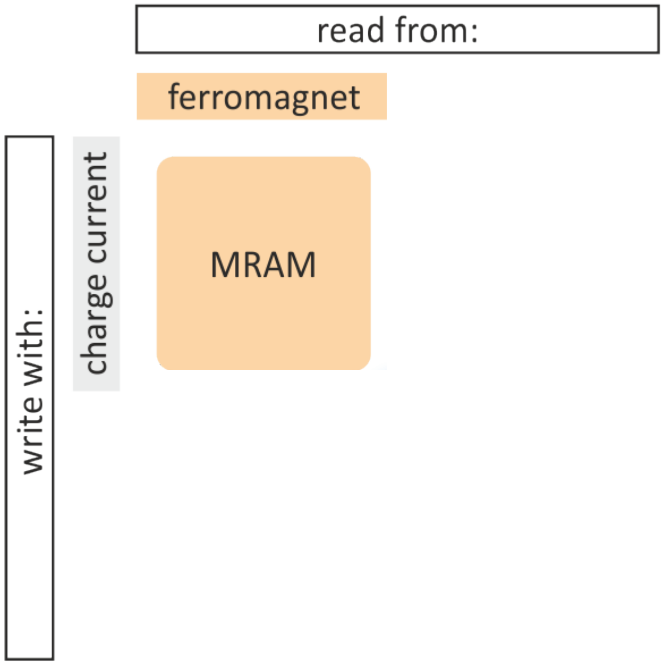

Spin transfer torque magnetic random access memory (STT-MRAM) is among the most promising spintronic memories

Still, it suffers from resistance scalability (resistance scales inversely proportional to the area and drive current densities) and intrinsically high energy/bit operation (>100 fJ/bit)

Families of Magnetic RAM

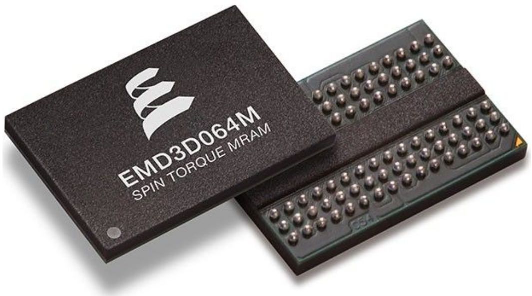

Courtesy: Everspin

write with:	read from: ferromagnet	read from: antiferromagnet
charge current	MRAM	AF-MRAM
electric field	MERAM	**AF-MERAM**

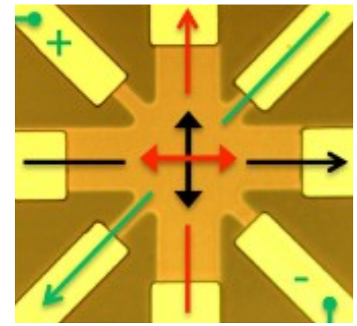

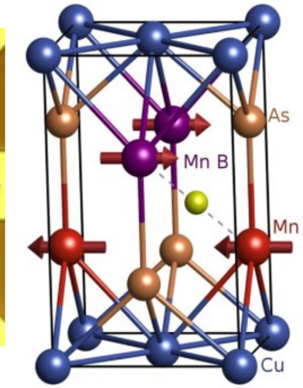

P. Wadley et al., *Science* (2016)

T. Kosub et al.,
Nature Commun. **8**, 13985 (2017)

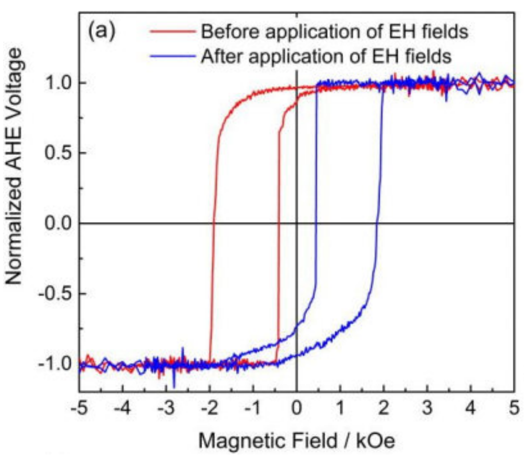

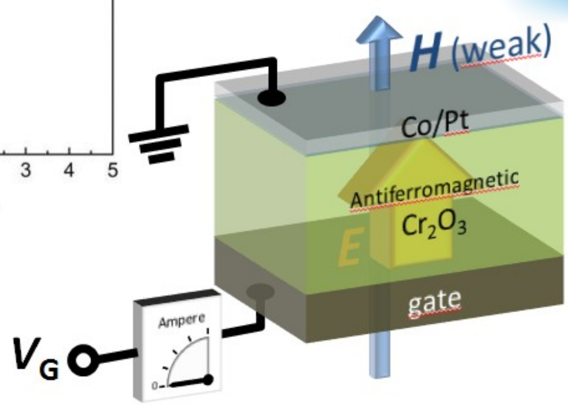

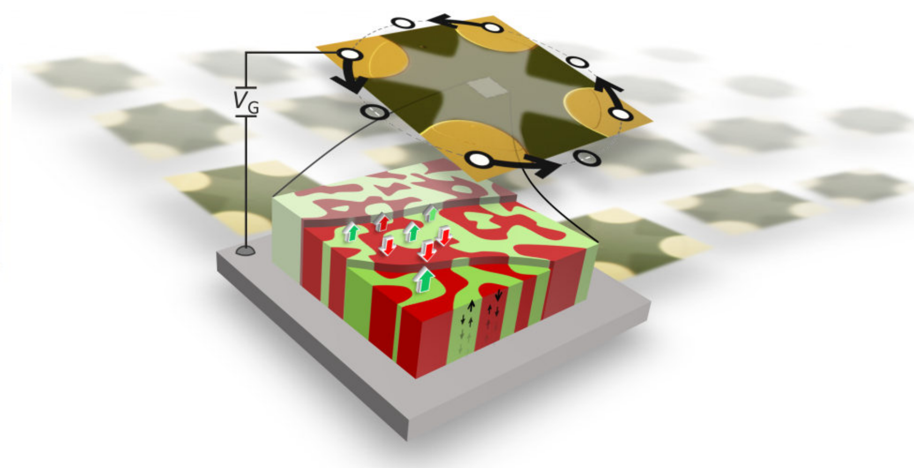

X. He et al., *Nature Mat.* **9**, 579 (2010)
K. Toyoki et al., *APL* **106**, 162404 (2015)

Lithography vs. Self Organization

Lithographically Defined

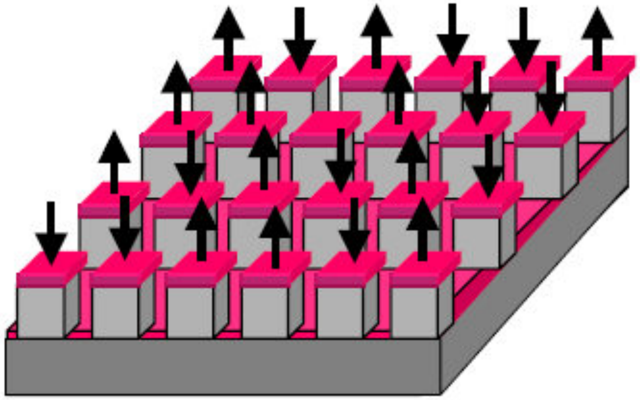

The major obstacle to smaller bit size is finding a low cost means of making media

- At 1 Tbpsi, assuming a square bit cell and equal lines and spaces, 12.5 nm lithography would be required
- Semiconductor Industry Association roadmap does not provide such linewidths within the next decade

FePt Self-Organizing Media

6 nm FePt particles

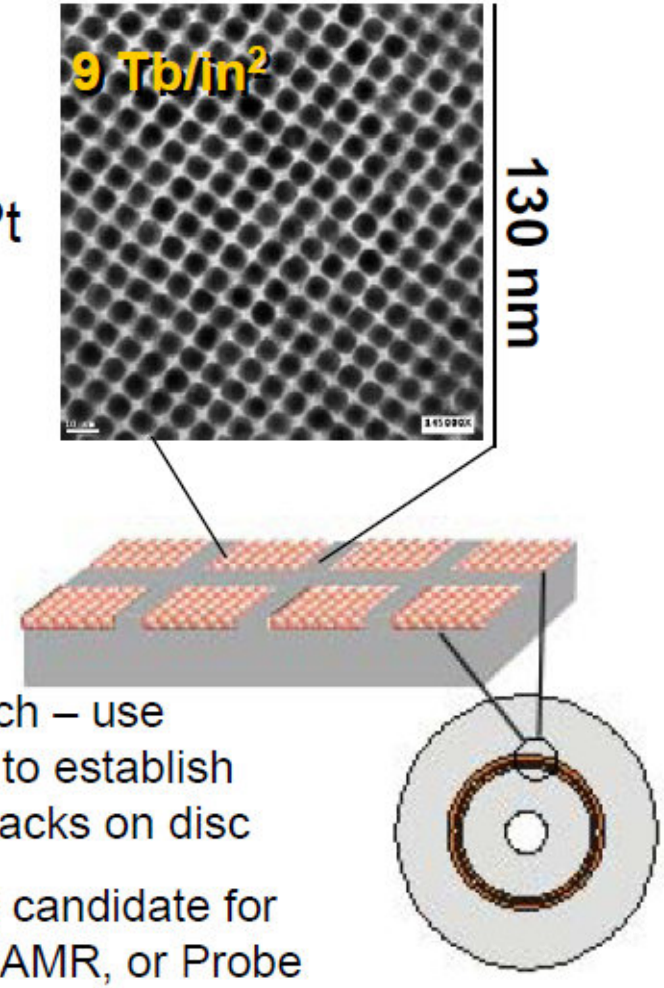

Potential approach – use patterned media to establish circumferential tracks on disc

Promising media candidate for Perpendicular, HAMR, or Probe

Source: M. Kryder, “Future storage technologies” (2006)

Hollow magnetic nanoobjects

Fabrication is based on Kirkendall effect
(different diffusion speed of ions at interfaces of two materials)

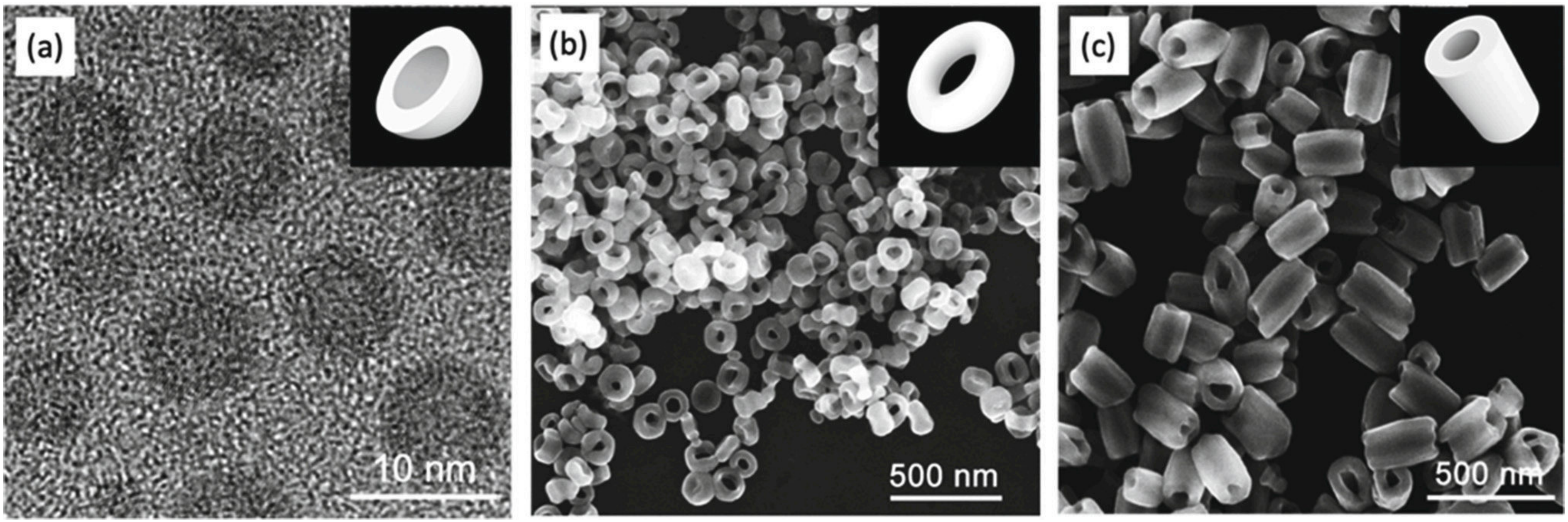

J. Phys. Chem. C 122, 7516 (2018); J. Am. Chem. Soc. 130, 16968 (2008); Appl. Surf. Sci. 492, 82 (2019)

Two photon photolithography & electrochemistry

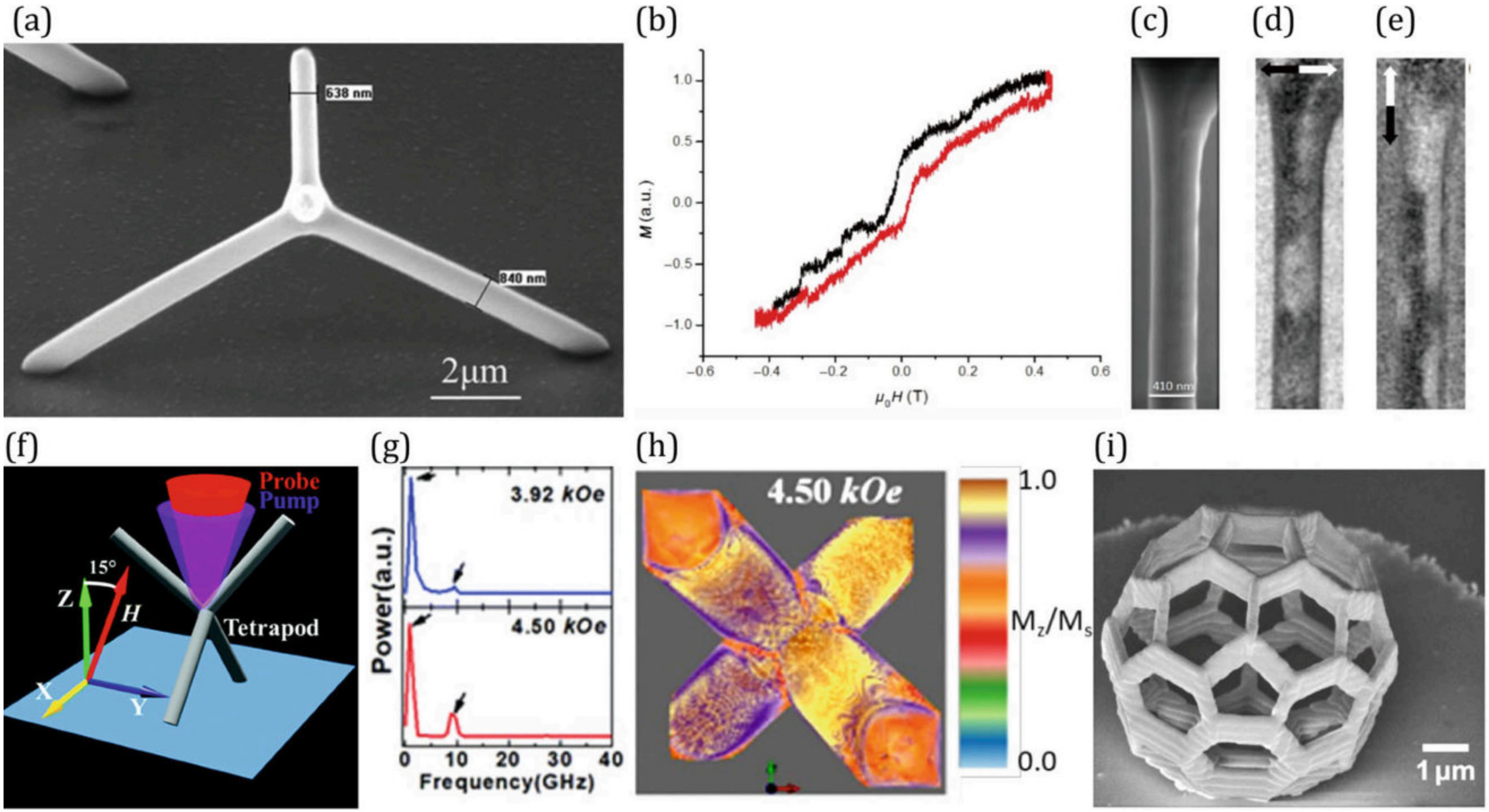

Nano Res. 11, 845 (2018); Nanoscale 10, 9981 (2018); Phys. Rev. Lett. 114, 115501 (2015)

Dobrovolskiy, O.V. et al. (2022). Complex-Shaped 3D Nanoarchitectures for Magnetism and Superconductivity. In: Makarov, D., Sheka, D.D. (eds) Curvilinear Micromagnetism. Topics in Applied Physics, vol 146. Springer. https://doi.org/10.1007/978-3-031-09086-8_5

Focused electron/ion beam induced deposition (FEBID/FIBID)

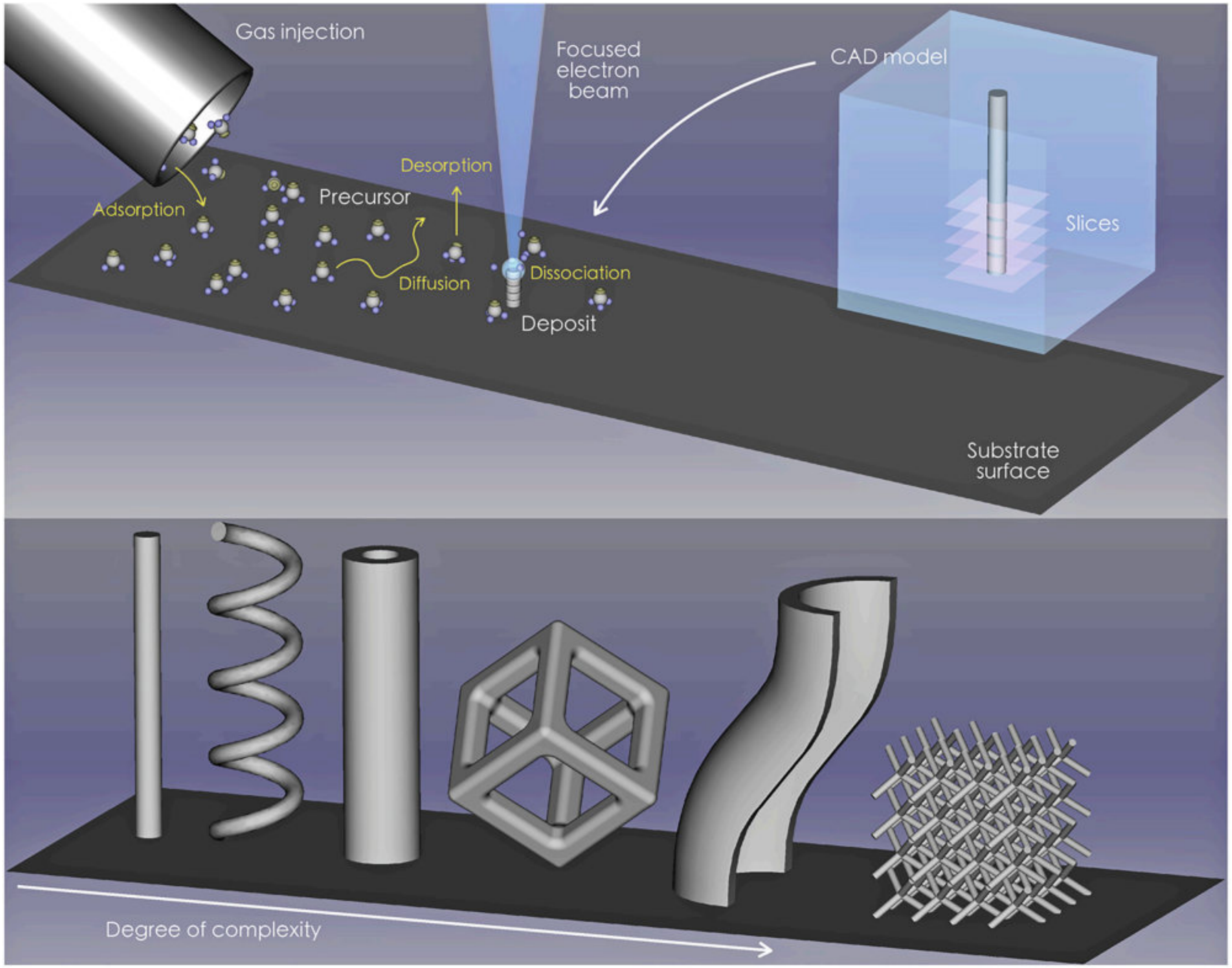

Dobrovolskiy, O.V. et al. (2022). Complex-Shaped 3D Nanoarchitectures for Magnetism and Superconductivity. In: Makarov, D., Sheka, D.D. (eds) Curvilinear Micromagnetism. Topics in Applied Physics, vol 146. Springer. https://doi.org/10.1007/978-3-031-09086-8_5

Focused electron/ion beam induced deposition (FEBID/FIBID)

Nano Lett. 20, 184 (2020); ACS Nano 14, 8084 (2020)

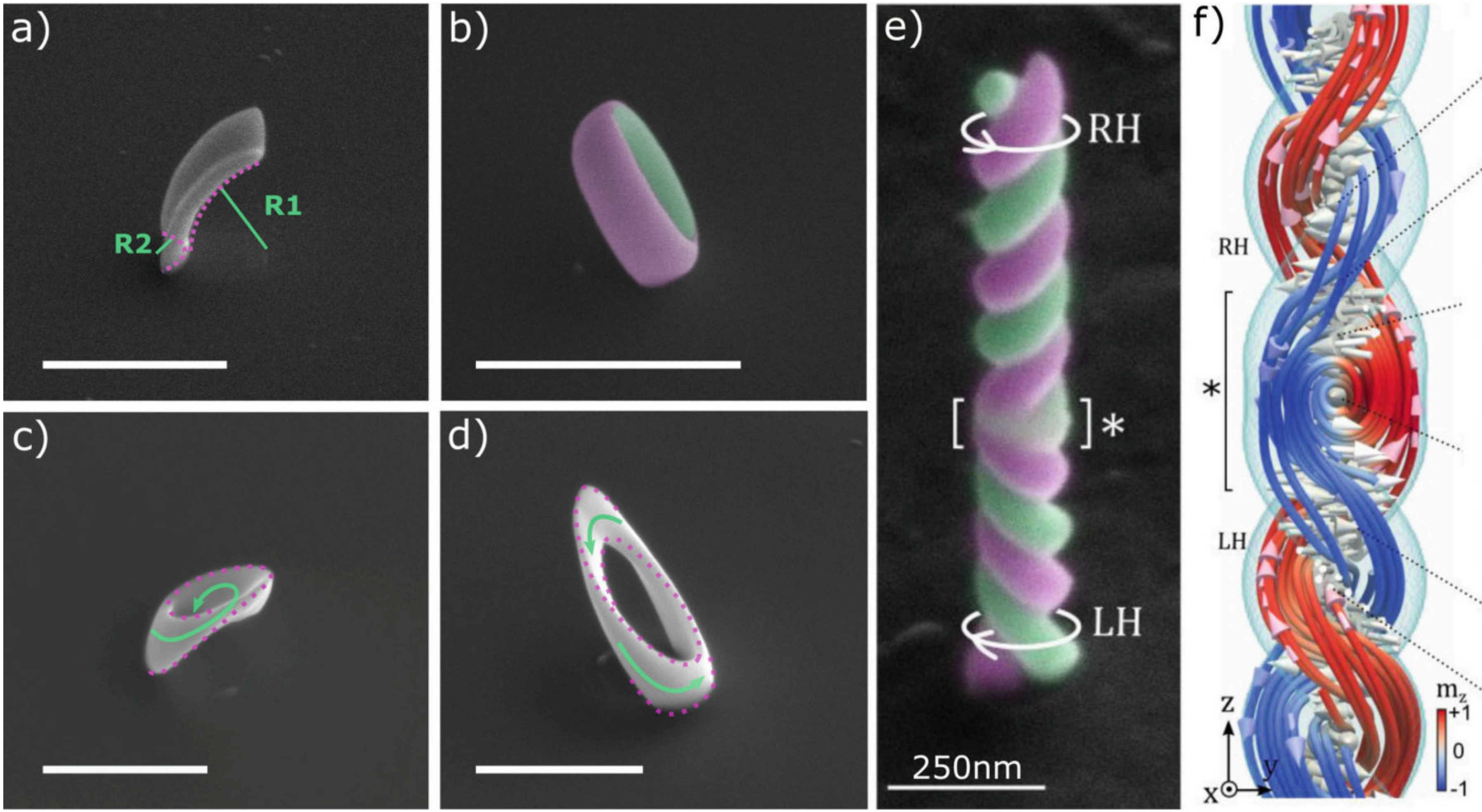

Dobrovolskiy, O.V. et al. (2022). Complex-Shaped 3D Nanoarchitectures for Magnetism and Superconductivity. In: Makarov, D., Sheka, D.D. (eds) Curvilinear Micromagnetism. Topics in Applied Physics, vol 146. Springer. https://doi.org/10.1007/978-3-031-09086-8_5

Site-Selective Chemical Vapor Deposition on Direct-Write 3D Nanoarchitectures

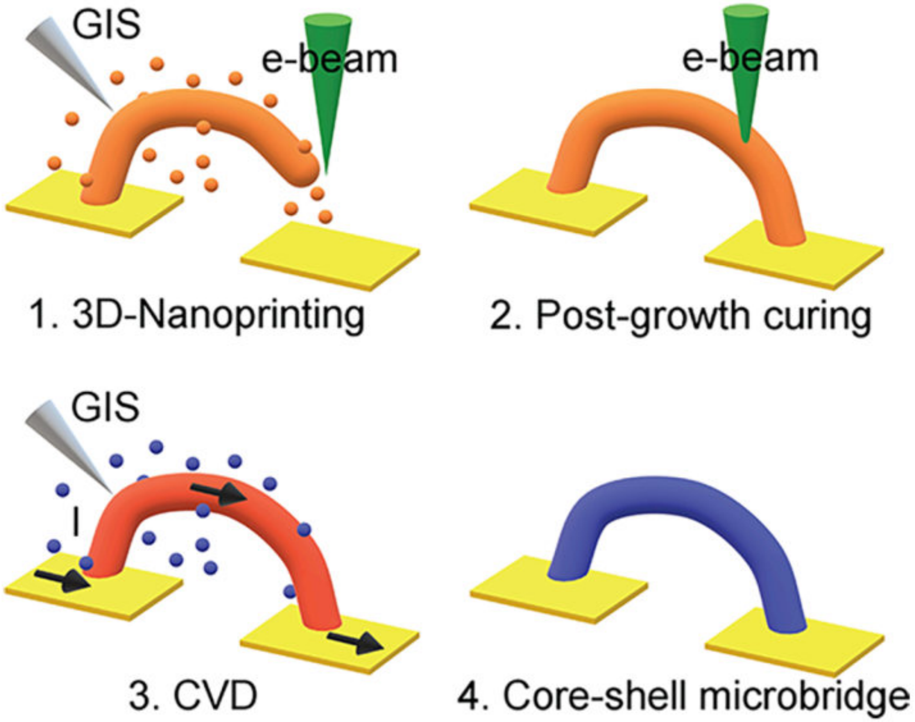

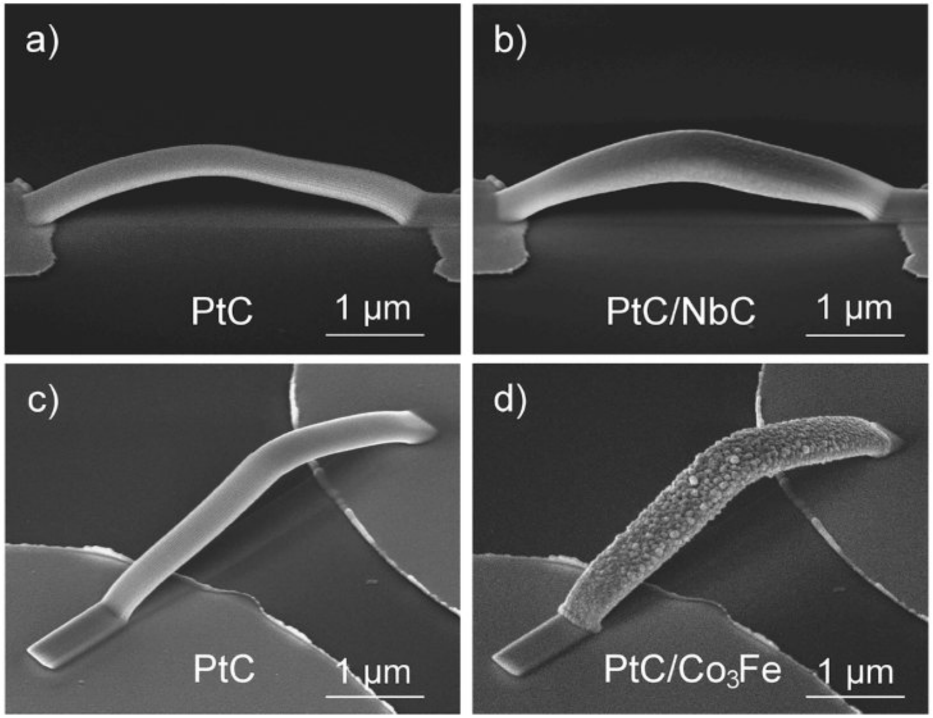

Fabrizio Porrati et al., ACS Nano 17, 4704 (2023)

Curvilinear magnetic nanostructures

Dr. Denys Makarov I E-Mail: d.makarov@hzdr.de I Intelligent Materials and Systems

Patterned Magnetic Media

Single grain ⇔ Single bit => Patterned Magnetic Media

Electron beam lithography

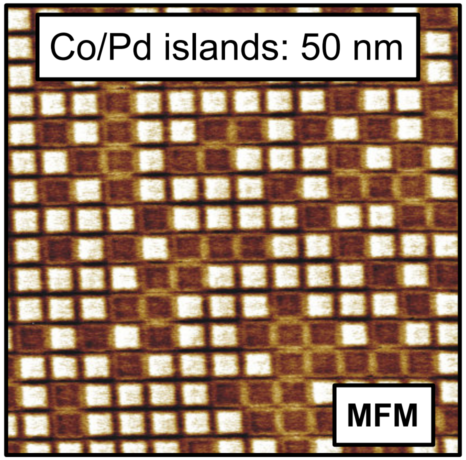

Hu et al., *J. Appl. Phys.* **95** (2004) 7013

Drawback of the approach:

i. Expensive

ii. Time consuming

iii. Size limited

X-ray/nanoimprint lithography

Ross, *An. Rev. Mat. Res.* **31** (‘01) 203;

Chou et al., *J. Appl. Phys.* **76** (‘94) 6673

Magnetic particles self-assembly

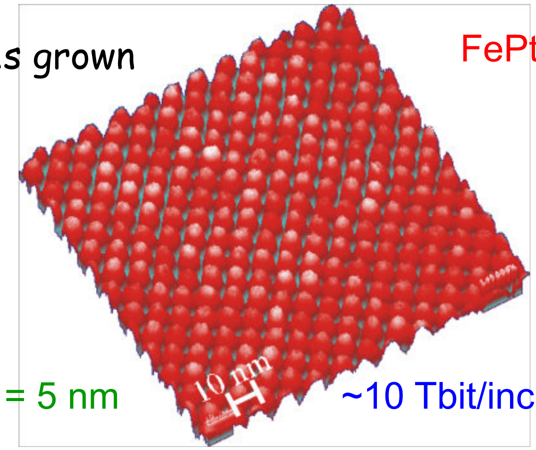

Sun et al., *Science* **287** (2000) 1989

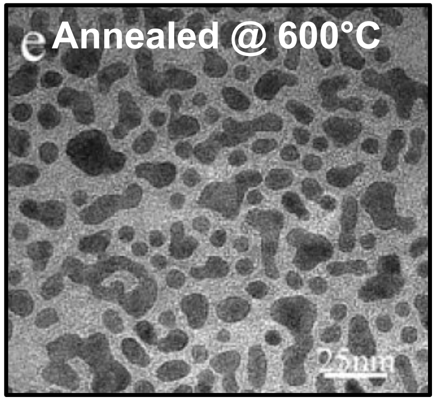

!!! Agglomeration !!!

Dai et al., *NanoLett.* **1** (2001) 443

Magnetic films on nanospheres

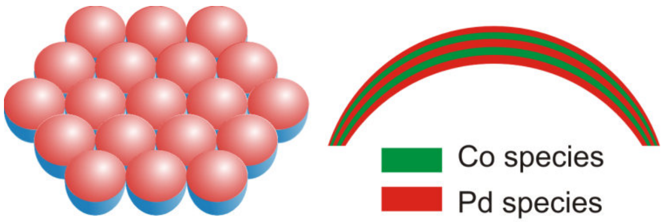

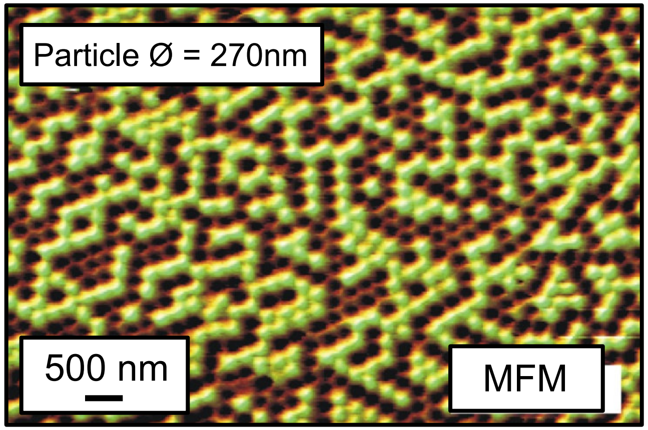

Magnetic properties

- Perpendicular anisotropy
- Single-domain state
- Exchange isolated caps

Albrecht et al., *Nature Materials* **4** (2005) 203

Curvature-induced thickness gradient

- Self-assembling of spherical particles via drop-cast approach

  ➜ Extended monolayers and individual spheres with ∅ = 100, 160, 330, 800 nm

- Magnetron sputter deposition of soft-magnetic permalloy film ($Ni_{80}Fe_{20}$, t = 10, 20, 30, 40 nm)

- Thickness gradient

  ➜ **Curvature-driven modification of magnetic properties**

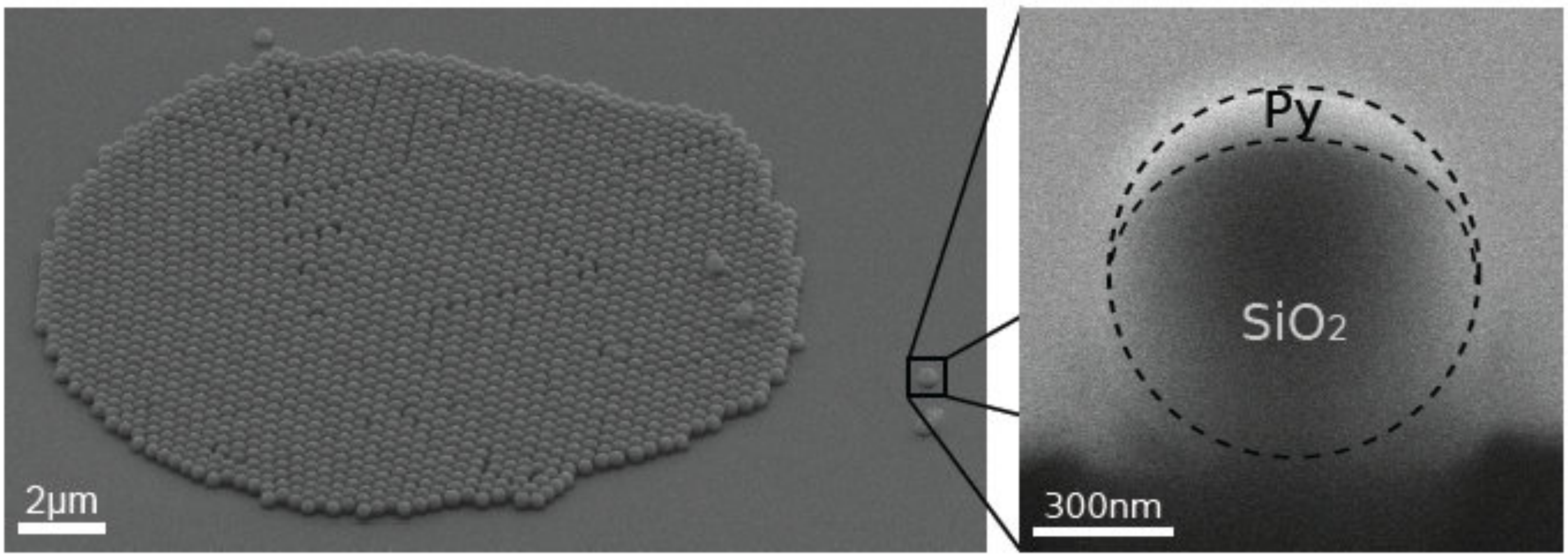

Courtesy: Dr. Robert Streubel (Leibniz IFW Dresden)

Assemblies of spherical nanoparticles

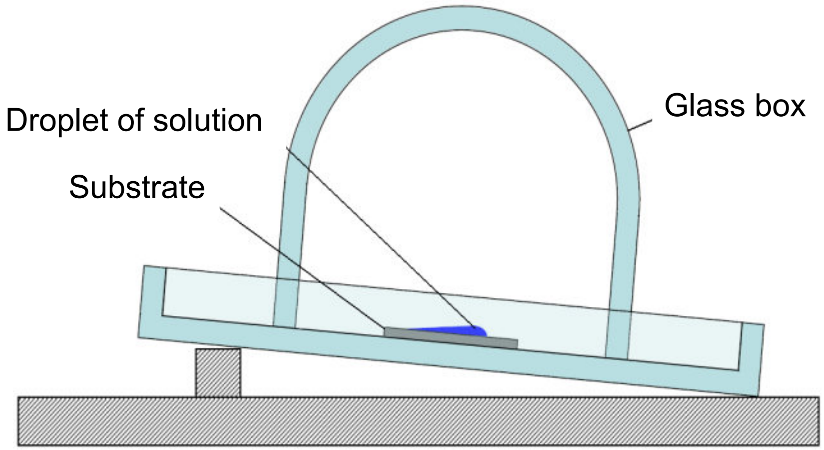

Preparation route

Ultrasonication of the substrate in acetone, ethanol, and purified water & oxygen plasma for 4 min

Droplet of a particle/water dispersion is deposited onto the cleaned substrate

Evaporation process of the droplet takes place in a small and tilted box

SEM study on particles morphology after metal film deposition

50 nm Particles

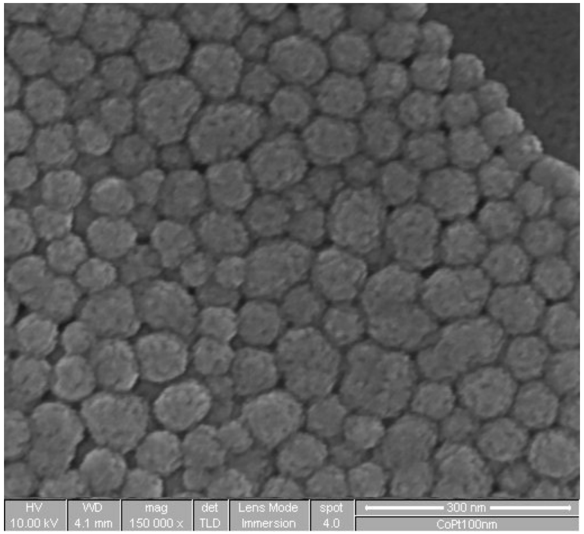

100 nm Particles

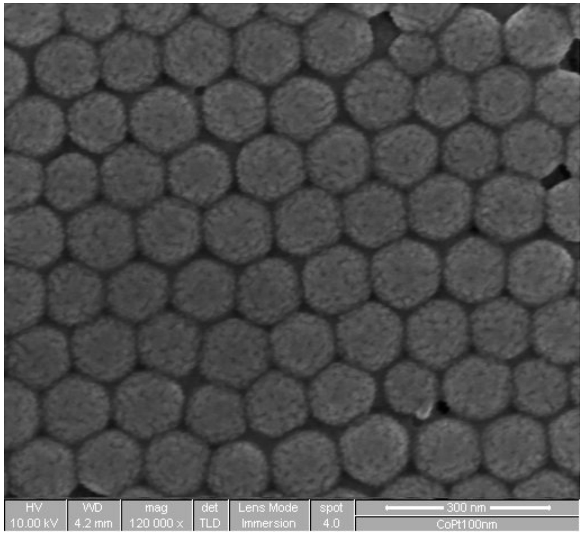

160 nm Particles

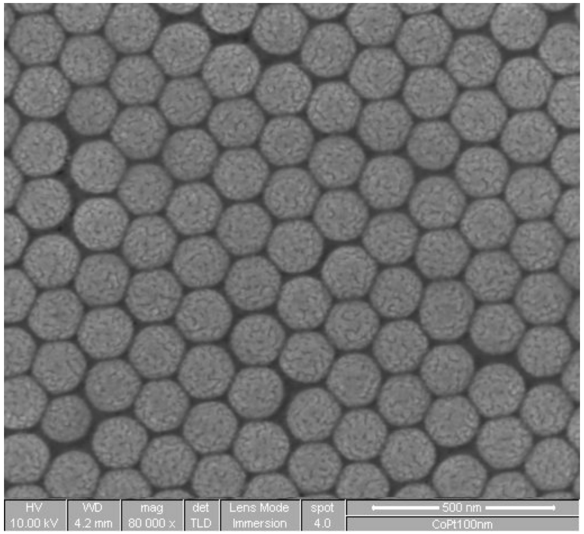

Structural TEM investigation

[Pd(1.8nm)/Co(1.8nm)]$_8$ stack on 50 nm SiO_2 particles

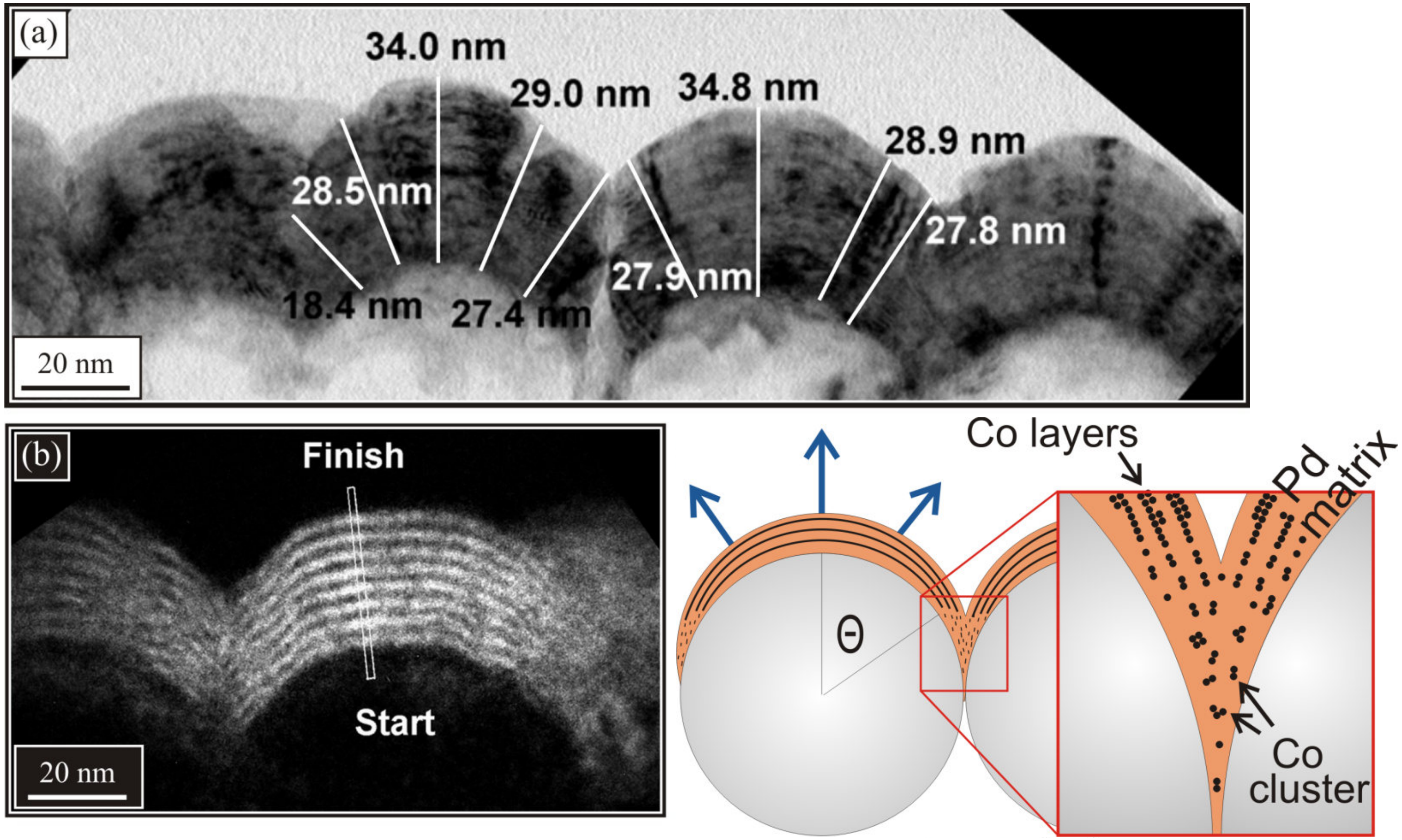

Grainy film morphology: grain size ~15 nm

Multilayer structure for θ up to about 50º

Film thickness is angle-dependent

Ulbrich et al., *Phys. Rev. B* **81** (2010) 054421

Magnetic states

- Integral magnetization loop shows typical vortex behavior
- Comparison with simulation of magnetic states and reversal process
- Qualitatively similar states compared to planar disks

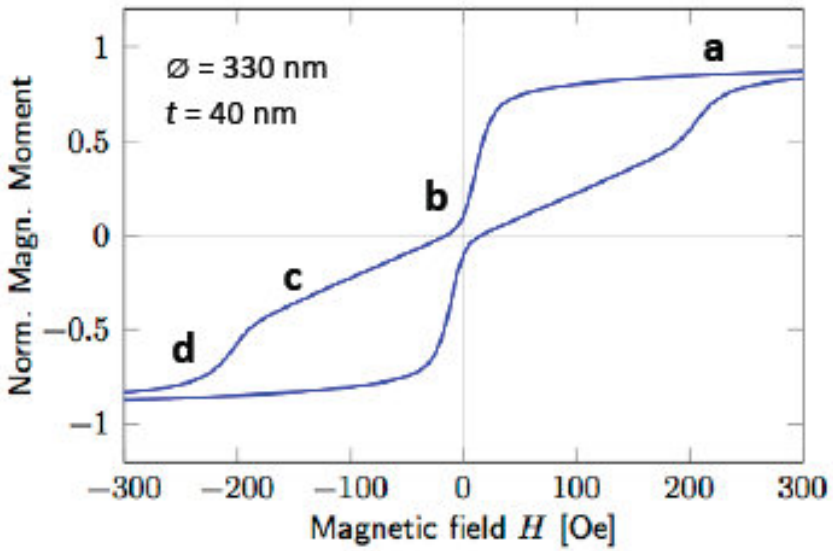

a) onion state **b) vortex state** **c) shifted vortex state** **d) *C*-state**

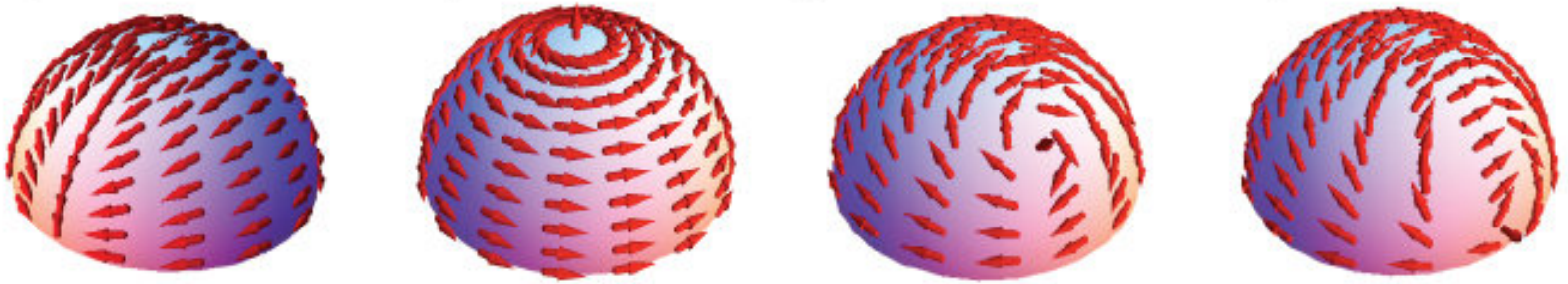

saturation — remanence — right before saturation

decreasing and inversing magnetic field

Courtesy: Dr. Robert Streubel (Leibniz IFW Dresden)

Vortex in a symmetric nanodisk

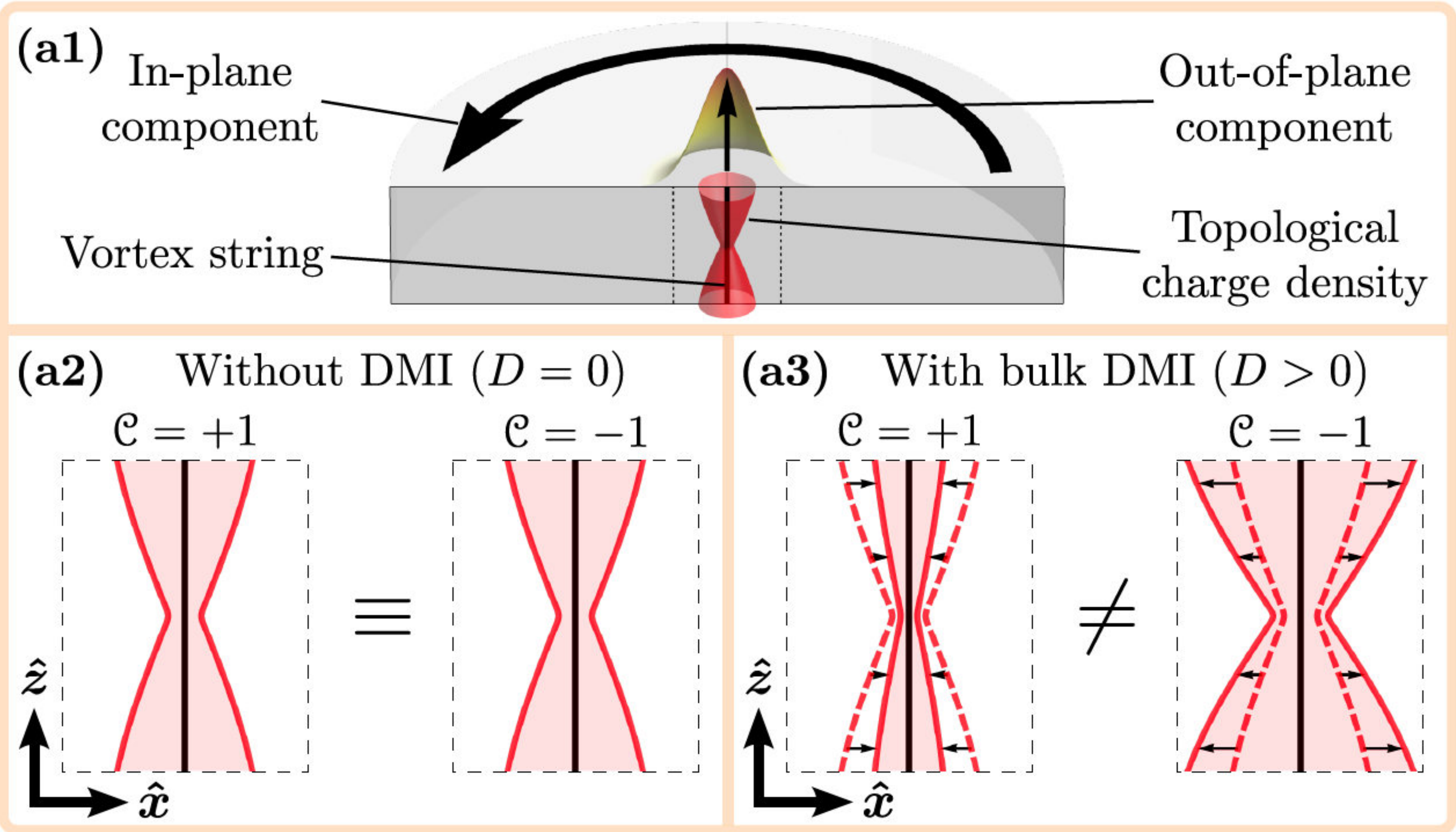

A. Butenko et al., *Physical Review B* **80**, 134410 (2009)

Vortex in 80-nm-thick Permalloy nanocap

Non-local chiral symmetry break:

Coupling of chiralities in topological textures with multiple magnetochiral parameters

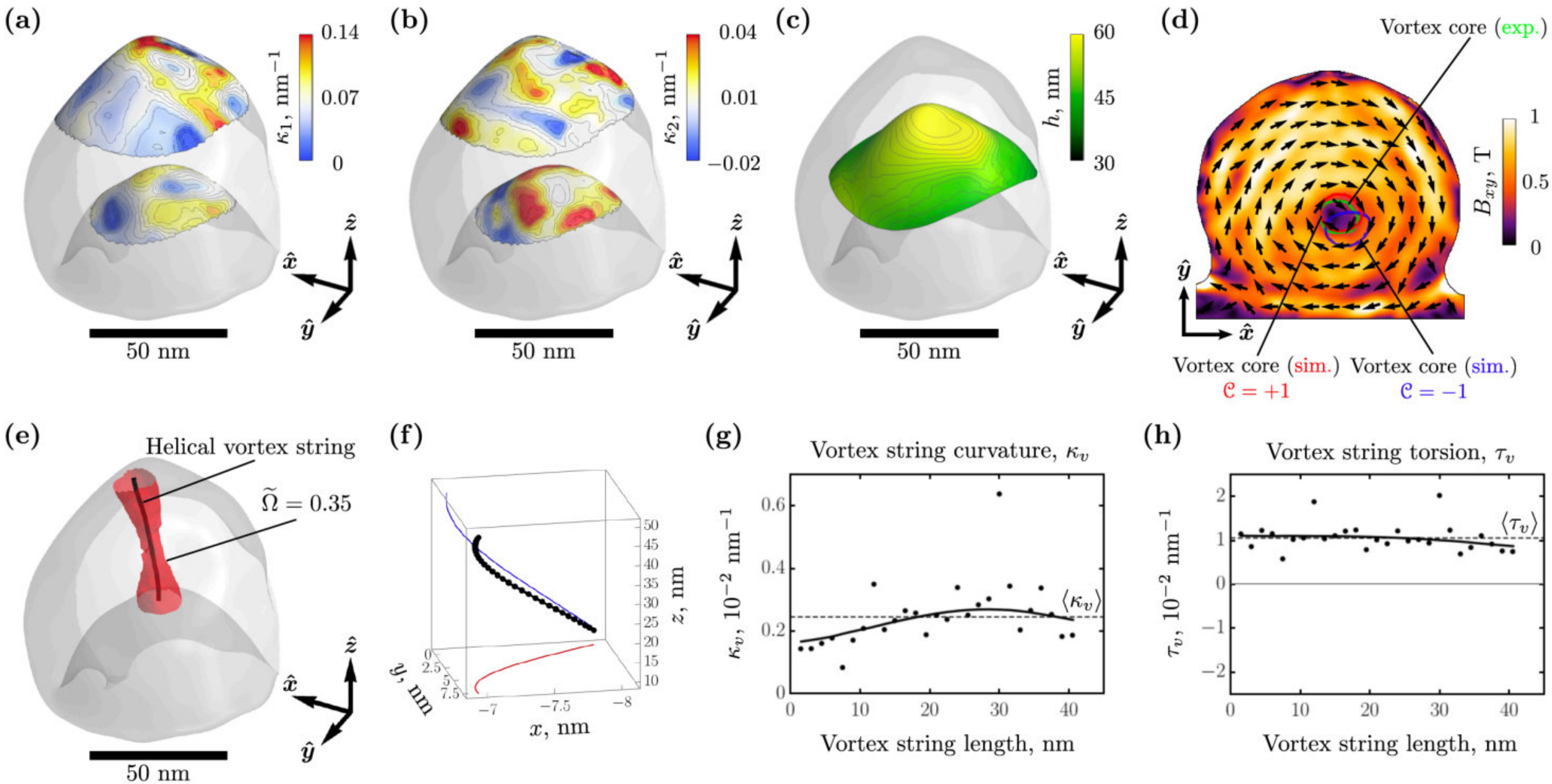

O. Volkov et al., *Nature Communications* **14**, 1491 (2023)

Coupling of two magnetochiralities within one object

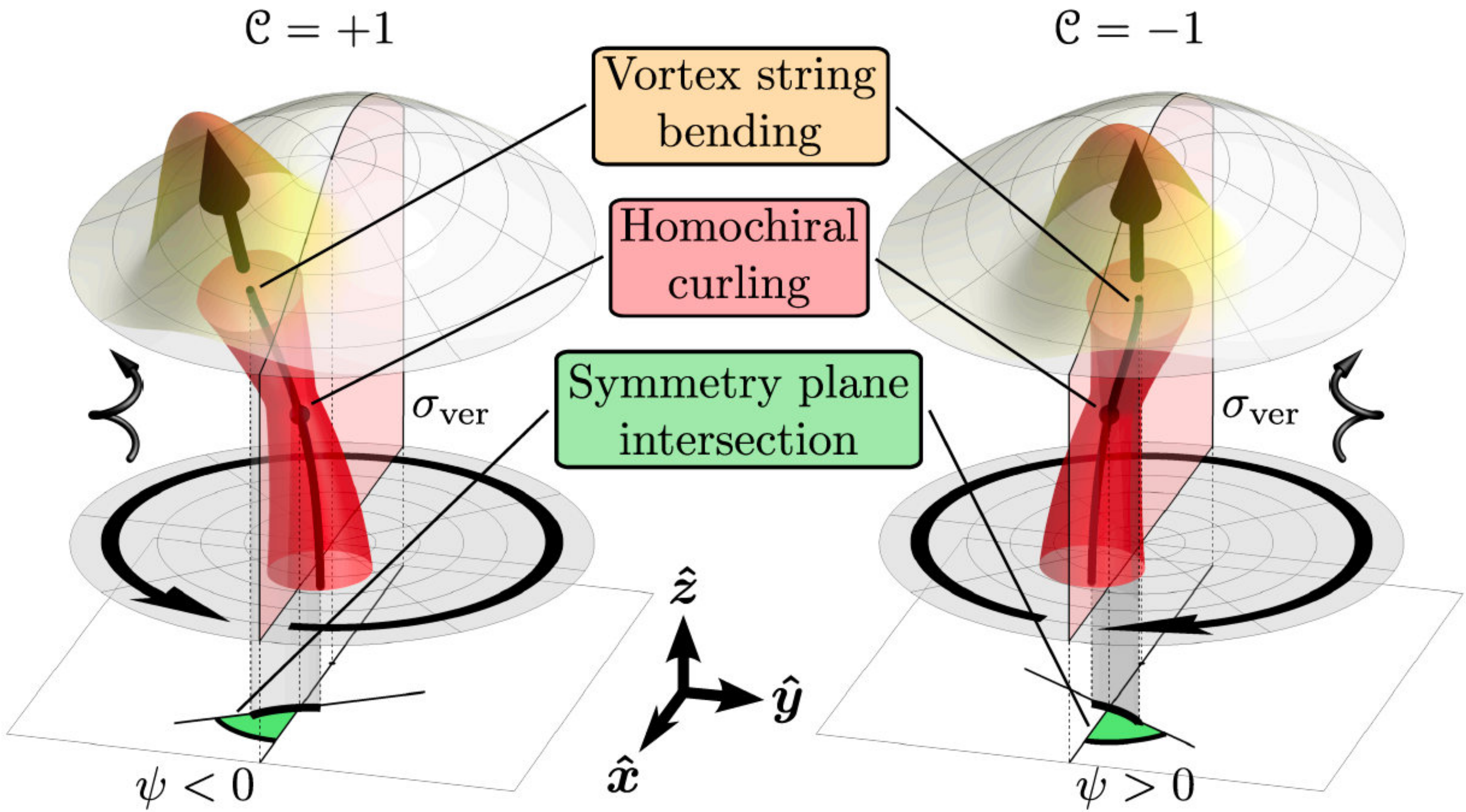

O. Volkov et al., *Nature Communications* **14**, 1491 (2023)

Guided self-assembly

Template-directed self-assembly

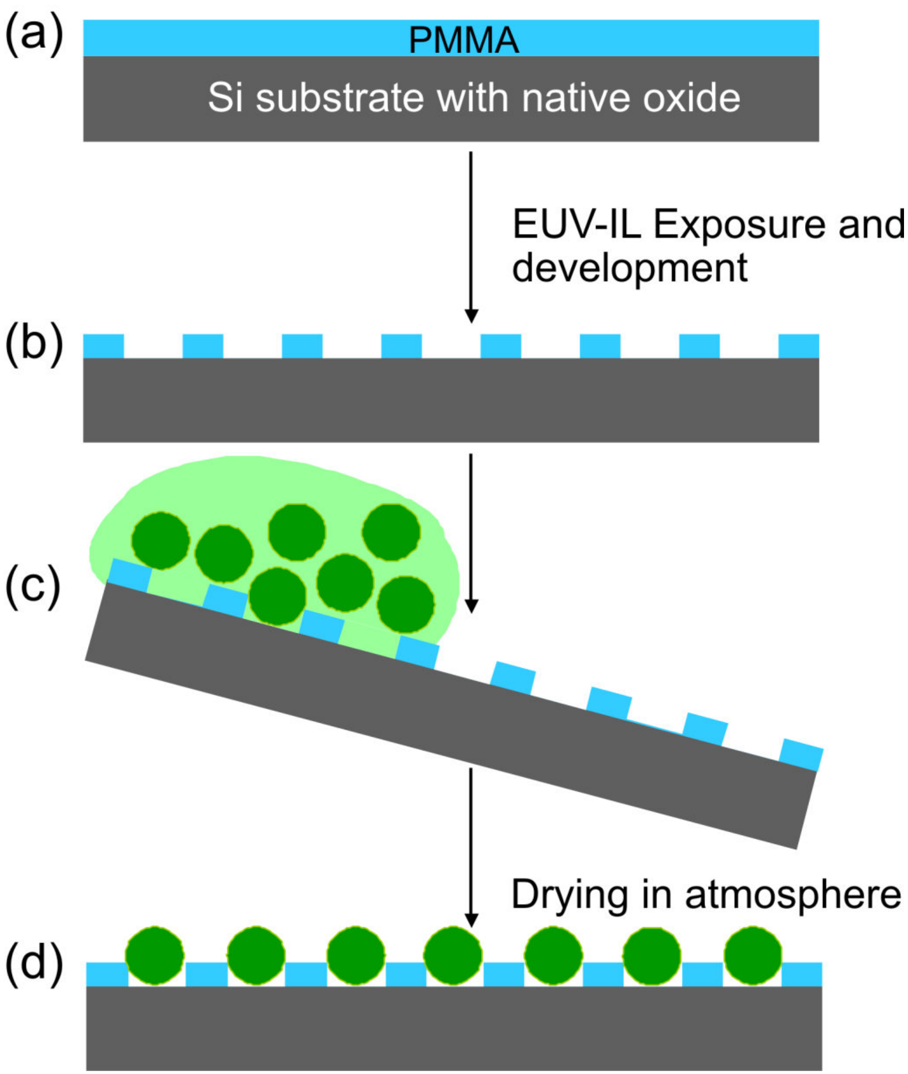

Templates were formed by EUV-IL in PMMA resist

Hole size: 60 nm & Period: 100 nm

Hole size: 30 nm & Period: 50 nm

Hole size: 22 nm & Period: 42 nm

Kappenberger et al., *Appl. Phys. Lett.* **95** (2009) 023116

Template-directed self-assembly

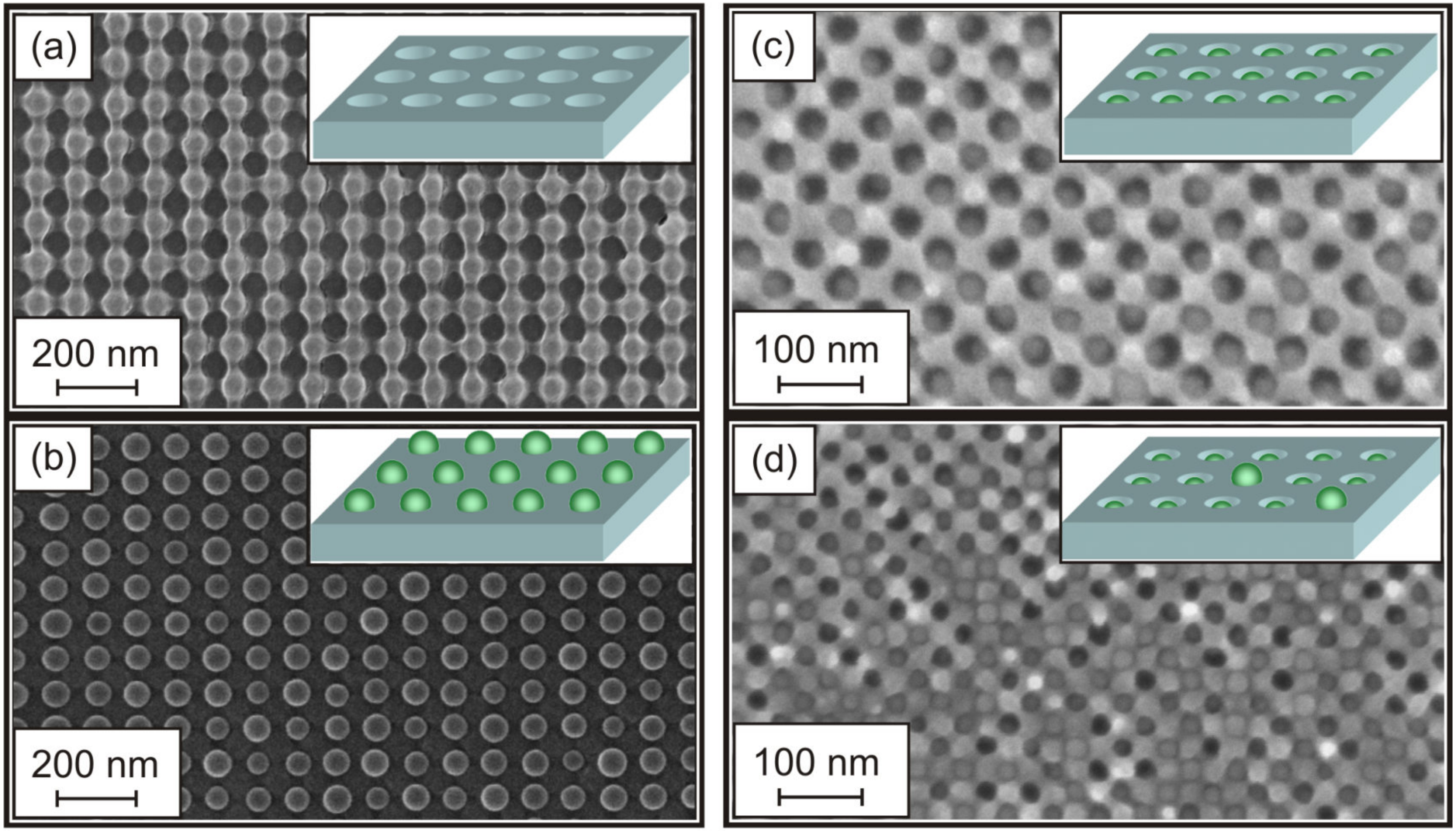

Kappenberger et al., *Appl. Phys. Lett.* **95** (2009) 023116

Recording tests on nanocaps

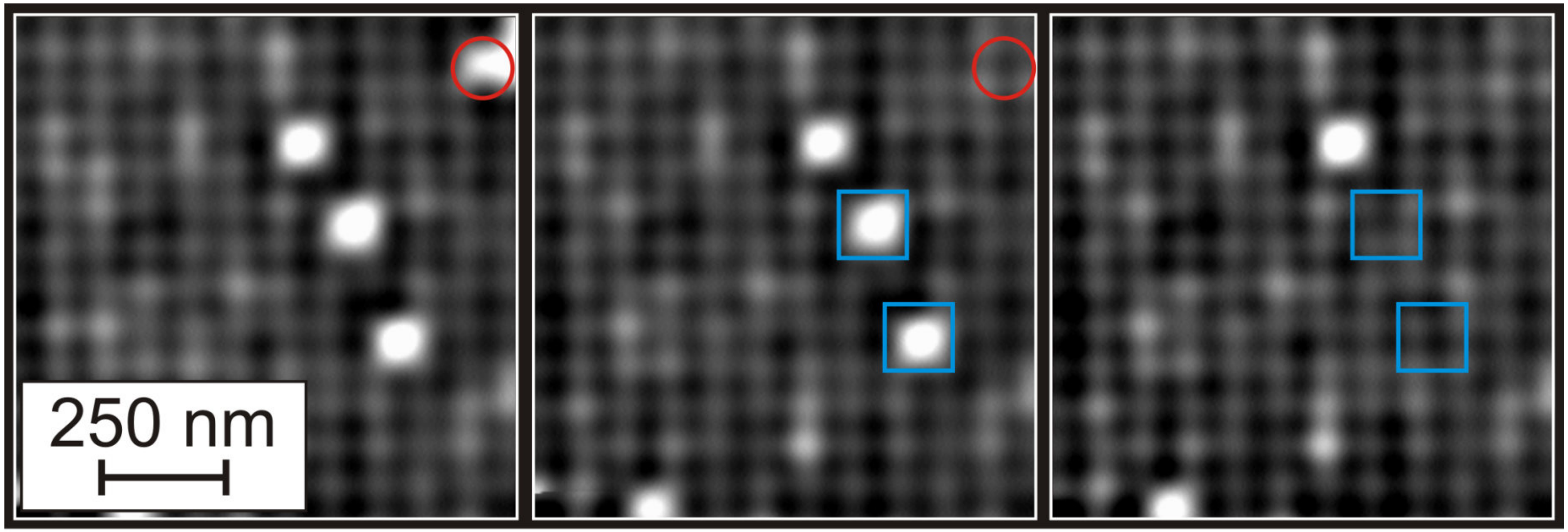

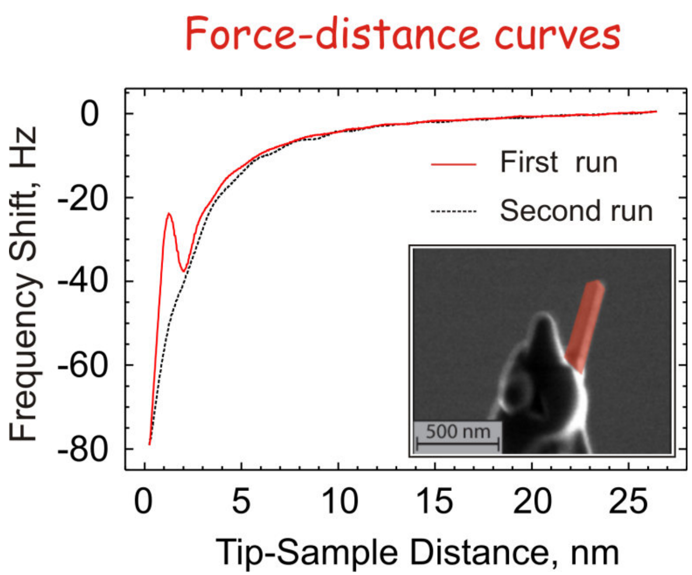

Magnetization of caps is switched by the field of MFM tip
(transition from bright to dark contrast)

Magnetic probe recording study

Performed using custom made MFM tip

Force-distance curves were used to detect writing events

Nanocaps are switched individually in a controlled fashion

Additional magnetic field of 405 mT was applied

Kappenberger et al., *Appl. Phys. Lett.* **95** (2009) 023116

BPM based on block copolymer directed assembly

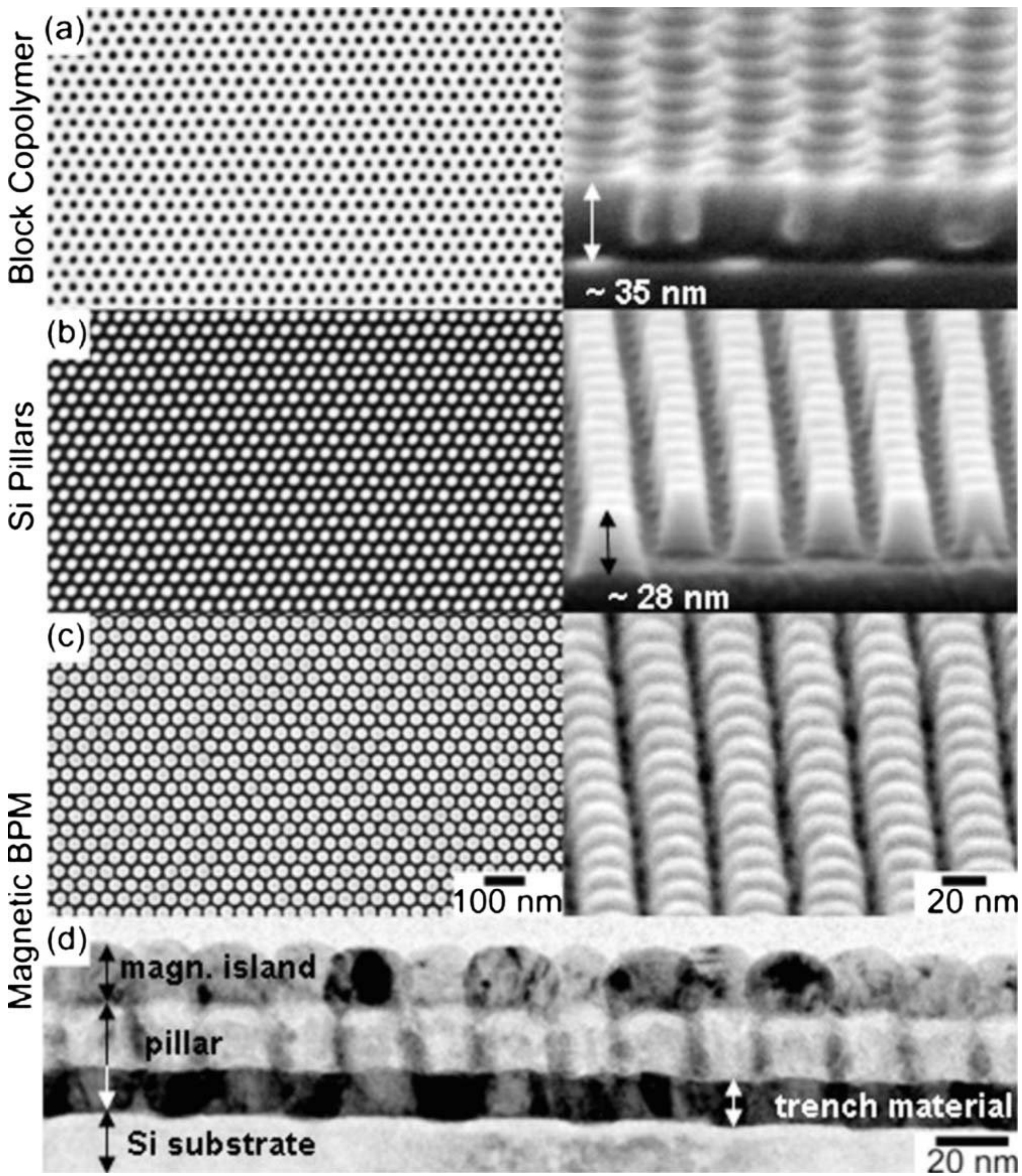

Array with a period of 38 nm

Substrate:
Si pillar substrates fabricated via e-beam directed assembly of block copolymer films

Magnetic film:
Co/Pd multilayer stacks

Areal density:
1 Tbit/inch^2 is already demonstrated

Hellwig et al., Appl. Phys. Lett. 96 (2010) 052511

3D architectures via strain engineering

Strain relaxation in thin films

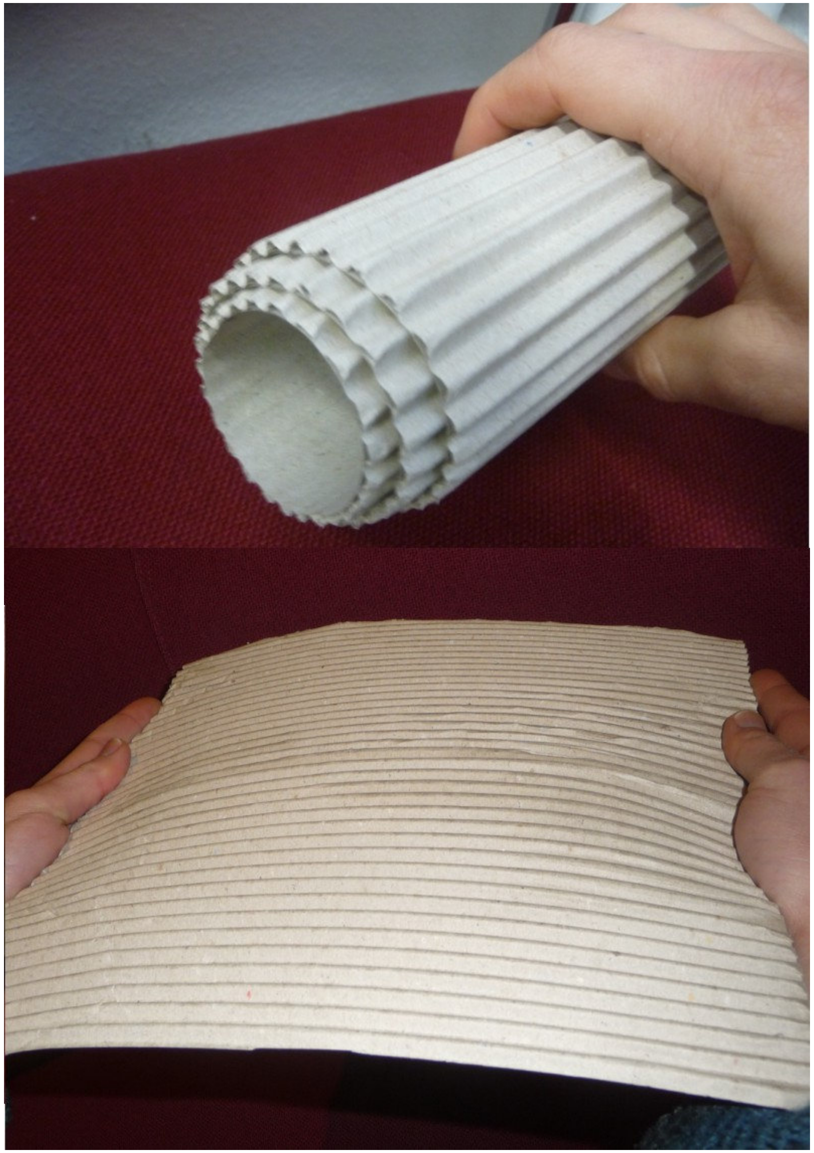

Cendula et al., *Nano Lett.* **11**, 236 (2011)

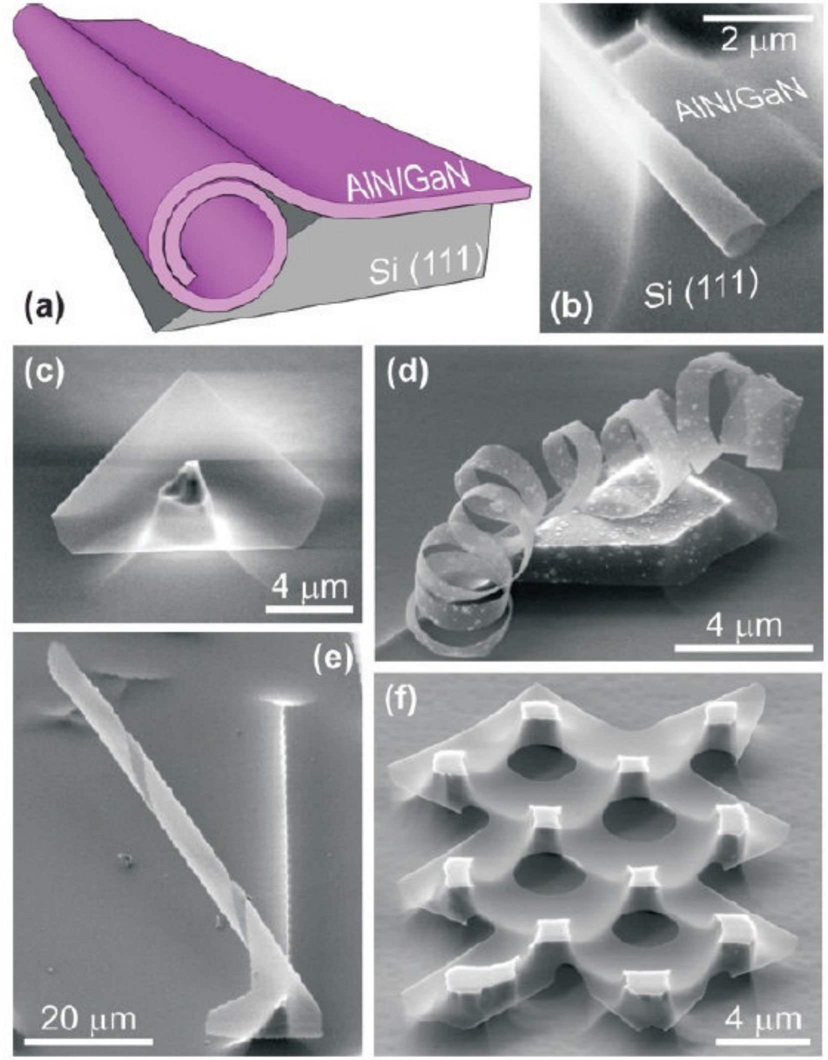

Mei et al., *ACS Nano* **3**, 1663 (2009)

Roll-up technology

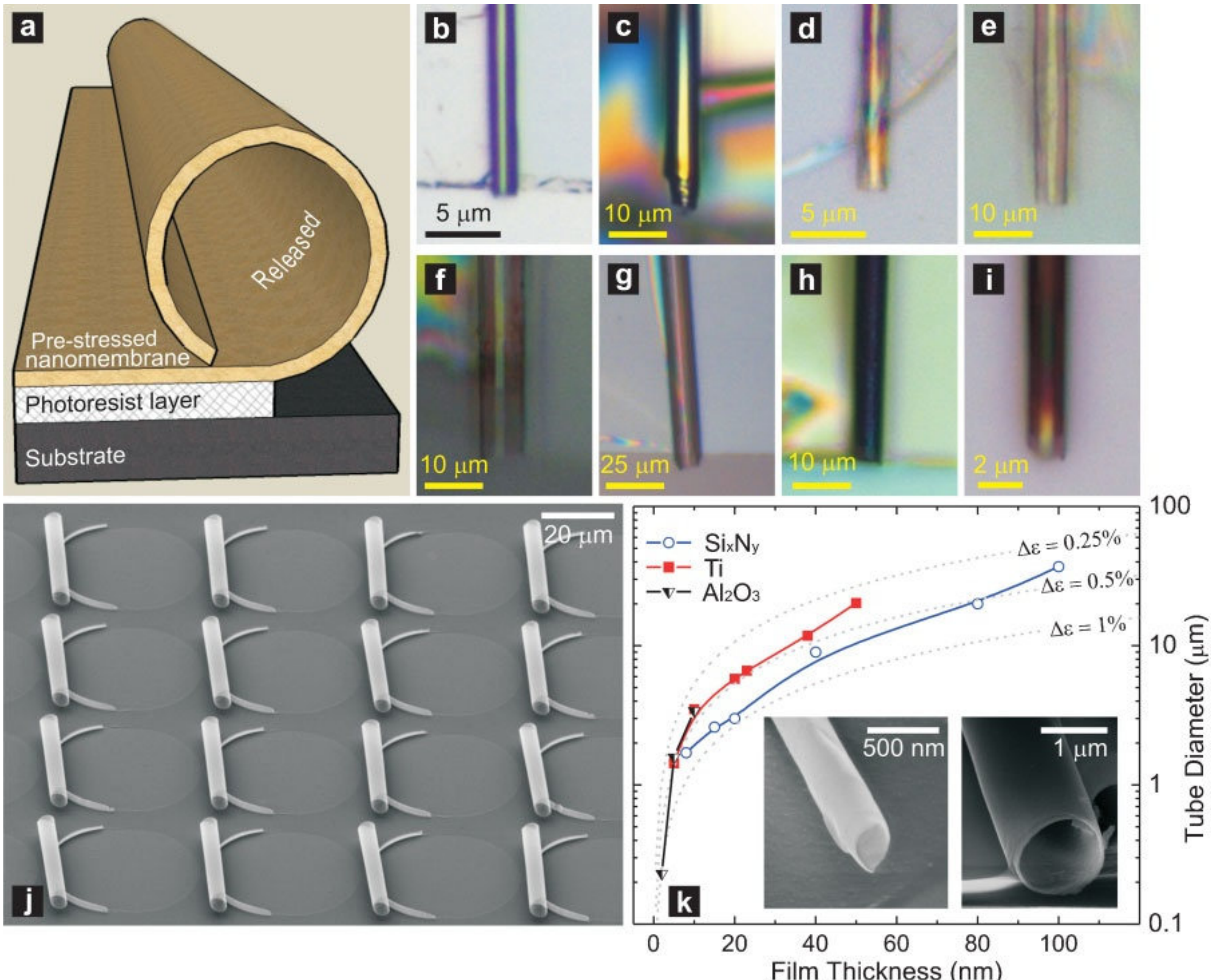

Mei et al., *Adv. Mater.* **20**, 4085 (2008)

Tubular architectures

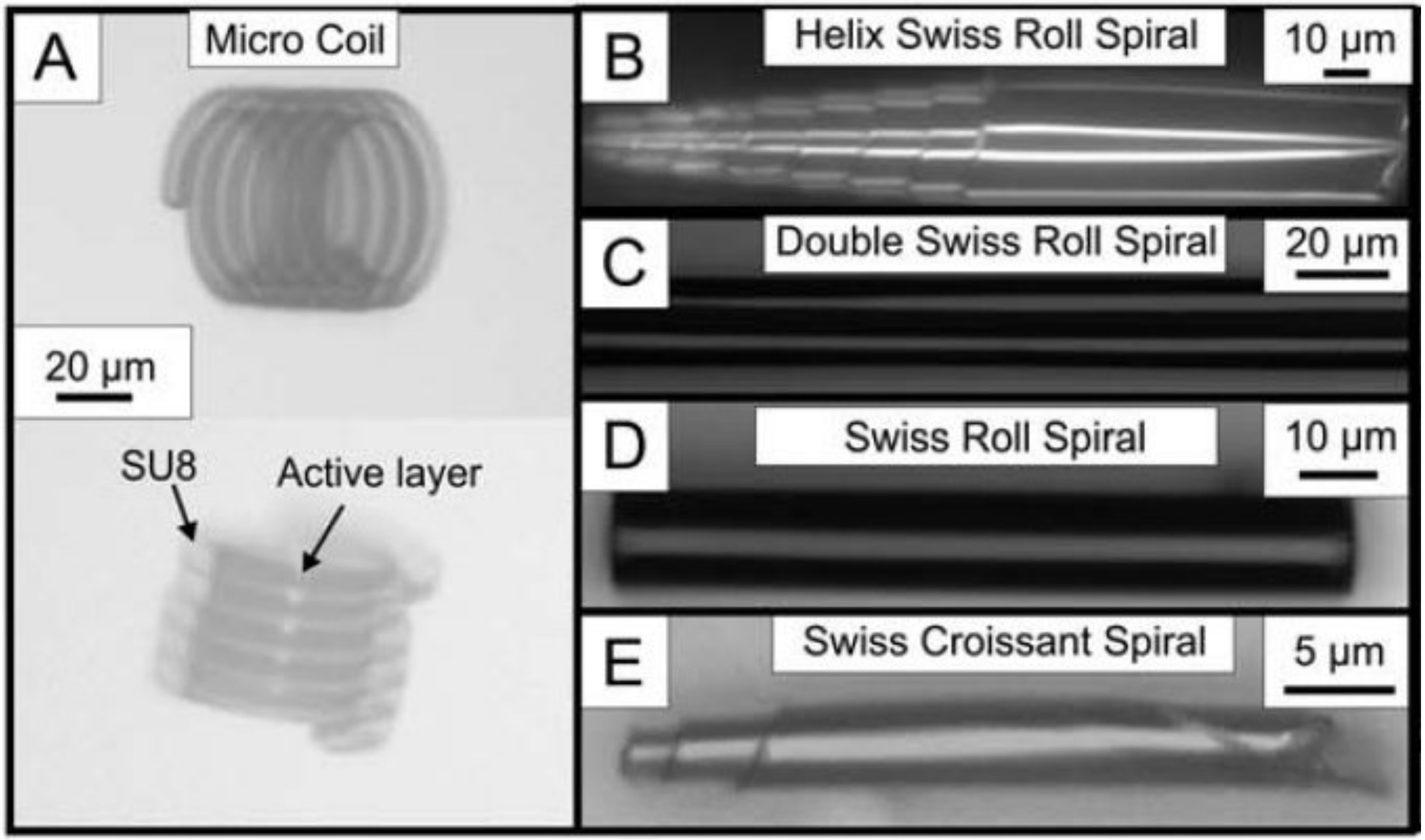

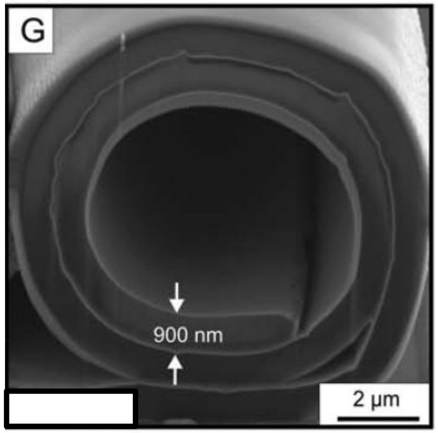

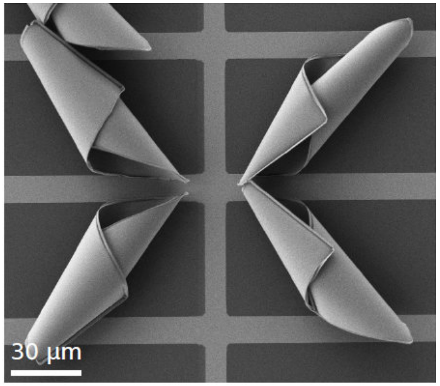

Smith et al., *Soft Matter* **7**, 11309 (2011)

Magnetization configurations

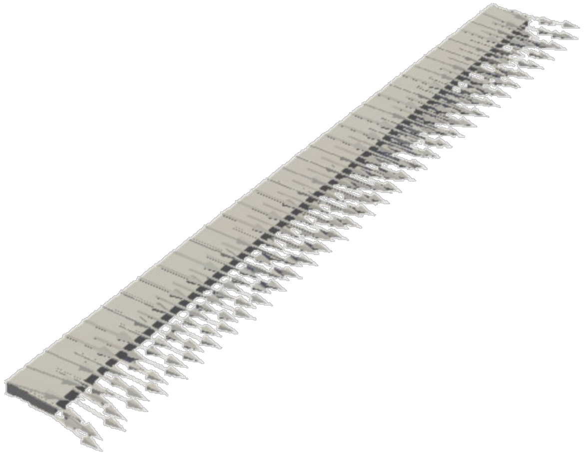

In-plane magnetized perpendicular to strip

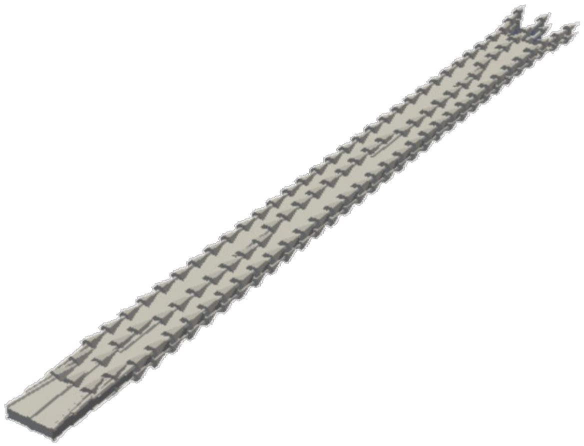

In-plane magnetized parallel to strip

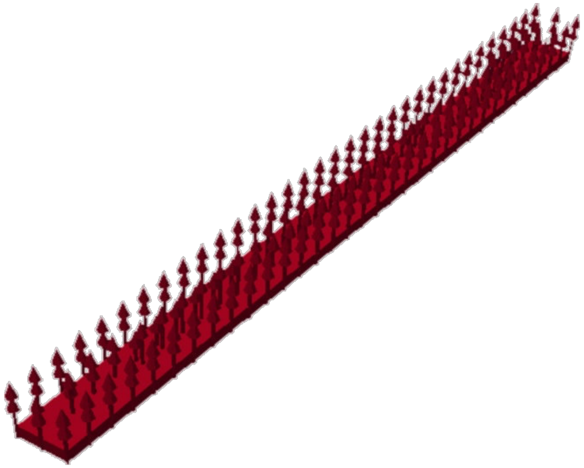

Out-of-plane magnetized

Smith et al., *Phys. Rev. Lett.* **107**, 097204 (2011); Smith et al., *Soft Matter* **7**, 11309 (2011)

Magnetization configurations

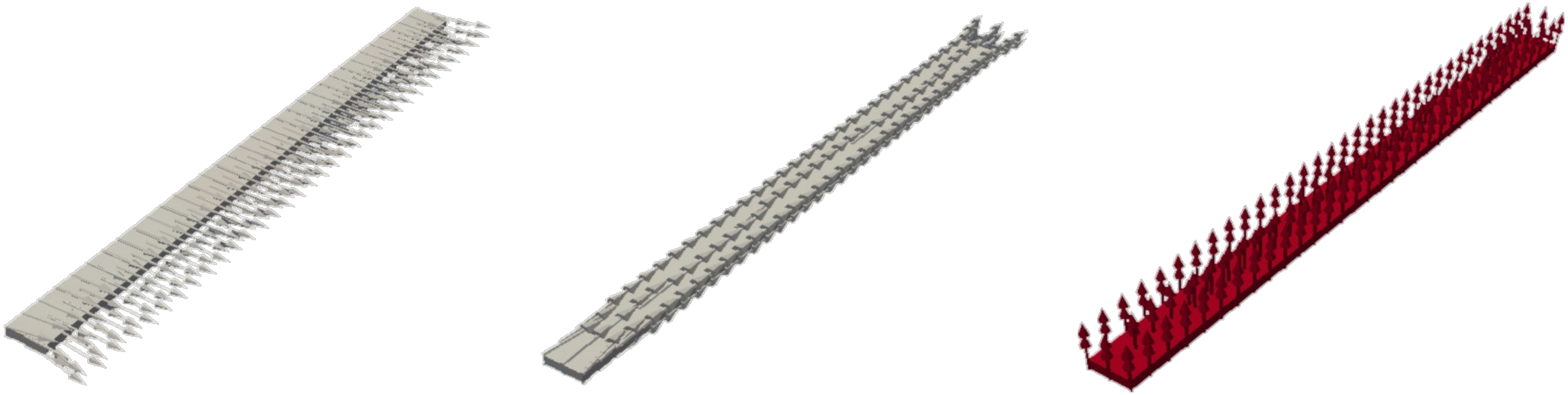

Magnetic configurations after coil-up

Hollow-bar-magnetized

Corkscrew-magnetized

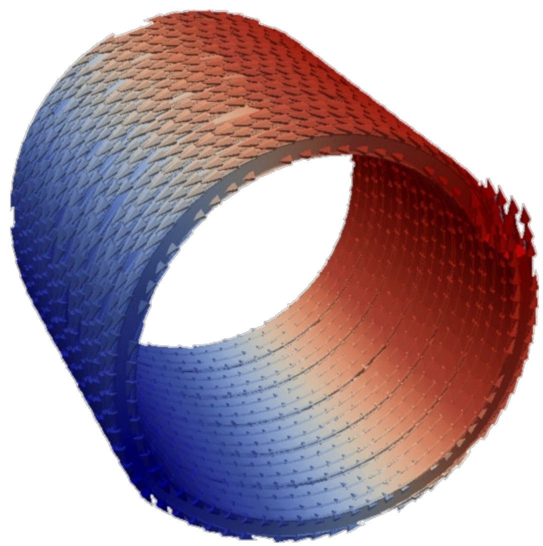

Radial-magnetized

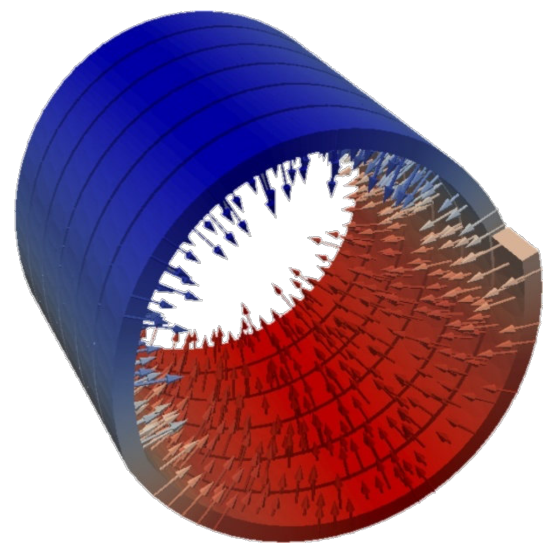

Smith et al., *Phys. Rev. Lett.* **107**, 097204 (2011); Smith et al., *Soft Matter* **7**, 11309 (2011)

Rolled-up technology

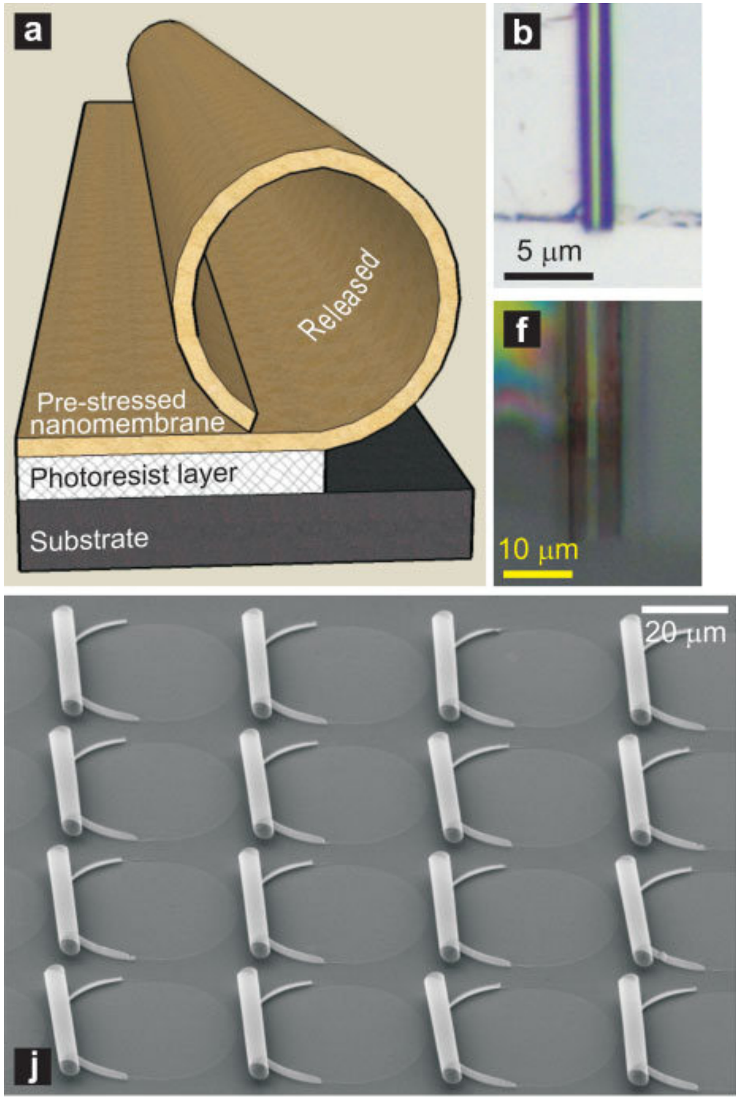

Straightforward on-chip integration

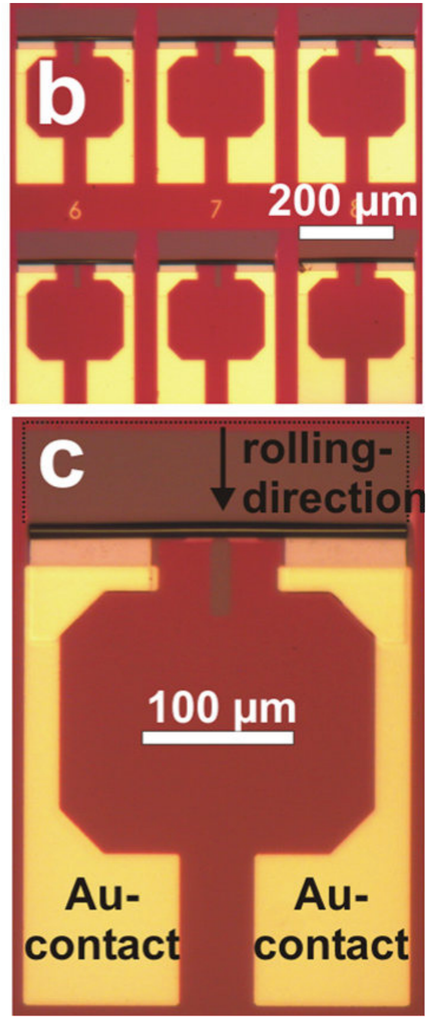

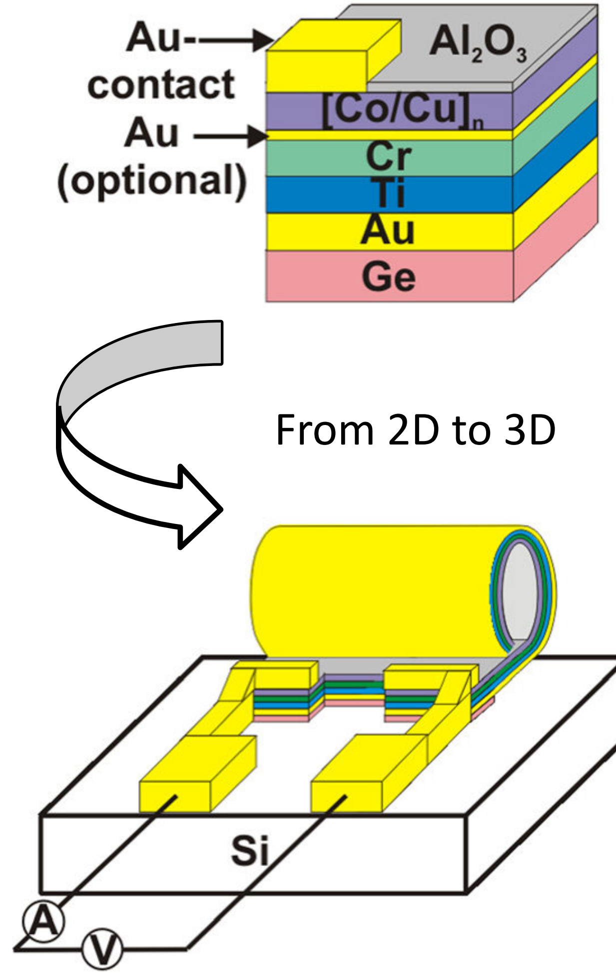

Mei et al., *Adv. Mater.* **20**, 4085 (2008); Müller et al., *Appl. Phys. Lett.* **100**, 022409 (2012)

Flexible substrates

Mechanically flexible magnetic field sensors

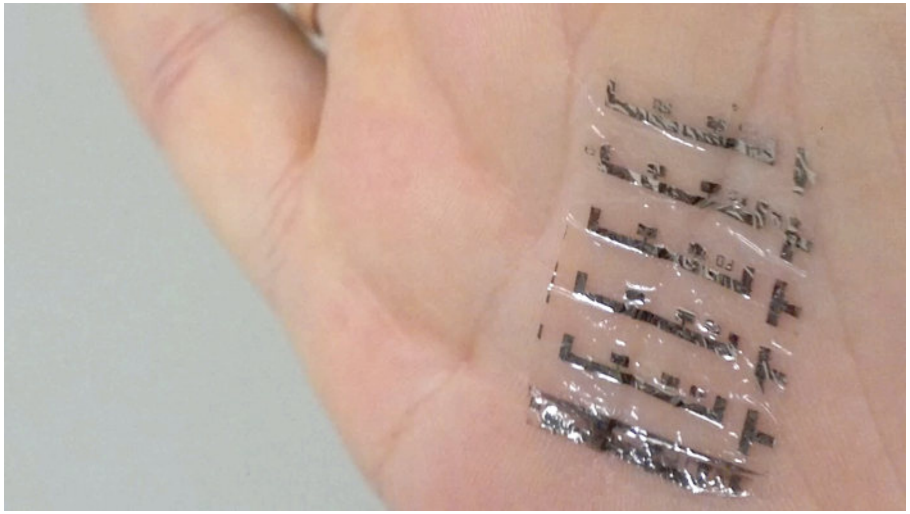

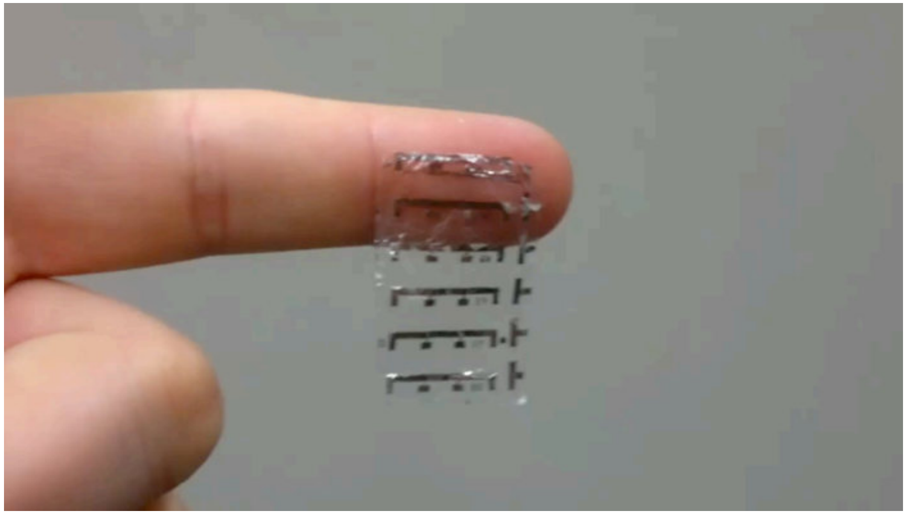

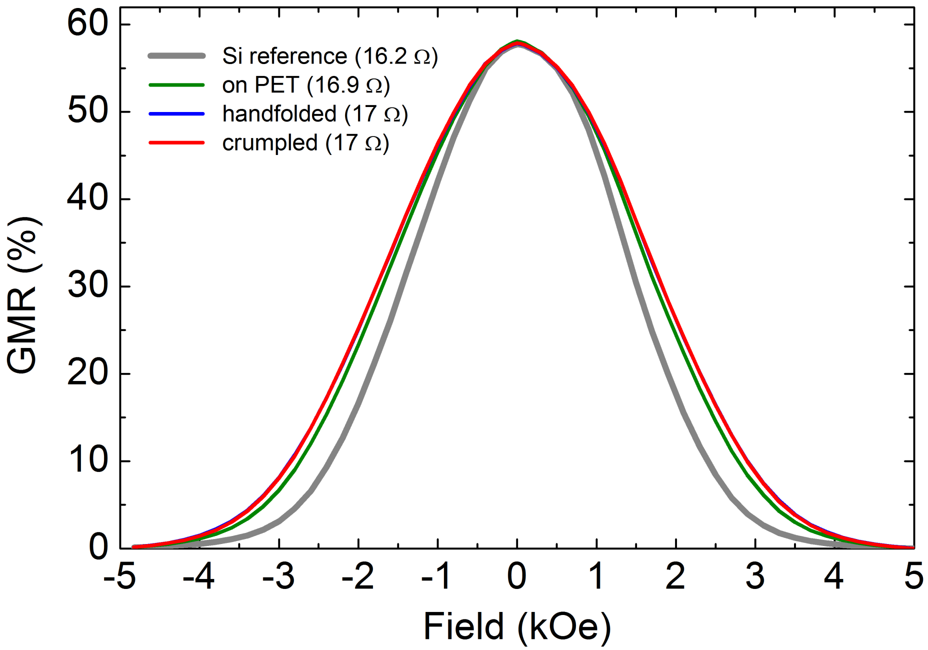

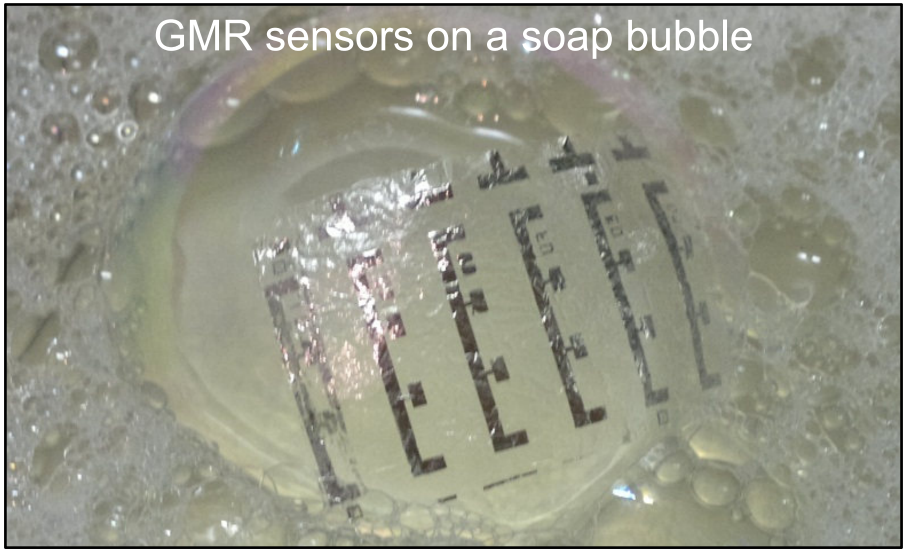

Melzer et al., *Nature Commun.* **6**, 6080 (2015)

DRESDEN concept HZDR

Characterization of skin conformal sensors

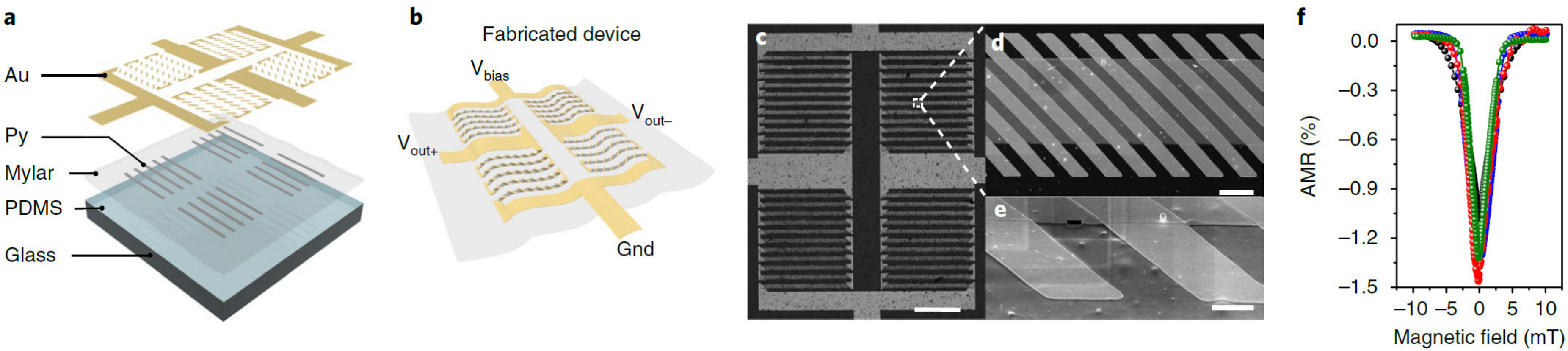

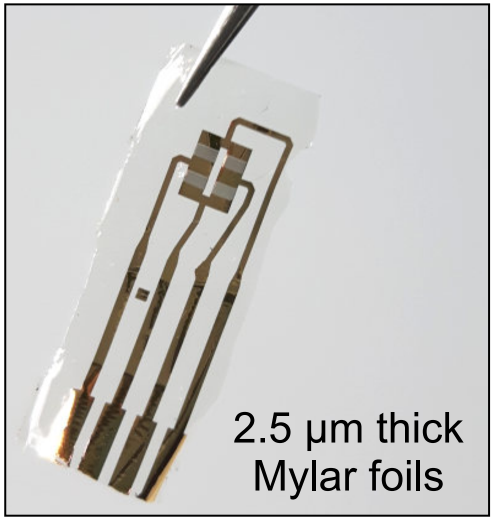

G. S. Canon Bermudez et al., *Nature Electronics* **1**, 589 (2018)

Characterization of skin conformal sensors

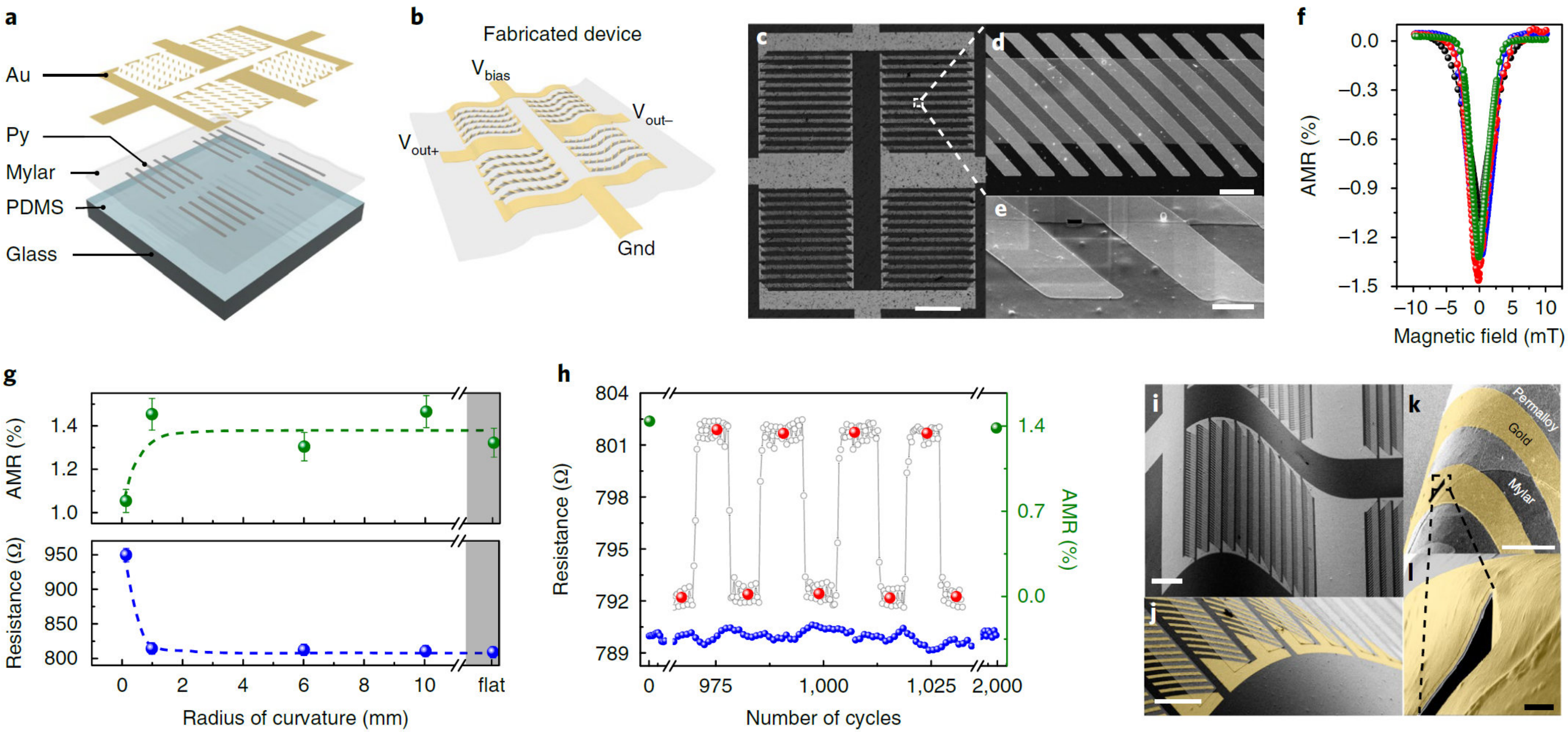

G. S. Canon Bermudez et al., *Nature Electronics* **1**, 589 (2018)

On-skin magnetoelectronics for touchless interaction

Augmented reality applications

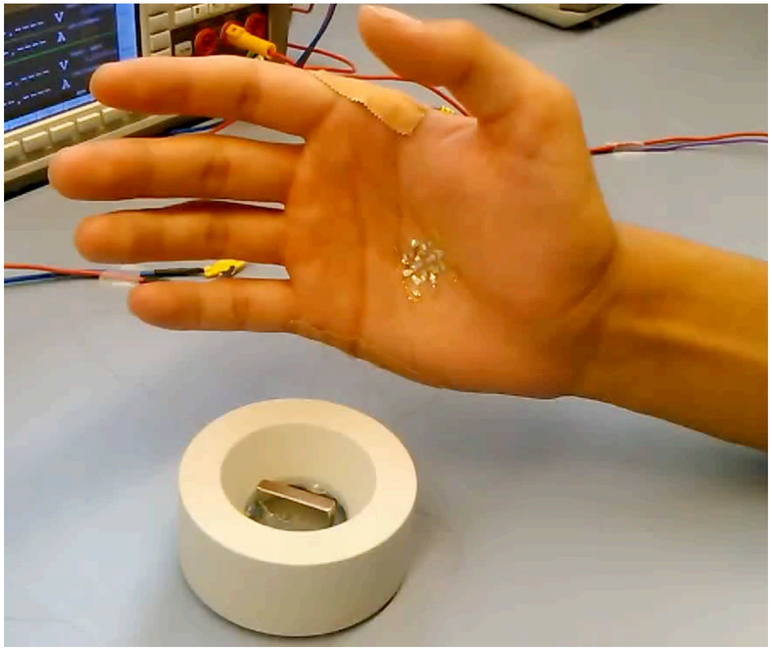

Magnetic field of a permanent magnet (4 mT)

G. S. Canon Bermudez et al.,
Science Advances **4**, eaao2623 (2018)

Virtual reality applications

Geomagnetic field (40 μT)

G. S. Canon Bermudez et al.,
Nature Electronics **1**, 589 (2018)

Tactile and touchless interactivity with magnetic MEMS

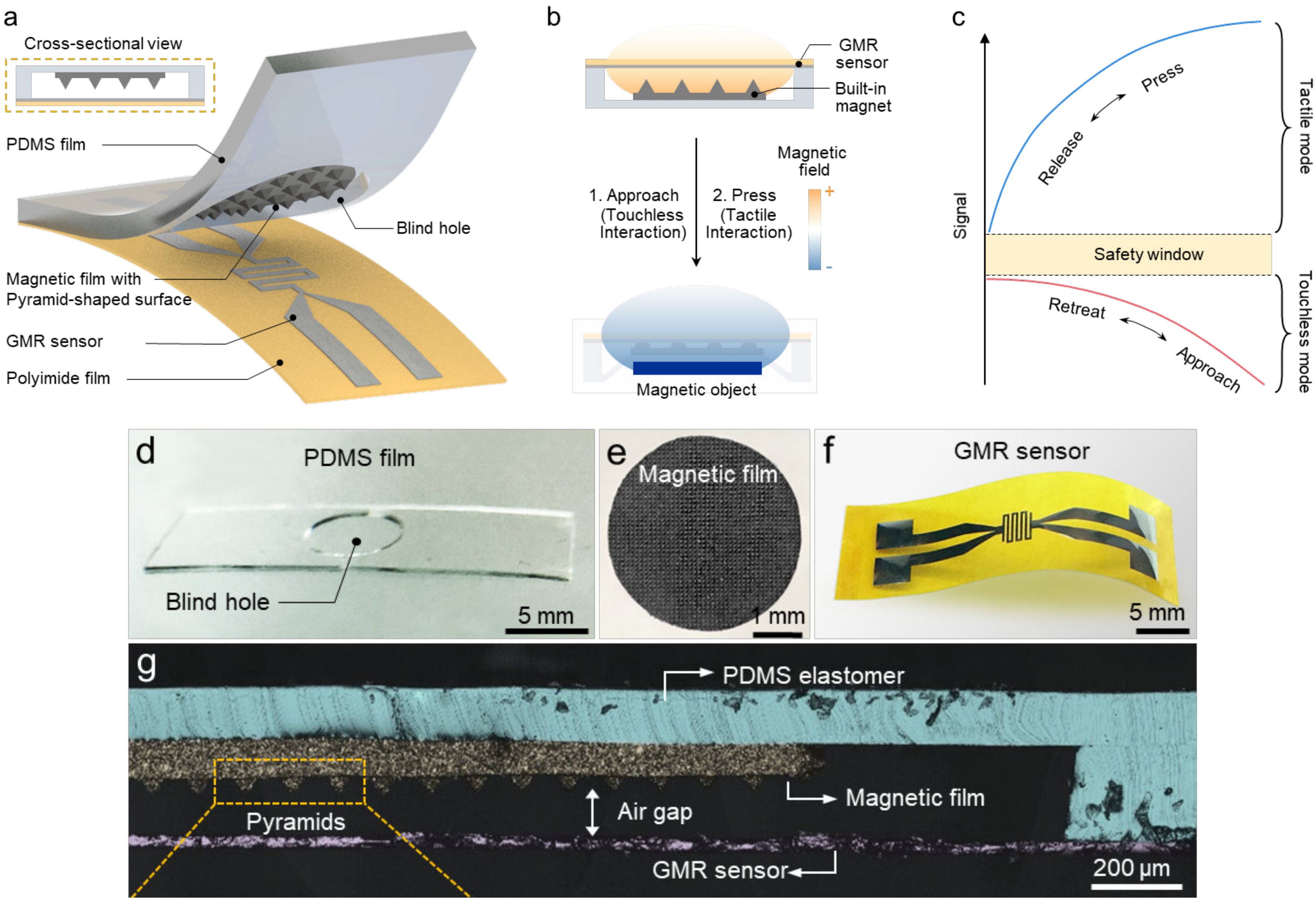

Jin Ge et al., *Nature Communications* **10**, 4405 (2019)

Magnetosensitive smart skins for immersive VR

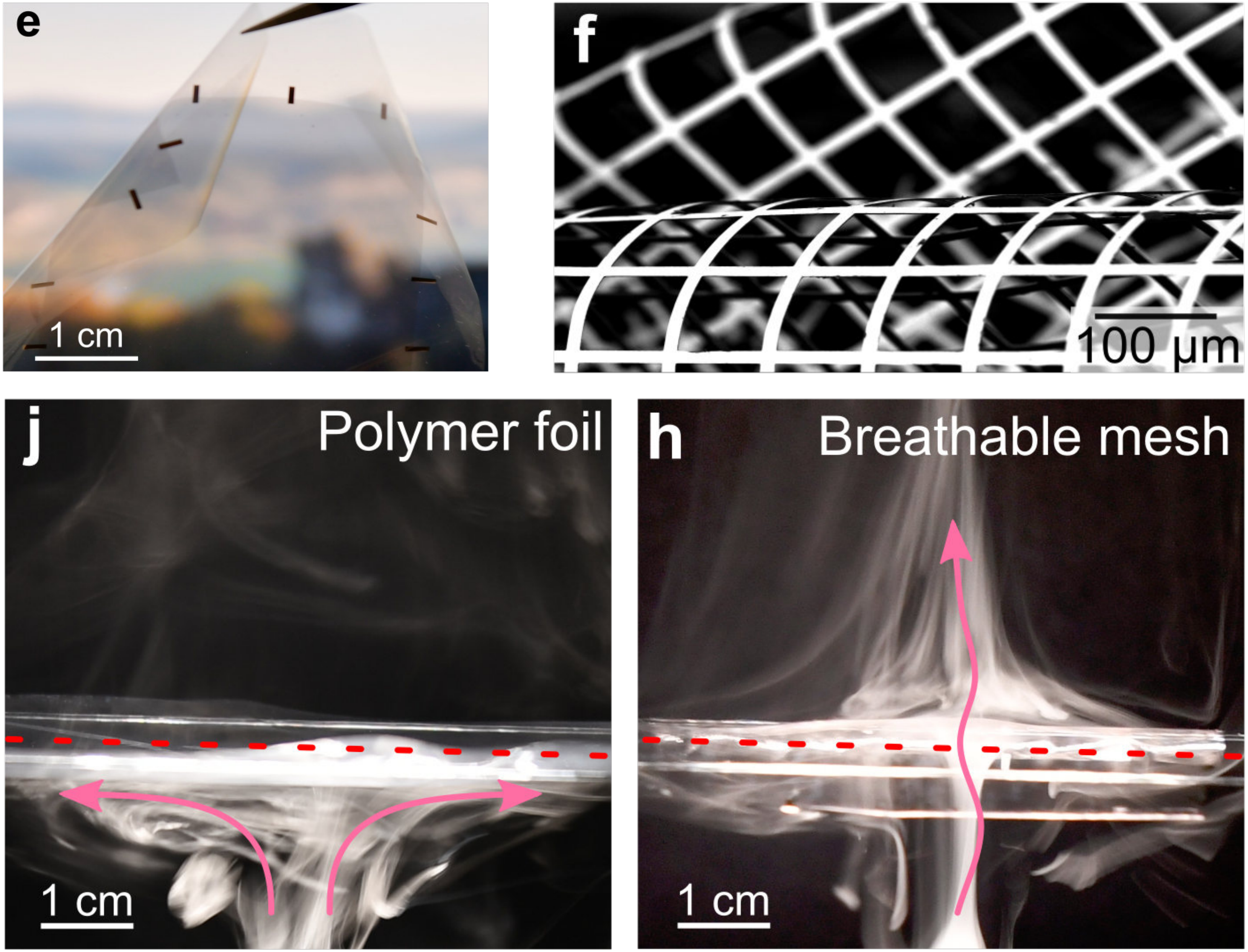

Magnetosensitive smart skins for immersive VR

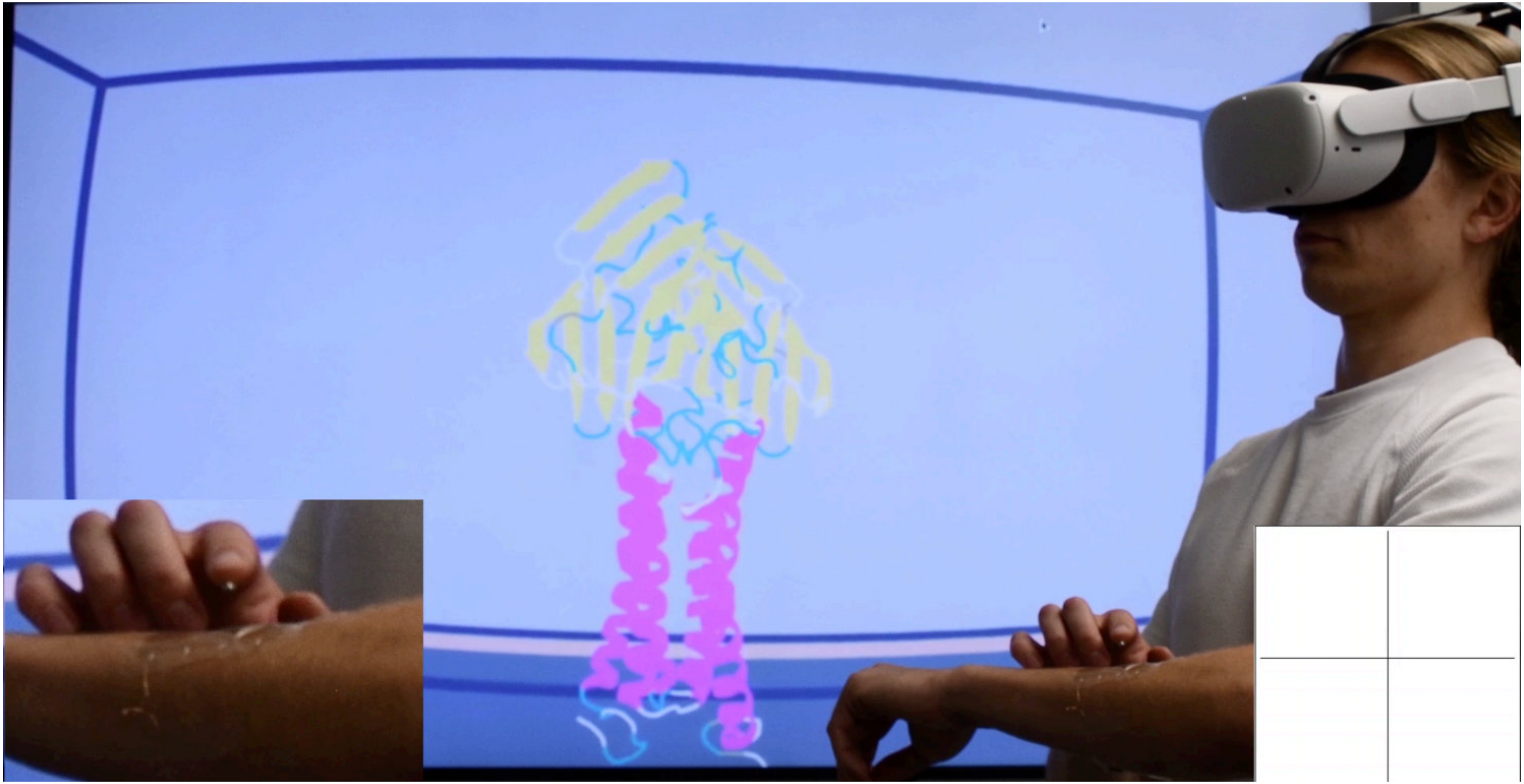

Collaboration: Dr. Stanislav Avdoshenko (Leibniz IFW Dresden)

Printed materials

Dr. Denys Makarov I E-Mail: d.makarov@hzdr.de I Intelligent Materials and Systems

Magnetic field sensors on polymeric foils (1-100 µm)

Thin film technologies

Thin film processing over up to 300 mm wafer scale

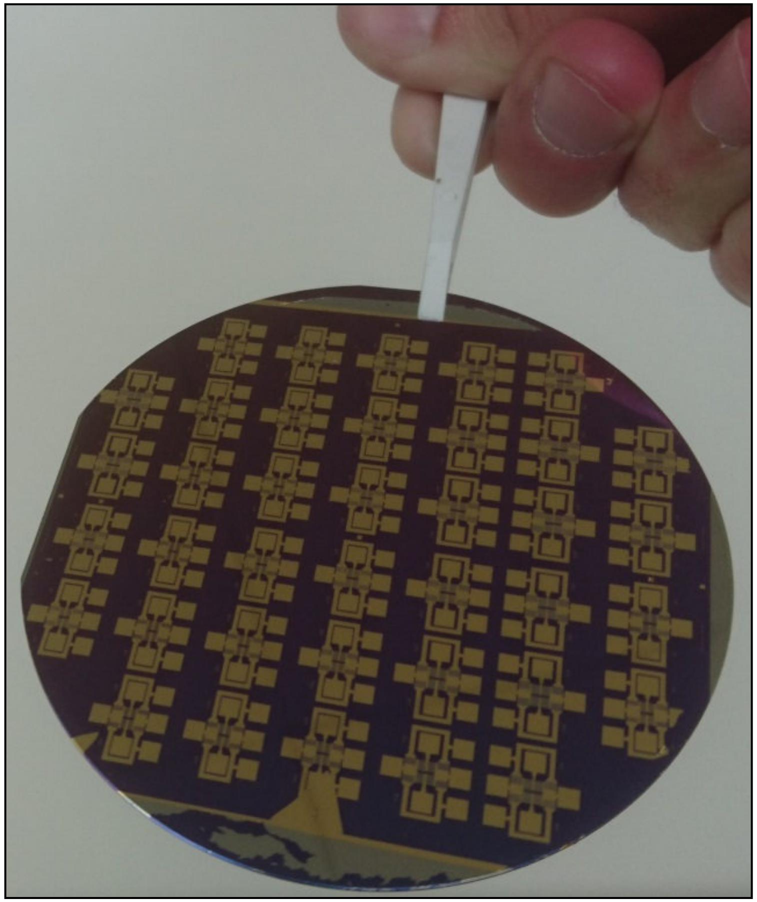

G. S. Canon Bermudez et al., *Nature Electronics* **1**, 589 (2018)

Printing technologies

Magnetic powder & Binder = Paste

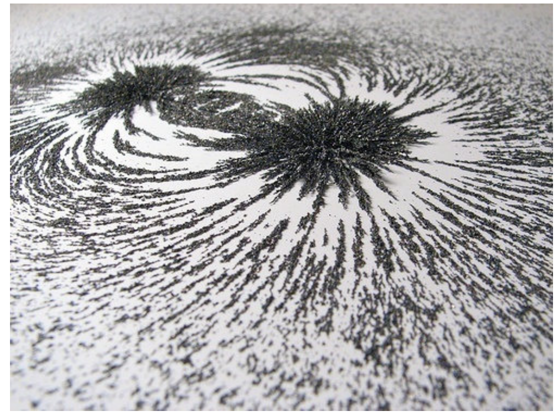

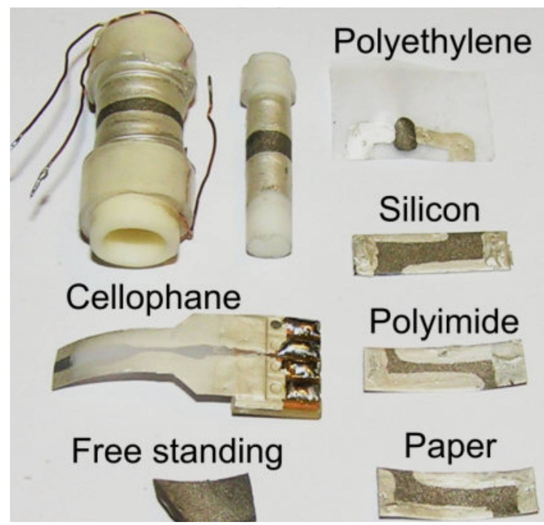

Patent: DE 10 2011 077 907.8

Patent: US 13/528,076

Adv. Mater. **24**, 4518 (2012)

Adv. Mater. **27**, 880 (2015)

Appl. Phys. A **127**, 280 (2021)

Adv. Mater. **33**, 2005521 (2021)

Nature Comm. **13**, 6587 (2022)

D. Karnaushenko et al., *Advanced Mater.* **24**, 4518 (2012)

Printable magnetic field sensors for switch applications

Patent application: DE 10 2019 211 970.0

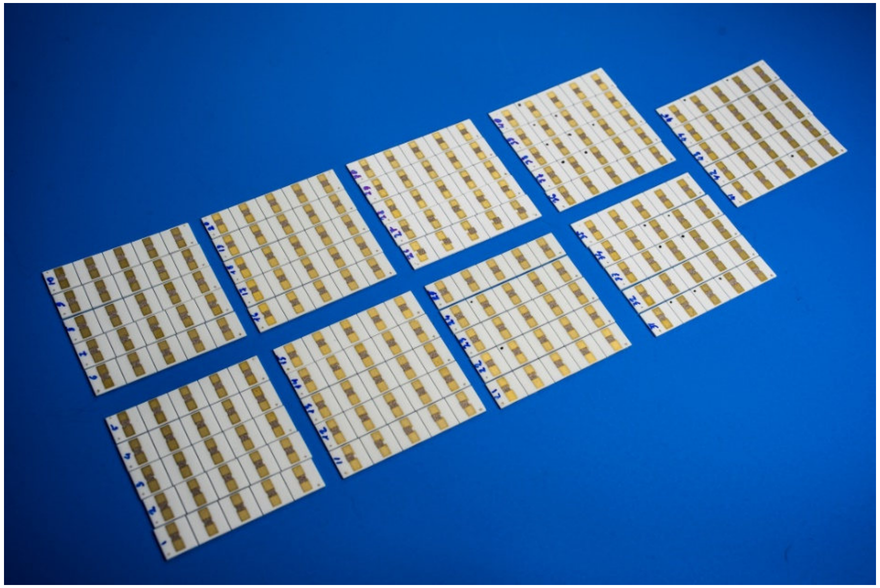

Cooperation with FhG-IKTS: Dr. Mykola Vinnichenko

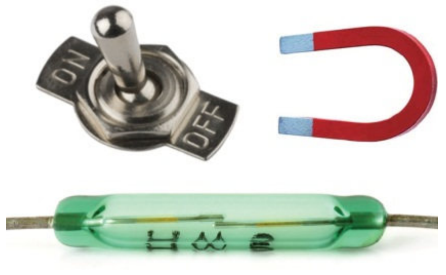

Sensors / Switches

Karnaushenko et al., *Adv. Mater.* **24**, 4518 (2012)

- ❑ REED contacts: 100s Mio sensors per year
- ❑ New application fields including printable and wearables
- ❑ No mechanical parts
- ❑ Isotropic magnetic field sensing performance

Not an improvement only but a shift in technology

Dispenser printed Bi-based magnetic field sensors

E. S. Oliveros Mata et al.,
Adv. Mater. Technol. **7**, 2200227 (2022)
(Cooperation with FhG-IKTS)

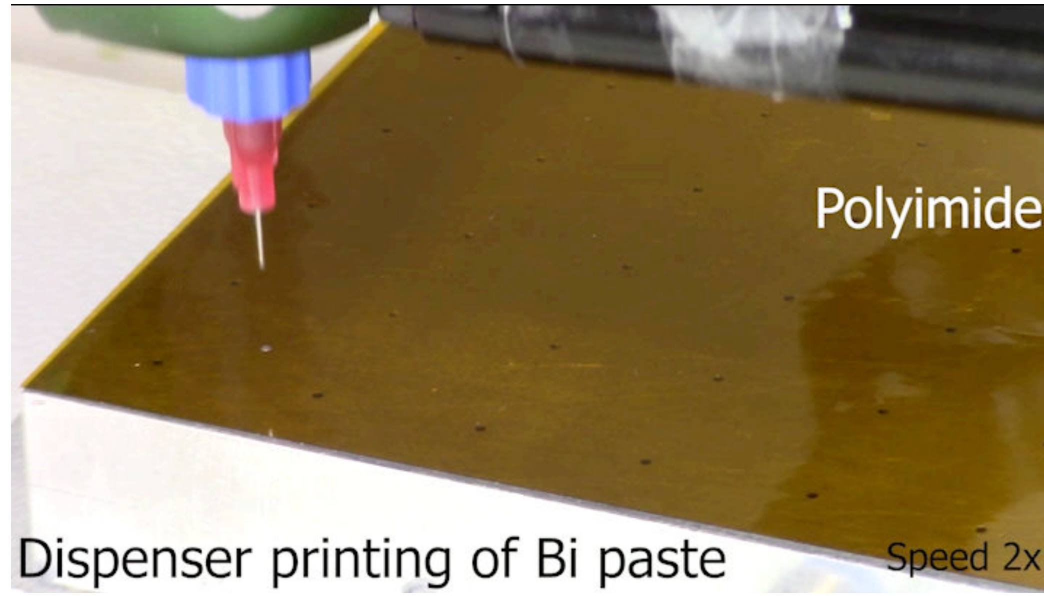

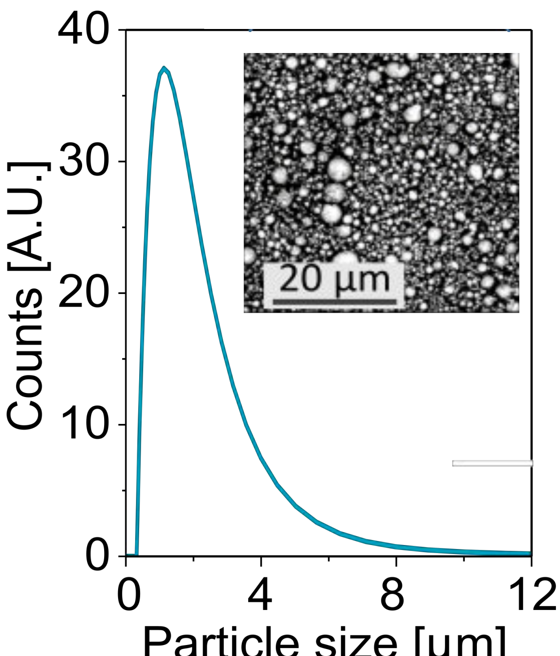

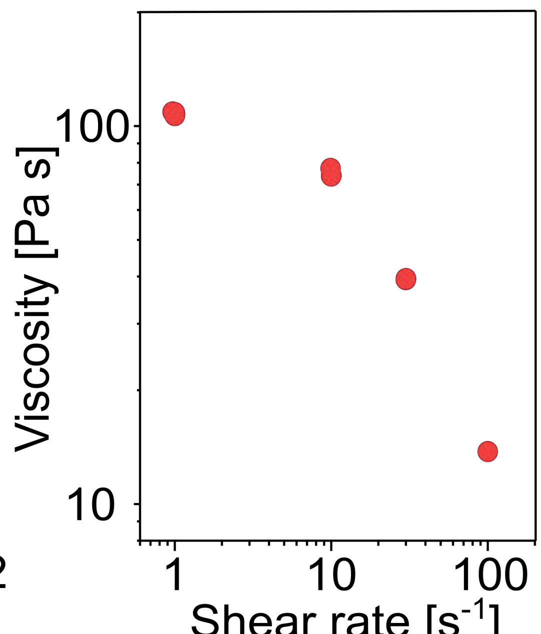

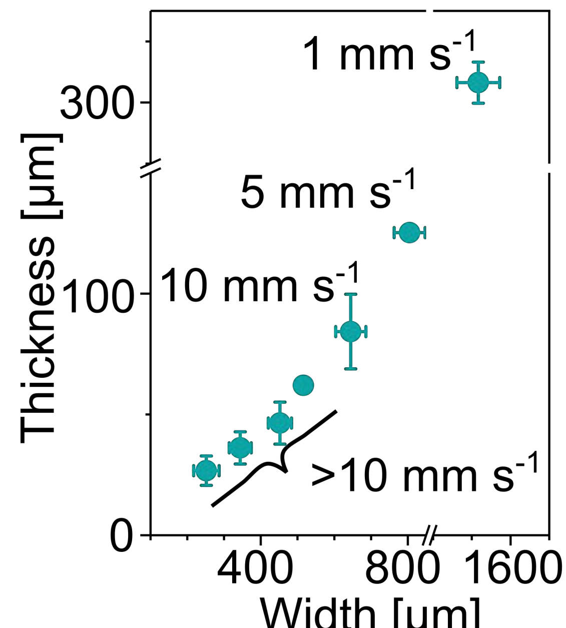

Converting any surface to become interactive

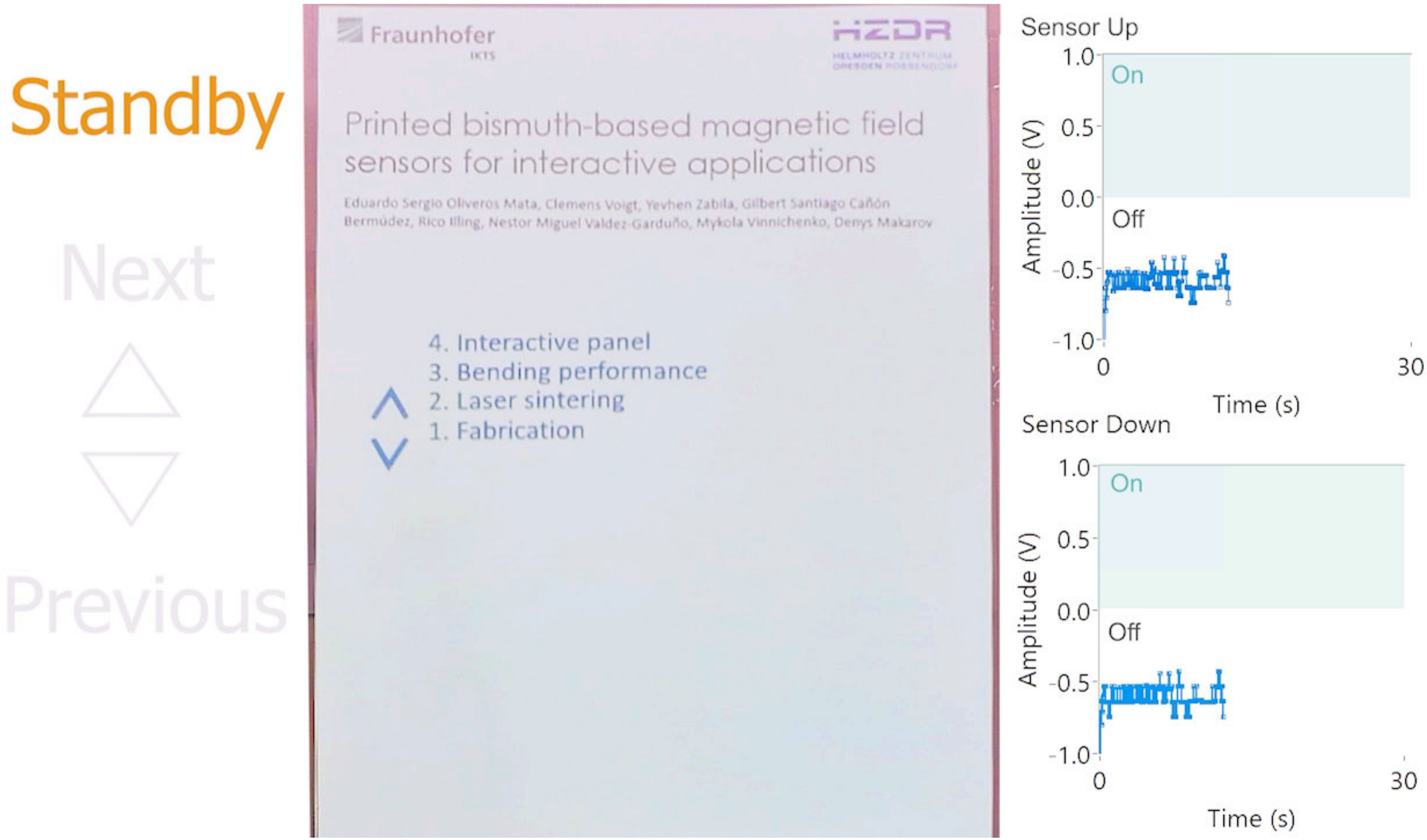

E. S. Oliveros Mata et al., *Adv. Mater. Technol.* **7**, 2200227 (2022)

3D printing: hunt for electromagnetic functionalities

https://all3dp.com

http://www.telegraph.co.uk

http://www.engineering.com

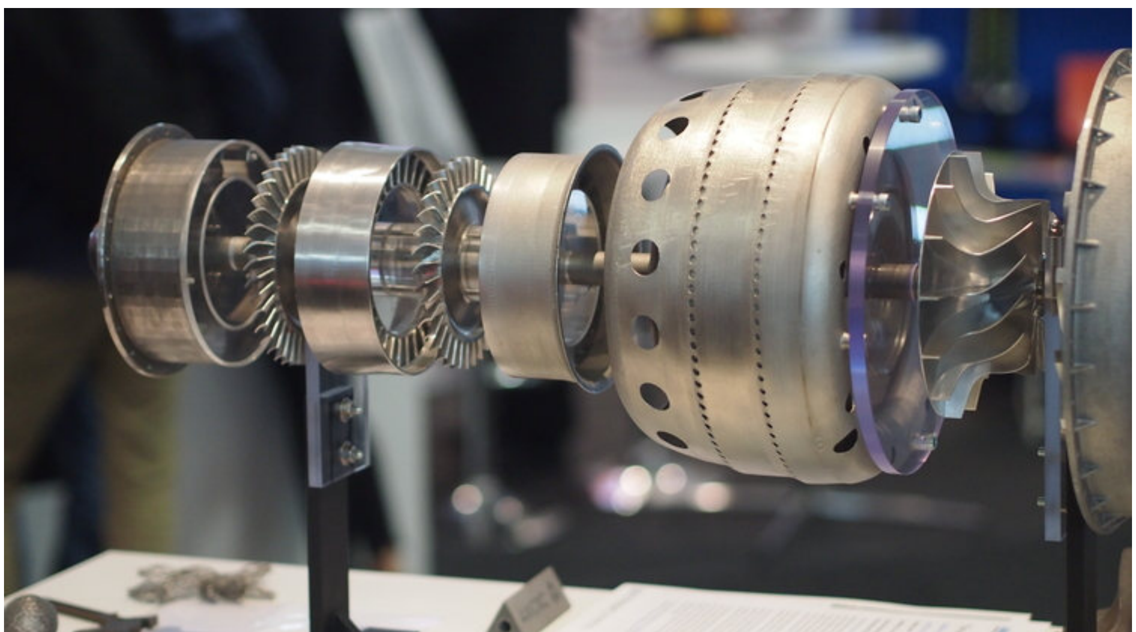

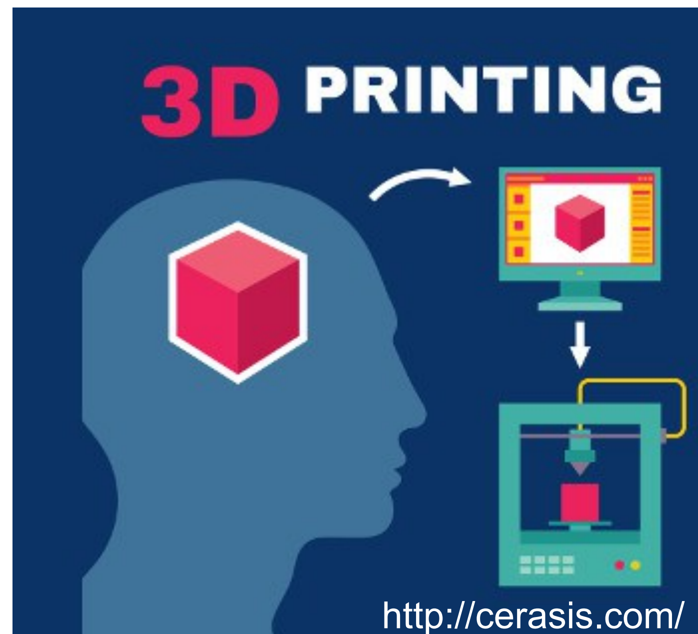

http://cerasis.com/

Self-healable magnetoelectronics

Permalloy microparticles in PDMS-PBS matrix

Permalloy spherical particles (5 µm) | PDMS: polydimethylsiloxane | PBS: polyborosiloxane

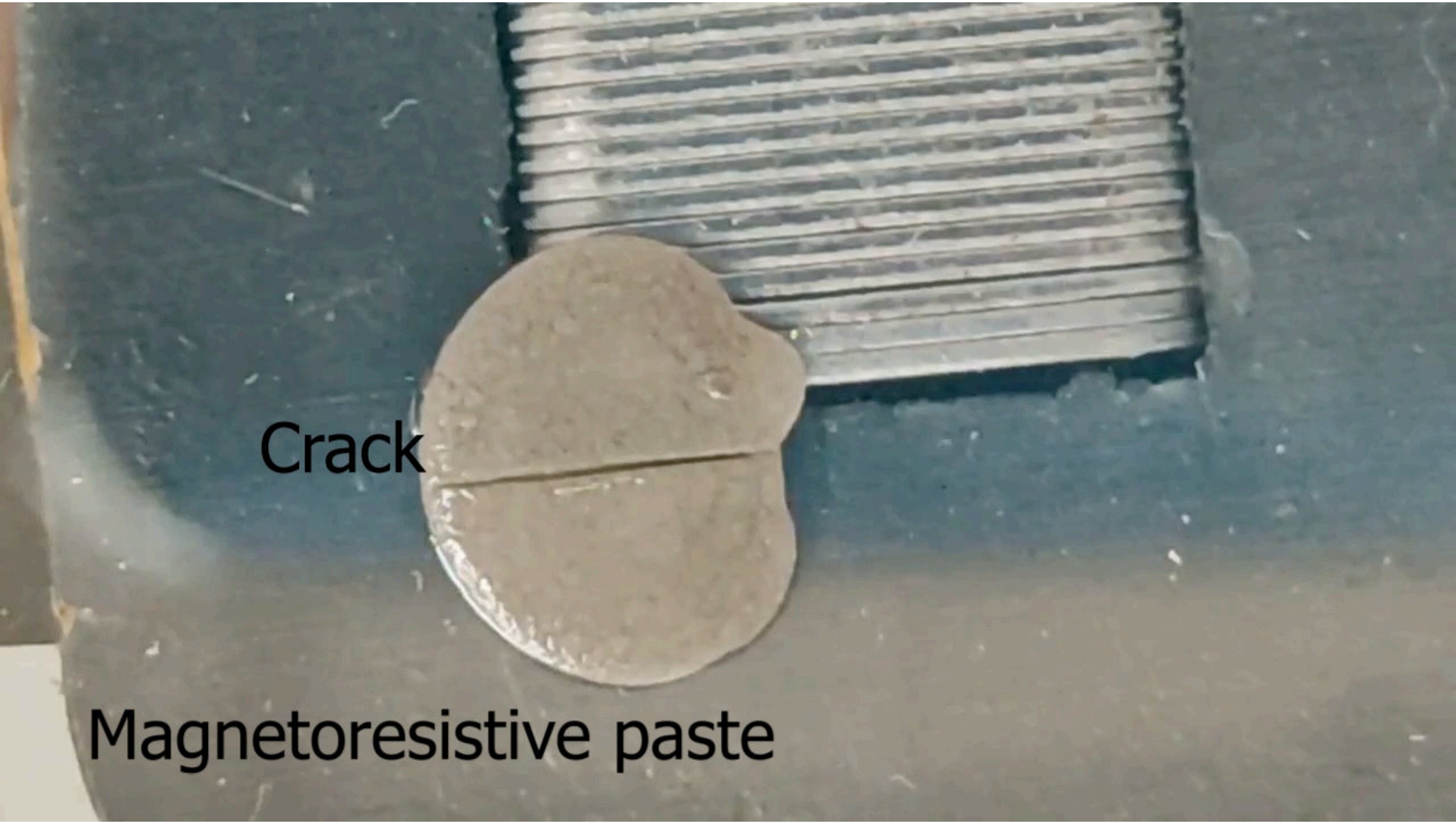

Rui Xu et al., *Nature Communications* **13**, 6587 (2022)

Self-healable printed AMR sensor

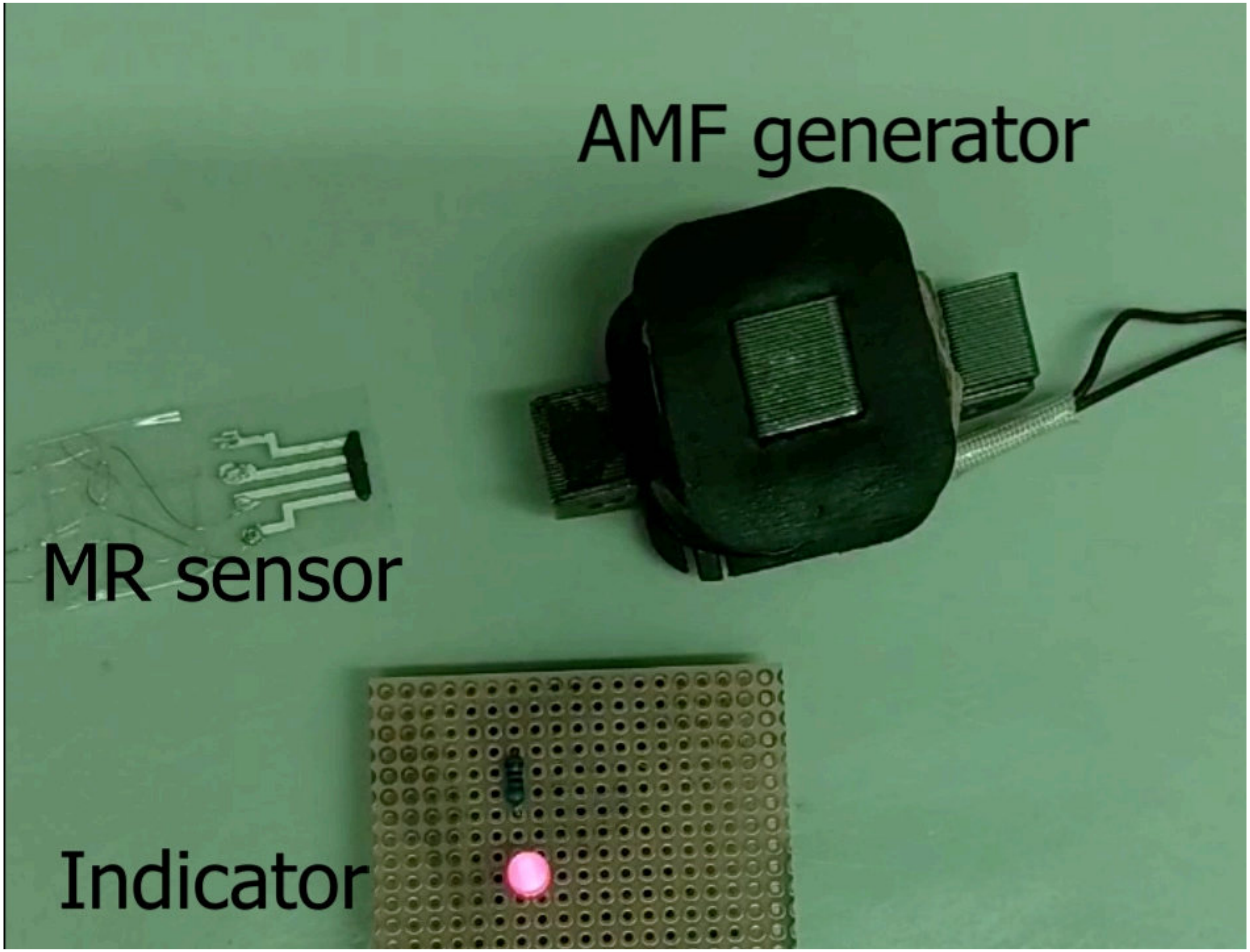

Rui Xu et al., *Nature Communications* **13**, 6587 (2022)

Alternating magnetic field heals damaged composites

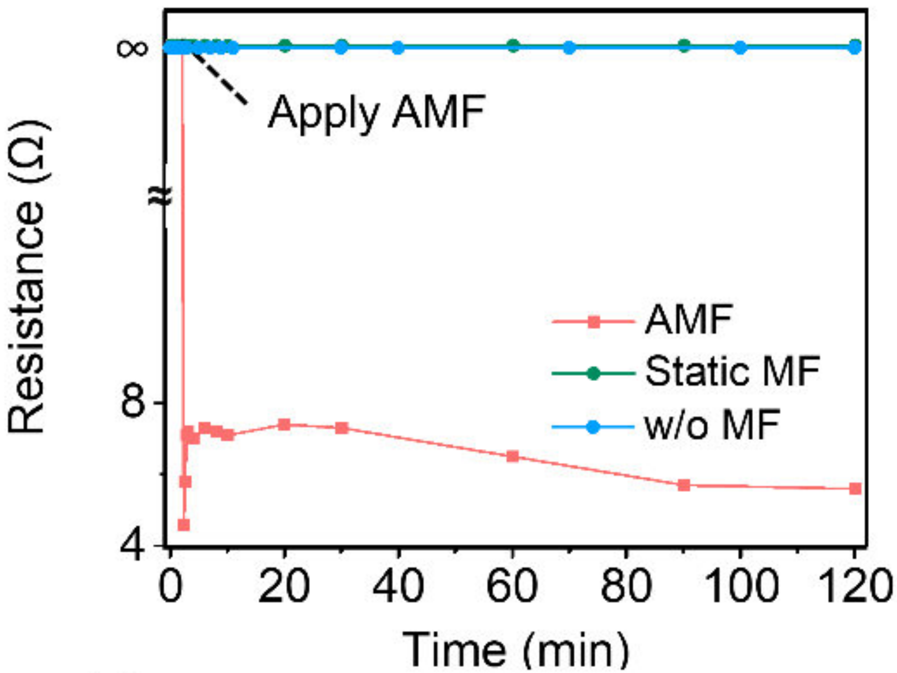

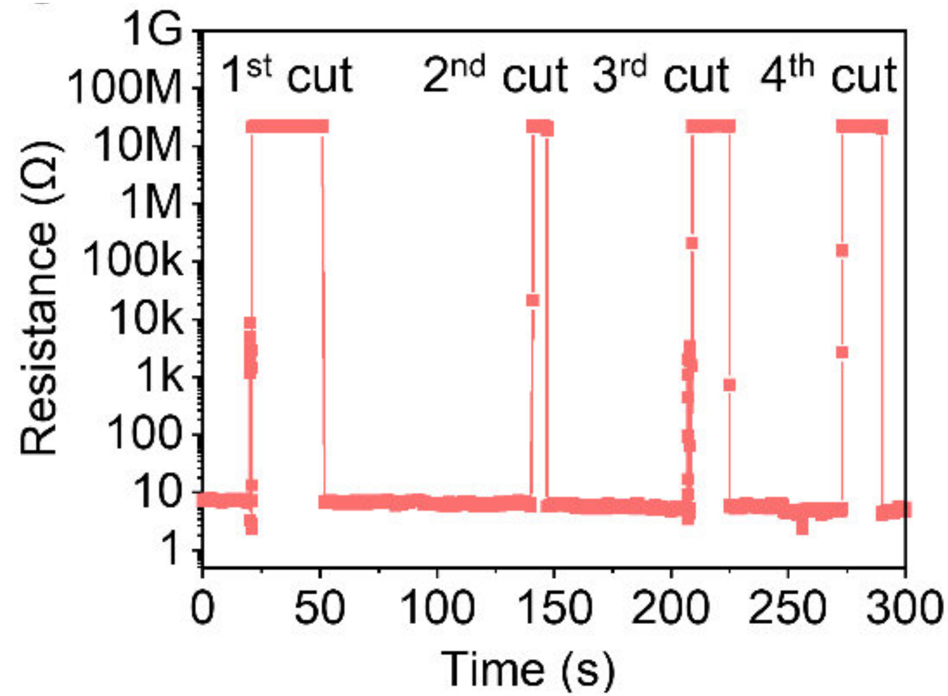

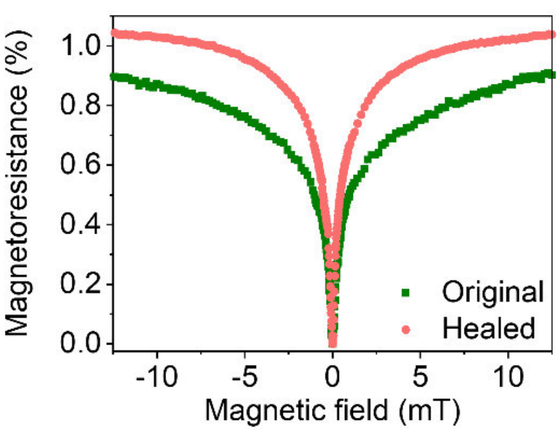

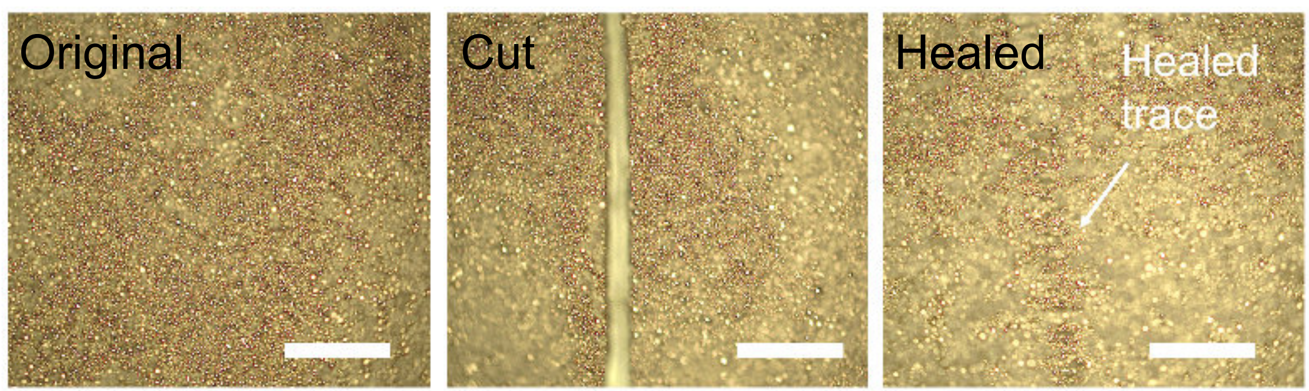

Rui Xu et al., *Nature Communications* **13**, 6587 (2022)

Permalloy microparticles in PDMS-PBS matrix

Permalloy spherical particles (5 µm) | PDMS: polydimethylsiloxane | PBS: polyborosiloxane

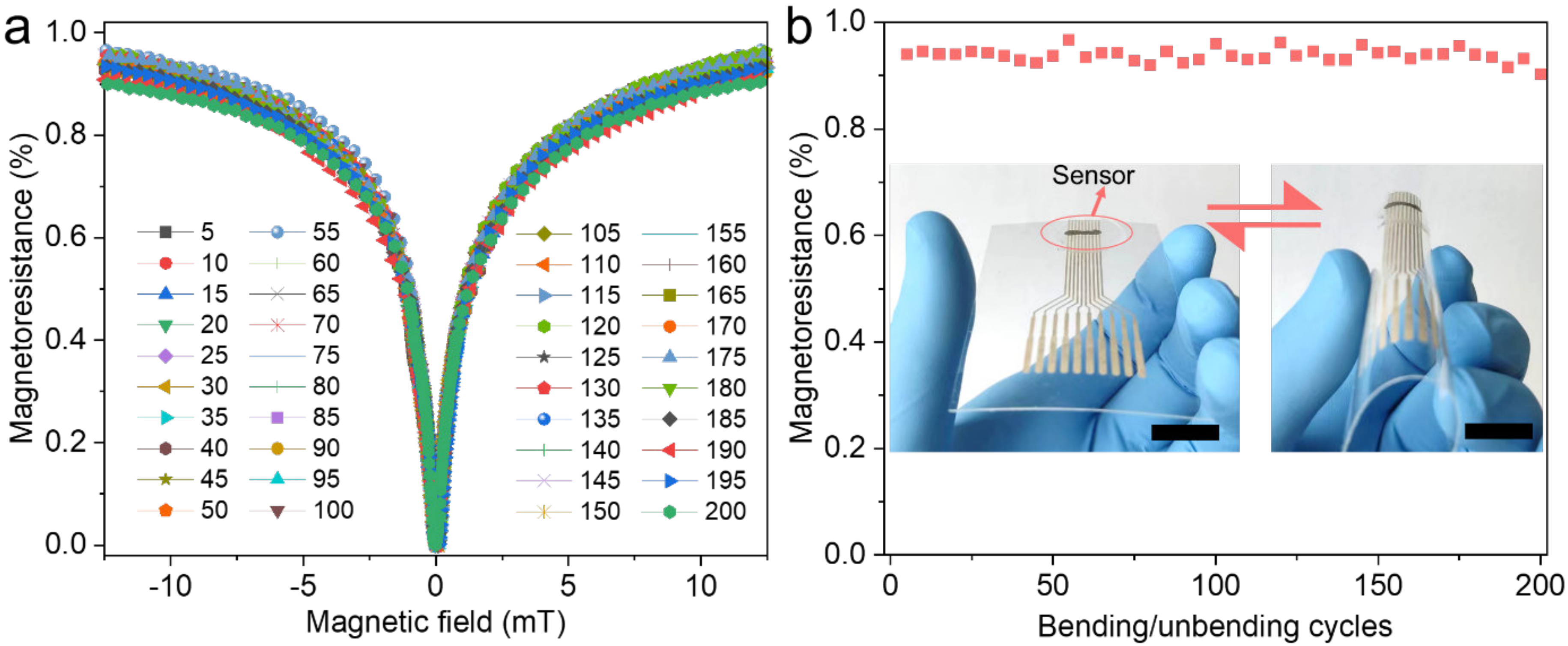

Rui Xu et al., *Nature Communications* **13**, 6587 (2022)

Printed magnetic field sensor (AMR effect)

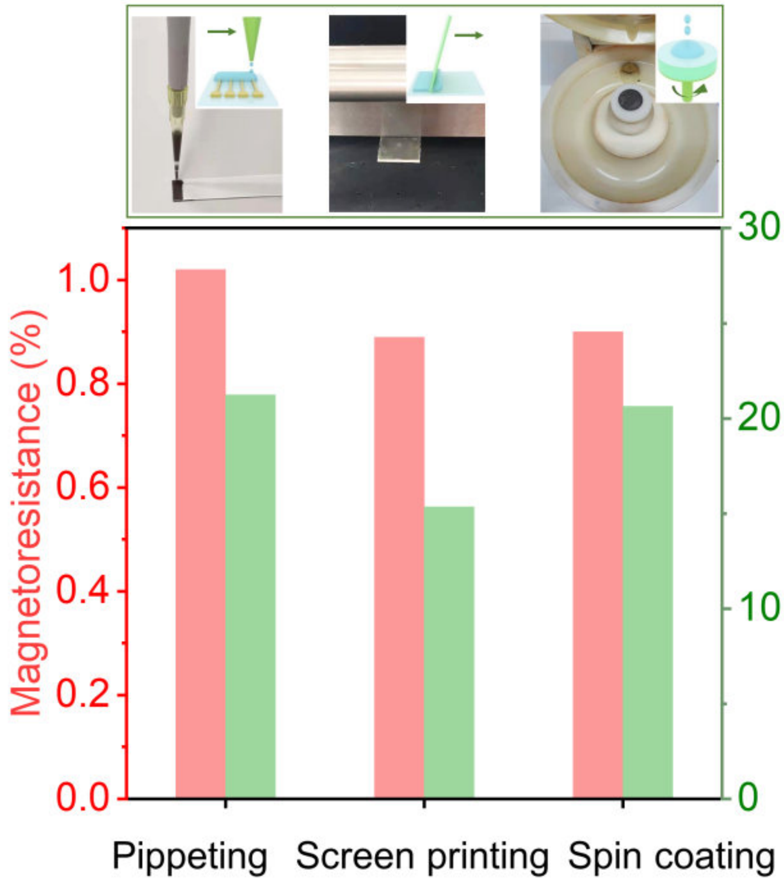

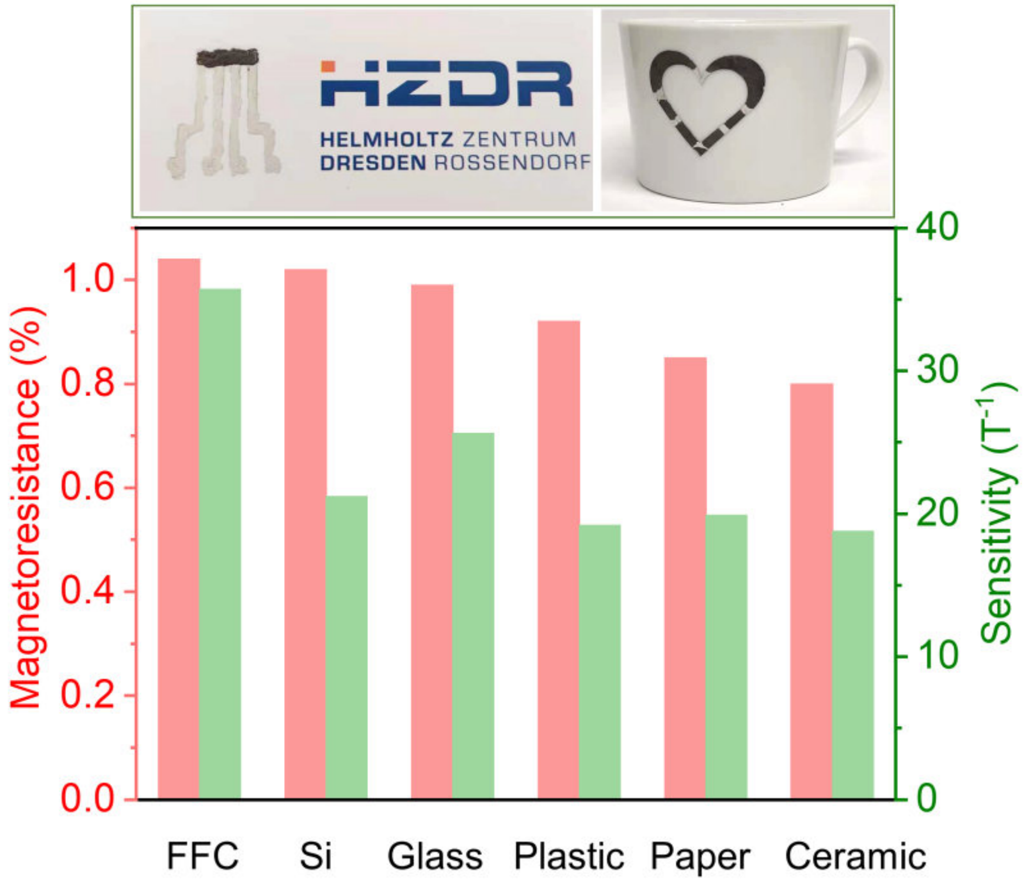

Rui Xu et al., *Nature Communications* **13**, 6587 (2022)

Thank you for your attention